CASE STUDY

5(20), October - December, 2019

ISSN
2394–8558
EISSN
2394–8566

Climate Change

Assessment of inter-seasonal, inter-annual and intra-annual variability in snow and rainfall recharged fresh water discharge under IPCC AR5 based climate change scenarios: A case study of Soan river basin, Potowar region, Pakistan

Muhammad Usman[1], **Burhan Ahmad**[2]✉, **Syed Ahsan Ali Bukhari**[2]

[1]Bahria University, Department of Earth and Environmental Sciences, Shangrilla Road., Sector E-8, Islamabad, Pakistan
[2]Pakistan Meteorological Department, Research and Development Division, Pitras Bukhari Rd., H-8/2, Islamabad, Pakistan

✉**Corresponding author:**
Pakistan Meteorological Department,
Research and Development Division, Pitras Bukhari Rd.,
H-8/2, Islamabad, Pakistan
E-mail: burhanahmadkhan@gmail.com

Article History
Received: 19 June 2019
Accepted: 30 August 2019
Published: October - December 2019

Citation
Muhammad Usman, Burhan Ahmad, Syed Ahsan Ali Bukhari. Assessment of inter-seasonal, inter-annual and intra-annual variability in snow and rainfall recharged fresh water discharge under IPCC AR5 based climate change scenarios: A case study of Soan river basin, Potowar region, Pakistan. *Climate Change*, 2019, 5(20), 264-326

ABSTRACT

Apart from being one of the most important natural resources, freshwater resources are also highly vulnerable to climate changes, especially over the past century, on global and regional levels. Freshwater resources in Pakistan are extremely exposed to climatic changes, and especially the semi-arid basins are susceptible to hydrological implications of climate change. This study aimed to investigate the variations in freshwater resources of the semi-arid Soan River Basin (SRB) under changing climate scenarios till mid of the twenty first century. In the present study, state of the art, conceptual, semi-distributed, lumped hydrological model, Hydrologiska Byrans Vattenavdelning (HBV) light, a modified version of the HBV model was implemented to simulate projected flows of two sub-catchments of the SRB namely, the Sihala sub-catchment (SSC) and the Kani sub-catchment (KSC). HBV-light is calibrated for the time period (1984–2008) and validated for (2009–2017) for both the sub-catchments of the SRB. HBV-light exhibited good performance both during calibration and validation for both the sub-catchments of the SRB. After calibration and validation, the hydrological model was induced with future climate projections data of the Swedish Meteorological and Hydrological Institute Rossby Centre Regional Atmospheric Model (SMHI RCA4), forced with the two Representative Concentration Pathways (RCPs), i.e. the RCP 4.5 and RCP 8.5 to simulate projected flows of the (SRB) for the time period (2018–2047). Climate changes in the future suggest warming under both the RCPs and a significant increase in precipitation amount (yearly and seasonal basis, while decrease and increase could be seen for monthly basis), and an increase in evapotranspiration (but the magnitude of change in precipitation outweigh the change in evapotranspiration). Mean annual flows of the SSC showed an increase of 467% (593%) and an increase of 270% (316%) for KSC under the RCPs 4.5 (8.5). A decrease of up to 39% and 29% is projected under RCP 4.5 for spring transitioning months for both sub-catchments and a decrease of up to 41% for winter months under RCP 8.5 for the SSC. Highest increase amongst all the seasons is projected for the summer season in the SSC under both the emission scenarios. However the winter flows seems to decrease under the RCP 8.5. Overall an increasing pattern could be observed for the rest of the seasons. This study would be beneficial for multiple stakeholders and sectors including water resource managers, agriculture, hydropower generation, and socioeconomic development.

Keywords: Climate change, Hydrology, Impacts assessment, HBV-light, Climate change scenarios, Water resources, Runoff, Hydrological modelling, Soan river basin.

1. INTRODUCTION

1.1. Climate Change

A variation in the state of climate (variation in average or its properties) that can be statistically identified is referred to as climate change, and it persists typically for decades or longer. Warming of the climate system in recent decades is unequivocal, as is now evident from observations of increase in global average air and ocean temperatures, rampant melting of snow and ice, and rising global sea level. Natural internal processes or external forcing such as volcanic eruptions and persistent anthropogenic changes in the composition of the atmosphere or in land use may lead to climate change. The United Nation Framework Convention on Climate Change (UNFCCC), in its article 1, defines climate change, as "a change of climate which is attributed directly or indirectly to human activity that alters the composition of the global atmosphere and which is in addition to natural climate variability observed over comparable time periods".

A warming of (0.65 °C to 1.06 °C), over the period1880-2012 has been observed from globally averaged combined land and ocean surface temperature data. Variations exist regionally in the global trend, but overall the entire globe has warmed during the period 1901-2012. Heavy precipitation events have been amplified on many land areas, but total and extreme precipitation showed certain trends as well. Theoretical and climate model studies propose that, in a globally warm climate that is due to increasing greenhouse gases, extreme precipitation is likely to show a greater increase, as compared to the mean precipitation, but regional variations in precipitation are also expected (Bott, 2014; IPCC, 2007; IPCC, 2014; Bates et al., 2008; Gebre, 2015).

1.2. Freshwater Resources

Water is an essential component of the natural environment, and the survival of all living species is dependent on water. Freshwater is a finite and vulnerable resource, crucial to sustain life, development and the environment. Due to tenacious increase in competing demands of fresh water resources, they are increasingly becoming more scarce (N.W. Policy, 2018). About 80% of the world's population already suffers from serious threats to its water security. The occurrence and movement of water through all biological

systems is the basis of life. Water is a vital resource for the livelihood of people and sustained development of any economy. Sustainable management of freshwater resources has attained importance regionally and globally, and 'Integrated Water Resources Management' has become the corresponding scientific paradigm.(WMO, 2009; Ali et al., 2017; Ky, 2014; Hoff, 2009; Hoegh-Guldberg et al., 2018)

1.3. Interrelation between climate change and assessment of freshwater resources

The World Meteorological Organization (WMO) Commission for hydrology has worked on hydrology and water resources assessment. At global scales, several initiatives aim at developing water resources assessments and water balances, such as the activities of the International Hydrological Program (IHP) of the United Nations Educational, Scientific and Cultural Organization (UNESCO)(European Commission, 2015).

The assessment of water resources is of critical importance to sound and sustainable management of the world's water resources (WMO, 2009). With the increasing imbalance between water supply and water demand, potentially exacerbated by changes in climate during the past few decades, water availability and water scarcity has progressively emerged as a key issue in water policy making and implementation (European Commission, 2015). Water resources are intricately connected with climate and the imminent climate change scenarios have serious ramification for water resources of Pakistan. The climate change impact assessment is one of the major policy objectives of the National Water Policy of Pakistan (Policy, 2018).

Renewable water resources are projected to decreases in some regions (in many mid-latitude and dry subtropical regions) and increases in others (at high latitudes and in many humid mid-latitude regions), albeit with large uncertainty in many places according to climate models. Even where increases are projected (in stream flows), there can be short-term shortages due to more variable stream flow (because of greater variability of precipitation) and seasonal reductions of water supply due to reduced snow and ice storage (IPCC, 2007). According to Islam (2013), it is a nationally prioritized agenda to assess the hydrological implications of climate change and how to cope with them.

1.4. Basin scale hydrological modeling and water resources management

The development of water quantity assessment frameworks focusing on water balances or asset accounts (which use hydrological information), have been identified as a useful tool for guiding water policy and management at different decision making scales. Which is particularly in regards to the quantitative management and efficient allocation of water resources (European Commission, 2015).

Significant information about the hydrological processes in the catchment is being provided by the applications of hydrological modeling(Nepal, 2016). Surface runoff modeling has been used for the purpose of understanding catchment yields and responses, estimation of water availability, identification of changes over time, and forecasting (Sitterson et al., 2017). Hydrologic models are widely used as a decision making tool at the catchment scale. In order to identify potential water resource problems and making better planning decisions, the quantitative estimation of the hydrological impacts of climate change is very essential (Ky, 2014), and according to Didovets et al., (2017) the climate change impacts on river discharge are also vitally important for planning adaptation measures.

A river basin has been recognized as the appropriate unitof analysis for addressing the challenges of water resources management with increasing competition for water use across regional and sectoral levels(Islam, 2013). There is general recognition that the natural management unit is the river basin. It makes sense to manage the water resources within a river basin and in a coordinated manner, as the water is often used several times as it moves from the headwaters to the river mouth. The projected impacts in a catchment depend on the sensitivity of the catchment to change in climatic characteristics and on the projected change in the magnitude and seasonal distribution of precipitation (which is a main driver of variability in discharge) along with, temperature, and evapotranspiration. Catchment sensitivity is largely a function of the ratio of runoff to precipitation: the smaller the ratio, the greater the sensitivity. Proportional changes in average annual runoff are typically between one and three times as large as proportional changes in average annual precipitation (WMO, 2009; McCabe and Wolock, 2014; IPCC, 2007). Water availability and its variability are when known is a base for improved Infrastructure design and long term planning.

1.4.1. Classifications of hydrological models

Based on the model structure, there are three types of hydrological models, as given in (Table 1.1). Another classification system, that is based on the spatial description of the watershed processes (spatial structure of catchment processes in rainfall-runoff models), divides the hydrological models into three further categories (Table 1.1).

Table 1.1
Classification of hydrological models based on model structures and spatial description of watershed processes (Sitterson et al., 2017; Islam, 2013); Jajarmizadeh et al., 2012).

Examples	Hydrological models based on model structure		
	Empirical (Black box)	Conceptual (Grey box)	Physical (White box).
	Soil and Water Analysis Tool (SWAT)	Hydrologiska Byrans Vattenavdelning (HBV)	Visualizing Ecosystem Land Management Assessments (VELMA)
	Artificial and Deep Neural Networks	Topography Based Hydrological Model (TOPMODEL)	Variable Infiltration Capacity (VIC)
		National Weather Service River Forecast System (NWSRFS)	European Hydrological System model (MIKE SHE)
		Hydrological Simulation Program - Fortran (HSPF)	Penn State Integrated Hydrologic Model (PIHM)
			Kinematic Runoff And Erosion Model (KINEROS)
	Hydrological models based on spatial description of the watershed processes		
	Lumped	Semi distributed	Fully distributed

Non-linear statistical relationship is used between inputs and outputs in the empirical models, also called as data-driven models. Most empirical models are black box models, which mean a minute detail is known about the internal processes that controls the determination of runoff results (Sitterson et al., 2017). Some of the examples of empirical models are given in (Table 1.1).

Simplified components are connected in the overall hydrological process to interpret runoff processes in conceptual models. For a conceptual idea of the behaviors in a catchment they are based on reservoir storages and simplified equations of the physical hydrological process. Water balance equation is represented in conceptual models with the conversion of rainfall to runoff, evapotranspiration, and groundwater. Models simulate the exchange in water among the atmosphere, hydrological components, and storage reservoirs, based on a water balance equation that is as follows (eq 1),

$$\frac{dS}{dt} = P - ET - Q_s \pm GW \qquad (1) \qquad \text{(Sitterson et al., 2017).}$$

Where $dS/dt$is change in reservoir storage, P is precipitation, ET is evapotranspiration, Q_s is surface runoff and GW is groundwater. Some of the examples of conceptual models aregiven in (Table 1.1).

Physical models, also known as process-based or mechanistic models, are based on the understanding of the physics related to the hydrological processes (Sitterson et al., 2017). In physically based models the detail physical processes can be represented in a deterministic way by depictions of mass, momentum and energy conservation (Islam, 2013). Some of the examples of physical models are given in (Table 1.1).

The spatial processes in runoff models provide a means of representing the catchment for modeling. They are based on input data and how runoff is generated and routed over the catchment. In a lumped model the spatial variability of watershed characteristics are ignored, while in a distributed model the spatial variability of vegetation, soil, topography, etc are taken into account and is processed by grid cells. While semi-distributed models reflect some spatial variability, they also take spatial variability into consideration at smaller scales than lumped models, but do not calculate runoff at every grid cell (Islam, 2013; Sitterson et al., 2017).

1.4.2. The Hydrologiska Byrans Vattenavdelning (HBV) model

The Hydrologiska Byrans Vattenavdelning (HBV) light model can be classified as a semi-distributed conceptual model (rainfall-runoff model) of catchment hydrology. This model is based on conceptual representations of the physical processes of the water flow lumped over the entire catchment area. It can reproduce historical daily discharge with an acceptable accuracy (Abebe and Kebede, 2017).

It depends on the daily rainfall, mean daily air temperature, long-term monthly mean potential evapotranspiration, and daily discharge to be used as input data. This is also considered as its advantage over other physically based hydrological models which are used to simulate the daily stream flow at a basin outlet. (Al-Safi and Sarukkalige, 2017; Vormoor et al., 2017; Zhao, 2015; Dicam and Szolgay, 2010).

The HBV model was developed at the Swedish Meteorological and Hydrological Institute (SMHI), where its development started in the 1970s. It is named after the Water Balance Department (which is Hydrologiska Byrans Vattenavdelning in Swedish language) of the SMHI, and is abbreviated as HBV). The original purpose of this hydrological model was to forecast the inflow to hydropower stations, but over the years it had been used for various applications due to its development, such as, for hydrological impacts of projected climate change, flood forecasting (Lawrence et al., 2009). During the last 20 years the HBV model has become widely used for runoff simulations in Sweden as well as 30 other countries and regions in modified versions.

The HBV light (which is being implemented in the present study) was developed at the Uppsala University in 1993. HBV light is programmed in visual basic, and in 2009/10 the code was re-written for the migration from visual basic 6 to visual basic.NET by Marc Vis. A latest version (4.0.0.22)of the HBV light that is used in this study was developed at the University of Zurich, Department of Geography, Switzerland and.

The basic equations are in accordance with the SMHI-version HBV-6, two main changes in light version is the inclusion of warming up period and the elimination of restriction for MAXBAS (which is parameter of the HBV-light that describes the length of triangular weighting function values) which were only integers in HBV-6.The conceptual models, are frequently used for catchment hydrology studies and can contribute to a better understanding of hydrological variables and their interactions in a quantitative way (Eregnu, 2019; Seibert and Vis, 2012; Seibert, 2005; Report, 1999).

The philosophy behind the relative simplicity of the HBV model relies mostly on the ideas lined out by Nash and Sutcliffe among others, who saw the risk that increasing computer capacities may result in too complex model formulations, unless the significance of model components is carefully checked (Bergström, 1992).

1.4.3. General circulation models and regional climate models

A Global Climate Model or General Circulation Model (GCM) is a mathematical model of the general circulation of the earth's atmosphere or oceans. The GCM sare used for number of applications that includes climate change projections, seasonal weather forecasting and scientific research that provide assistance towards the improved understanding of the atmosphere and oceans behaviors (Rosanna and David, 2014). For the same emissions scenario, different GCMs produce contrasting geographical patterns of change, primarily with respect to precipitation, which is considered as the most important driver for freshwater resources (IPCC, 2007).

A Regional Climate Model (RCM) is run over a narrow part of the earth's surface by using the GCM data for input at the lateral boundaries. Because the RCM is run at higher resolutions than the GCM, it could characterize the projected climate changes more accurately than global models for localized areas (Rosanna and David, 2014).

For regional assessments of hydrological impacts of climate change, the use of the GCM output is used as well Breach et al., (2016). In most of the hydrological projection studies, downscaled precipitation and temperature from the GCMs have been used to drive the hydrological models as described in the Fifth Assessment Report (AR5) Xu and Luo, (2015).

1.5. Representative concentration pathways (RCPs) and climate scenarios

The Representative Concentration Pathways (RCPs) are the latest generation of the GHGs emission scenarios that provide input to climate models. In climate research, emissions scenarios are used to explore how much humans could contribute to future climate change due to uncertainties in factors such as population growth, economic development, and development of new technologies. The scenarios are not used to predict future, but to explore both the scientific and real world implications of various plausible futures. Scientists insert the GHG Concentrations, land use, land cover, and pollution changes, to their climate models to calculate effect of human activities on the climate system (Bjørnæs, 2013).

A climate projection is usually a statement about the likelihood that something will happen several decades to centuries in the future if certain influential conditions develop. Scenarios however, are not projections or predictions, but rather representation of alternative, possible ways in which the future may reveal. The additional energy that the earth system takes due to the enhanced greenhouse effect is the radiative forcing, expressed as $w/m^{2.}$ It can also be defined as the difference in the balance of energy that enters the atmosphere and the amount that is returned to space compared to the pre-industrial situation. Total radiative forcing is determined by both positive forcing from greenhouse gases and negative forcing from aerosols. The dominant factor by far is the

positive forcing from Carbon Dioxide (CO_2). Global temperature rises as the radiative forcing increases. However, the precise relationship between these factors is not fully known (Bjørnæs, 2013).

The rate of climate change is characterized by the four RCPs (Arnell and Lloyd-Hughes, 2014), which are the RCP 8.5, the RCP 6.0, the RCP 4.5 and the RCP 2.6, the last is also referred to as RCP3-PD. The number refers to forcings and PD to Peak and Decline. For each category of emissions, an RCP contains a set of starting values and the estimated emissions up to 2100. The name "Representative Concentration Pathways" was chosen to emphasize the rationale behind their use. The RCPs are referred to as pathways in order to emphasize that their primary purpose is to provide time-dependent projections of the atmospheric GHG concentrations. In addition, the term pathway is meant to emphasize that it is not only a specific long-term concentration or radiative forcing outcome, such as a stabilization level that is of interest but also the trajectory that is taken over time to reach that outcome. They are representative in that they are one of several different scenarios that have similar radiative forcing and emissions characteristics (Wayne, 2013). All the four RCPs are explained below:

RCP 8.5 – High emissions, this RCP is consistent with a future with no policy changes to reduce emissions. It was developed by the International Institute for Applied System Analysis (IIASA) in Austria and is characterized by increasing GHG emissions that lead to high greenhouse gas concentrations over time

RCP 6.0 – Intermediate emissions, this RCP is developed by the National Institute for Environmental Studies (NIES) in Japan. Radiative forcing is stabilized shortly after year 2100, which is consistent with the application of a range of technologies and strategies for reducing greenhouse gas emissions

RCP 4.5 – Intermediate emissions, this RCP is developed by the Pacific Northwest National Laboratory (PNNL) in the United States (US). Here radiative forcing is stabilized shortly after year 2100, consistent with a future with relatively ambitious emissions reductions

RCP 2.6 – Low emissions, this RCP is developed by Planbureau voor de Leefomgeving (PBL) Netherlands Environmental Assessment Agency. Here radiative forcing reaches 3.1 w/m^2 before it returns to 2.6 w/m^2 by 2100. In order to reach such forcing levels, ambitious GHG emissions reductions would be required over time (Bjørnæs, 2013).

1.6. Global hydrological implications of climate changes

Changes in climate and related changes in hydrological systems owe their existence to emission of the Greenhouse Gases (GHGs). Climate change inevitably causes changes in the hydrological cycle, and change the spatial and temporal distribution of water resources. Climate change may have the marked influence on volume of water and can alter the availability of water resources. An enormous challenge to water management has emerged over the past few centuries, because of climate change and its effects on hydrological systems.

More consideration should be given to the effects of climate change on the distribution of rainfall, and runoff, besides the wide exposure to relationship between increased global temperatures and greenhouse gas induced warming. Along with the changes in temperature and precipitation, evapotranspiration has also been decreased since 1960. Climate change has a strong impact on freshwater resources, which are vulnerable already, and likely changes in streamflow, seasonality and amount of water flow from river systems are significant consequences of climate warming.

A wide variety of trends in stream-flows have been detected and attributed, for example, South and East Europe, U.S. Pacific Northwest, Southern Atlantic-Gulf regions, and Yellow river in China have observed decreased in streamflow, while Northern Europe, Mississippi basin in North America, and Yangtze river in China has shown an increase in the stream-flows. Out of 200 top rivers of the World, 45 showed decreased streamflow and 19 showed an increased trend. The detected stream-flows are consistent with precipitation and temperature changes since 1950. Seven percent of the global population is expected to be exposed to decreased renewable water resources for each degree of global warming. Semiarid and arid areas are particularly exposed to these threats.

These effects of climate change are with respect to both mean states and variability (e.g., water availability as well as floods and droughts). Increases in temperature and sea level, local changes of precipitation, and changes in the variability of these quantities are the major cause of observed and projected impacts of climate change on freshwater systems and their management (Jones, 2011; IPCC, 2001; IPCC, 2010; Gunasekara et al., 2014; Dingding et al., 2012; WMO, 2009; Aguilera and Murillo, 2009; Hoegh-Guldberg et al., 2018; IPCC, 2007; Hoff, 2009).

1.7. Regional hydrological implications of climate changes

At least 14 major international river watersheds exist in Asia, temporal and spatial distribution of water is expected to be highly vulnerable due to anticipated climate change. Across different regions of Asia, availability of water varies widely, from 77,000 m^3/ year per capita to less than 1,000 m^3/year per capita. Water availability is expected to rise in some areas of Asia, and reduction is projected for other areas.

Higher runoff is projected over Asia because of enhanced hydrological cycle and an increase in area-averaged annual rainfall. There is very considerable uncertainty in the magnitude and direction of projected precipitation, specifically in south Asia. Over 2 billion people living in different countries are currently experiencing high water stress. One hundred and eighty five to nine hundred and eighty one million people are expected to suffer from increased water stress by the mid of the twenty first century in Asia. (IPCC, 2007; Harasawa et al., 2007; United Nations, 2019).

1.7.1. Water resources situation in Pakistan

An increase in annual and seasonal precipitation in the past thirty to fifty years has been observed in Pakistan, although large differences between regions and seasons exist. Water availability per person is low and decreasing in Pakistan, the population of the country will be 309 million by mid of 21st century and it could lead to reduced water availability, and Pakistan ranked as among the most water stressed in the world and expected to be classified as "water scarce" in the coming years (UNDP, 2017). The main reason for declining water resources is increasing temperature and decreasing precipitation (Jia et al., 2017). Per capita water availability as declined from 5,260 cubic meters per year in 1951 to around 1,000 cubic meters in 2016. This quantity is likely to further drop to about 860 cubic meters by 2025 The situation calls for rapid development and management of the country's water resources on a war footing (N.W. Policy, 2018).

The water resources will continue to vary under climate change, urbanization, over population, industrialization, economic growth. Potential changes in agricultural practices and water requirements are expected to increase by 2050 (Ali et al., 2017; UNDP, 2017). Water use in rural and urban areas of Pakistan is 45 and 120 liter per capita per day. Over ninety percent of total annual water available in the country issued for agriculture (Ali et al., 2017). A 15 percent increase in agriculture water requirement is expected by 2050 (UNDP, 2017).

The vulnerability of Pakistan's water sector to the impacts of climate change. Identification of gaps and recommendations for action, is a research project of the Ministry of Climate Change and the United Nation Development Program that addresses the need of climate change impact studies. One of the major component of this project is to how water flow levels in the Indus river basin (Soan is its tributary) may or may not change in the future (UNDP, 2017).

A limited number of studies have been conducted that assess future changes in water flow in the Indus Basin, both in the short and longer term.The current density in the Upper Indus Basin represents one gauge for precipitation measurement per 5,000 square kilometers, which falls short of the one gauge per 250 square kilometers recommended by the World Meteorological Organization (UNDP, 2017).

According to UNDP. (2017), national climate change policy of Pakistan also acknowledge that Pakistan does not have a comprehensive evaluation of how changing climatic conditions are or could adversely affect its critical water resources.

Within the context of this situation discussed above, the assessment of climate change impact on future water resources is inevitable over the whole country, from the future projections of discharge it would be made clear that whether water abundant or water stressed, or no change conditions are expected in the future under climate change. That could be helpful (in either case, water abundance, water stressed or no change) in the development and implementation of policies regarding management of freshwater resources.

1.7.2. Current hydro-climatic state of Soan River Basin (SRB)

Discharge in the Sihala sub-catchment (SSC) varied from 69 mm up to 450 mm a year, while lower discharge could be seen in the Kanisub-catchment (KSC) varying between 38 mm and 285 mm a year as depicted in (Fig.1.1). Yearly precipitation in the SSC ranged between 268 mm to 815 mm a year. However the annual precipitation ranged between 246 mm to 579 mm a year in the KSC as shown in (Fig. 1.2). Evapotranspiration along-with the precipitation, plays a key role in non-glacierized catchments because the runoff is strongly influenced by these two climatic variables.

Evapotranspiration in the SSC was found out to be in the range of 21 mm to 107 mm a year, while in the KSC evapotranspiration lied between59 mm to 110 mm a year (Table 1.2). It makes it obvious that the evapotranspiration is much more significant in the KSC as compared to the SSC, and it may attribute to the low flows of the KSC. When it comes to temperatures, as seen in the (Fig.

1.2), the SSC has annual temperatures in the range of8 °C and12 °C, while higher temperatures are seen in the KSC ranging between 11 °C to 14 °C.

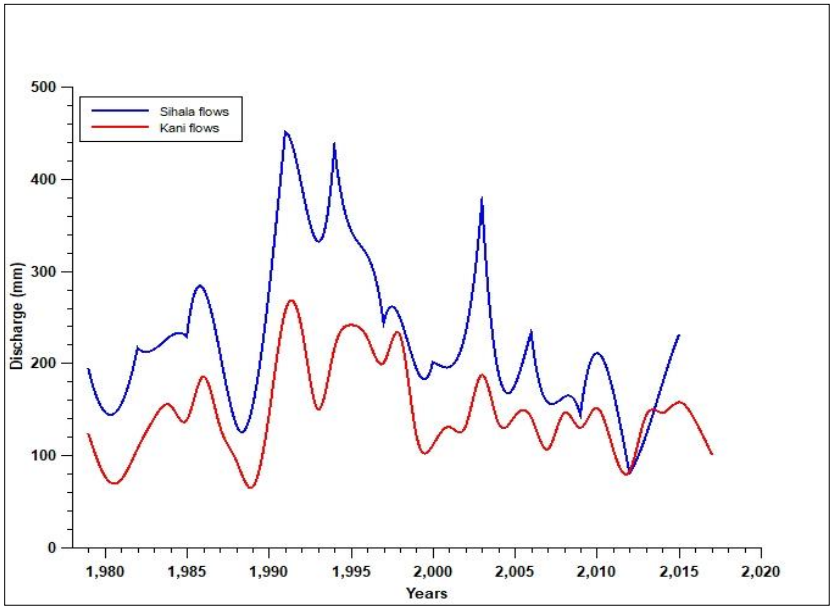

Figure 1.1
Yearly discharge of the Sihala and Kani sub-catchments for the observed time period (1979-2017): Data source (ECMWF)

Table 1.2
Yearly evapotranspiration of the Sihala and Kani sub-catchments for the observed time period (1979-2017): Data source (ECMWF)

Yearly Evapotranspiration (mm)		
Years	Sihala Sub-catchment	Kani Sub-catchment
1979	90	103
1980	95	106
1981	94	107
1982	90	102
1983	84	59
1984	82	73
1985	80	97
1986	88	100
1987	93	105
1988	99	110
1989	91	103
1990	95	108
1991	91	103
1992	91	103
1993	91	104
1994	94	105
1995	89	102
1996	88	101
1997	82	98
1998	90	103
1999	107	107
2000	90	103
2001	92	104
2002	94	106
2003	90	103
2004	95	108
2005	90	101
2006	98	109

2007	93	105
2008	93	104
2009	94	105
2010	93	105
2011	92	105
2012	91	103
2013	92	104
2014	88	101
2015	94	106
2016	97	110
2017	99	110

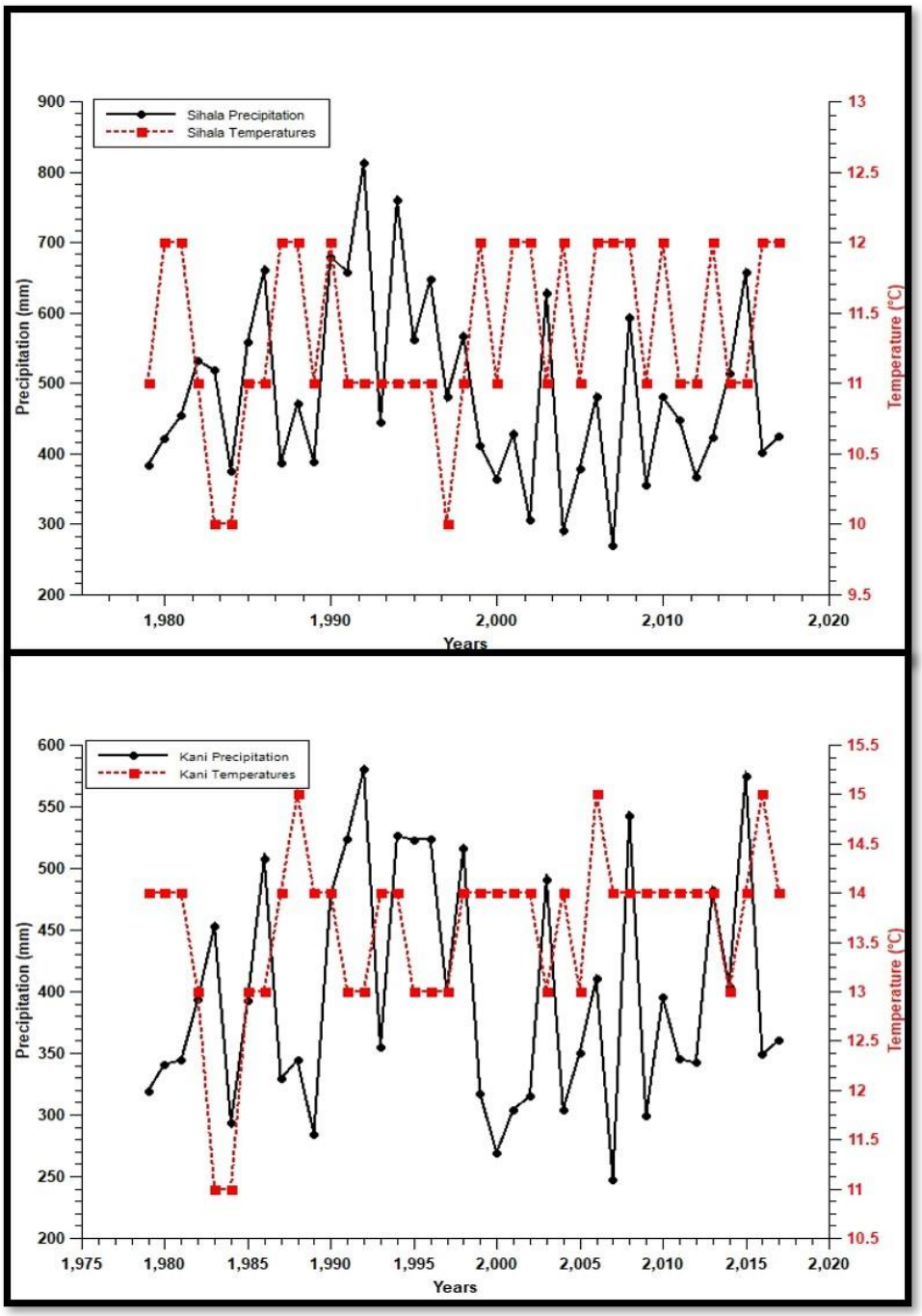

Figure 1.2

Yearly Precipitation and Temperature of the Sihala and Kani sub-catchments for the observed time period (1979-2017): Data source (ECMWF)

As seen in (Fig. 1.3), months with high flows and low flows are crucial for water balance estimation, and as it could be seen in the figure that high flows occurs in March, April, August and September in the SSC while March, August and September are high flow months in the KSC. Low flows months are January, June, November, December in the SSC while January, May, June, November, and December in the KSC.

Maximum precipitation in the SSC and the KSC could be seen in July with an average of 87 mm and 70 mm respectively as depicted in (Fig. 1.4), making July the wettest month, consequently producing highest flows in the upcoming month of August with an average of 44 mm and 31 mm as shown in (Fig. 1.3). The highest evapotranspiration is also observed in the month of July with an average of 11.8 mm 12.26 mm for the SSC and the KSC respectively, but the magnitude of increase in precipitation outweighs the increase in evapotranspiration, hence resulting in high flows. Minimum mean precipitation of 13 mm occurs in October making it the driest month in the SSC, while in the KSC the lowest rainfall occurs in the months of May and November with an average of 13 mm as illustrated in (Fig. 1.4), resulting in the low flows of 8 mm in the same month as presented in (Fig. 1.3).

Mean monthly evapotranspiration valued 7 mm a month with lowest of 1.29 mm in January in the SSC, while mean monthly evapotranspiration valued 8.6 mm a month with lowest of 2.8 mm in January in the KSC. The coldest month is of January in both sub-catchments with an average temperature of 1.12°C in the SSC and 2.52°C in the KSC, and the warmest month is of July with a mean temperature of 21.3°C and 23.6°C in the SSC and the KSC respectively as shown in (Fig. 1.4).

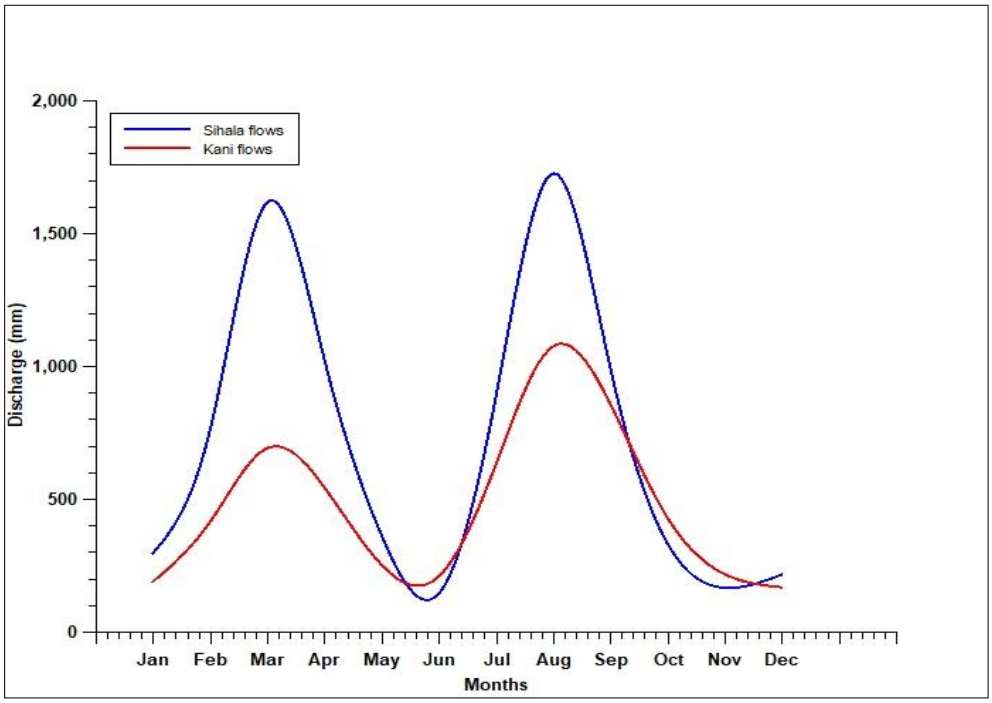

Figure 1.3

Monthly discharge of the Sihala and Kani sub-catchments for the observed time period (1979-2017): Data source (ECMWF)

Table 1.3

Monthly evapotranspiration of the Sihala and Kani sub-catchments for the observed time period (1979-2017): Data source (ECMWF)

Evapotranspiration (mm)		
Months	Sihala Sub-catchment	Kani sub-catchment
Jan	1.29	2.8
Feb	3.18	4.75
Mar	6.13	7.46
Apr	8.92	9.65
May	10.30	11.26
Jun	11.6	12.29
Jul	11.8	12.35
Aug	11.71	12.23
Sep	10.68	11.41

Oct	8.23	9.3
Nov	5.51	6.84
Dec	2.47	3.83

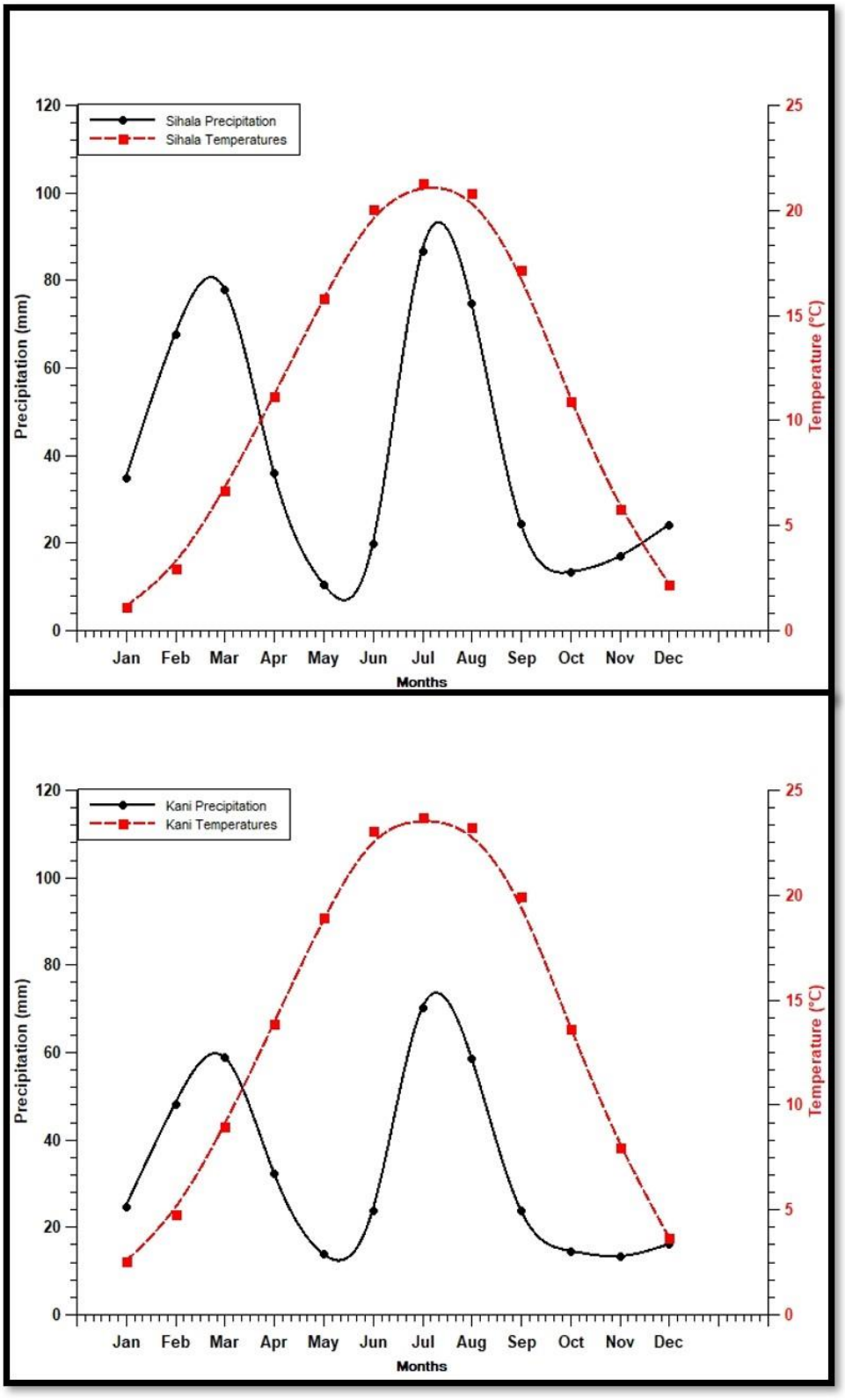

Figure 1.4

Monthly precipitation and temperatures of Sihala and Kani sub-catchments for the observed time period (1979-2017): Data source (ECMWF)

As depicted in (Fig. 1.5) highest flows could be seen in Spring (MAM i.e. March-April-May) season with an average of 77 mm, however highest flows in the KSC are seen in the Summers with an average of 16 mm. Low flows could be seen in the winter season with an average of 32 mm and 6.19 mm in the SSC and the KSC respectively.

Wettest season is summer (JJA i.e. June-July-August) with a mean precipitation of 181 mm in the SSC and 50 mm in the KSC and Autumn (SON i.e. September-October-November) is the driest season with a mean precipitation of 54 mm and 17 mm in the SSC and the KSC respectively as shown in (Fig. 1.6). Summer has the highest average temperature of about 20.73°C in the SSC and 23.3°C in the KSC. Winters (DJF i.e. December-January-February) has the lowest temperature of about 2°C and 3.6 °C in the SSC and the KSC respectively as illustrated in (Fig. 1.7). In summers, maximum evapotranspiration occurs with an average of 11.7 mm and 12.29 mm, while minimum evapotranspiration occurs in winters averaging 2.31 mm and 3.76 mm in the SSC and the KSC respectively (table 1.4).

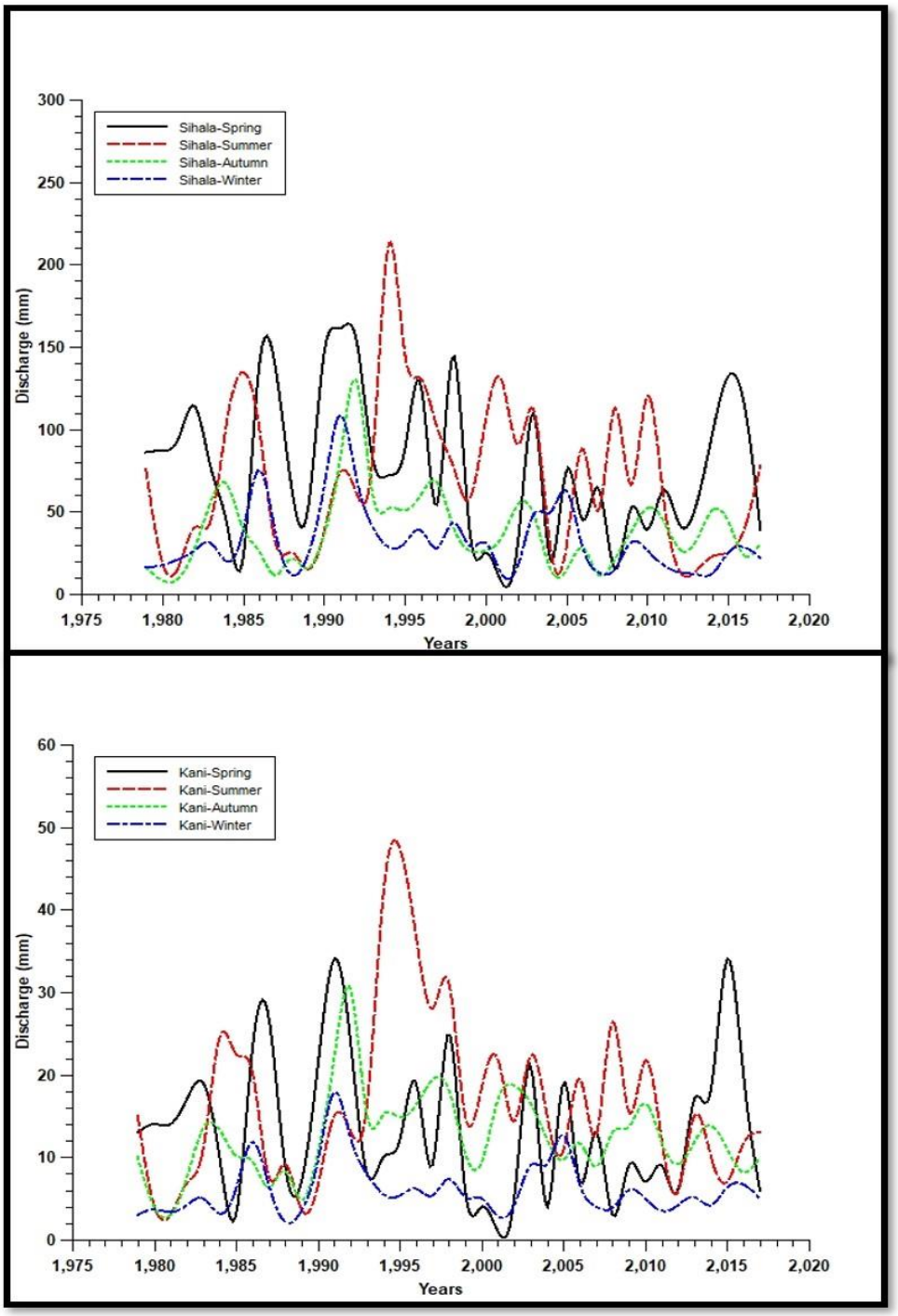

Figure 1.5
Seasonal discharge of Sihala and Kani sub-catchments for the observed time period (1979-2017): Data source (ECMWF)

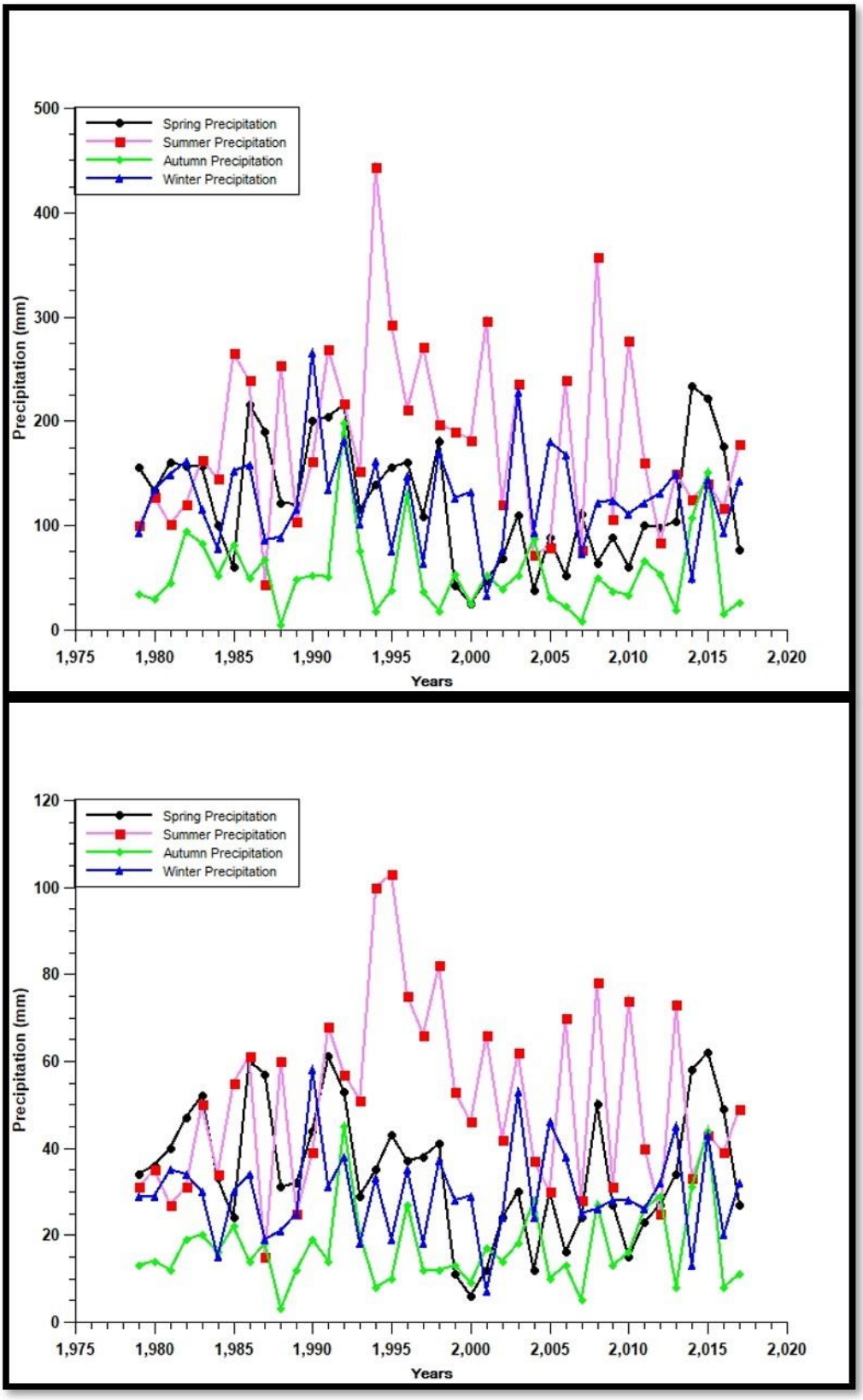

Figure 1.6

Seasonal Precipitation of the Sihala and Kani sub-catchments for the observed time period (1979-2017): Data source (ECMWF)

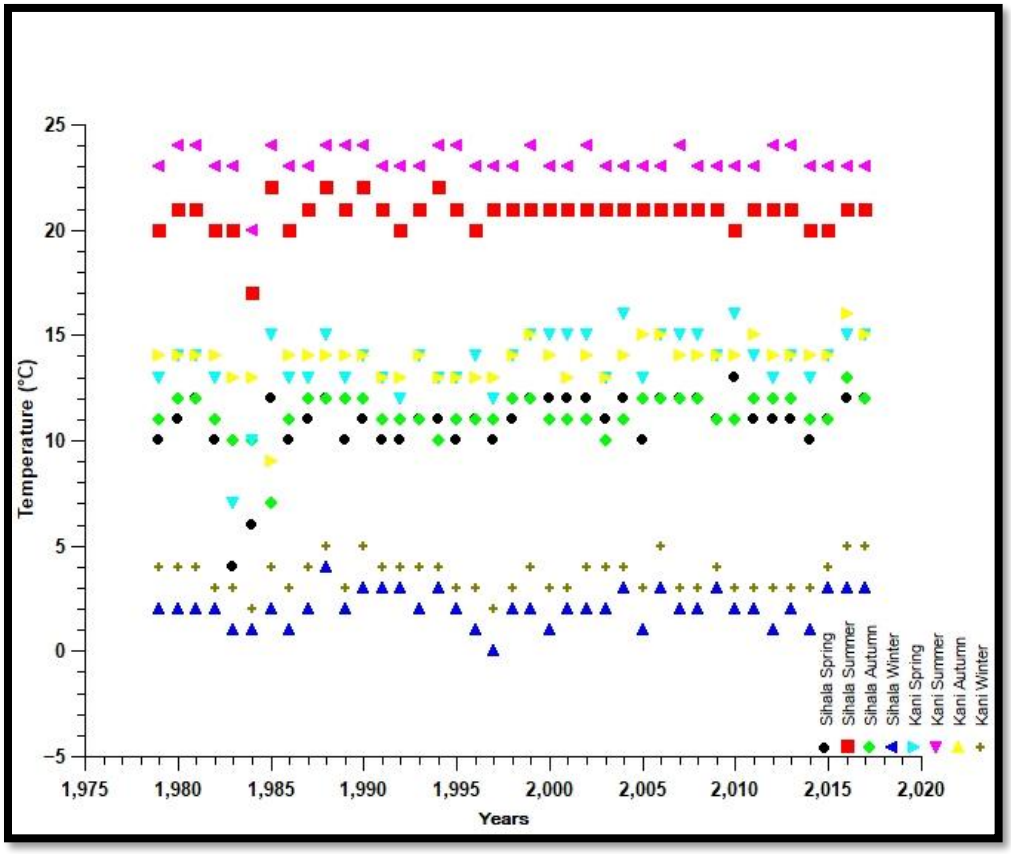

Figure 1.7

Seasonal temperatures of the Sihala and Kani sub-catchments for the observed time period (1979-2017): Data source (ECMWF)

Table 1.4

Seasonal evapotranspiration of the Sihala and Kani sub-catchments for the observed time period (1979-2017): Data source (ECMWF)

	Seasonal Evapotranspiration (mm)							
	Sihala Sub-catchment				Kani Sub-catchment			
Years	Spring	Summer	Autumn	Winter	Spring	Summer	Autumn	Winter
1979	24	35	25	6	27	37	28	11
1980	25	36	26	8	28	37	29	12
1981	26	35	25	8	29	37	28	13
1982	24	35	25	7	27	37	28	11
1983	22	35	23	5	26	36	27	10
1984	26	30	23	3	28	33	27	8
1985	27	36	12	6	30	38	18	12
1986	23	35	25	4	27	37	28	9
1987	25	35	26	7	28	37	28	12
1988	26	36	25	12	30	37	28	15
1989	24	35	25	7	27	37	28	11
1990	24	36	25	11	28	38	28	14
1991	24	35	23	9	27	37	27	12
1992	24	35	24	9	27	37	27	13
1993	25	35	25	7	28	37	28	12

1994	25	36	24	9	28	37	27	13
1995	24	36	24	5	27	37	27	10
1996	26	35	23	4	29	37	27	9
1997	24	35	24	0	27	37	27	7
1998	24	35	24	6	28	37	27	11
1999	39	36	26	7	30	37	29	12
2000	25	35	25	5	29	37	28	10
2001	26	35	24	6	30	37	27	10
2002	26	35	25	8	30	37	28	12
2003	25	35	23	7	28	37	27	12
2004	27	35	24	9	30	37	28	13
2005	24	35	26	5	27	37	28	9
2006	26	35	26	11	29	37	29	14
2007	25	36	26	6	29	37	28	11
2008	27	35	25	6	30	37	28	10
2009	25	35	24	10	28	37	28	13
2010	28	35	24	6	31	37	28	11
2011	25	35	26	6	29	37	30	11
2012	25	36	25	5	28	37	28	9
2013	25	36	25	7	28	37	28	11
2014	24	35	24	5	27	37	28	10
2015	25	35	25	9	28	37	28	13
2016	26	35	27	9	29	37	30	14
2017	27	35	26	11	29	37	29	15

1.7.3. Ranked annual flow of Sihala and Kani sub catchments

The ranked annual flow of both the sub-catchments of the SRB is illustrated in (Table 1.5). It could be seen from the table 1.5 that the year 1991 has the highest flows for the SSC and the KSC among all thirty nine years of observed period, while 2004 stood the year with least flows in the SSC, and 1989 was the year of lowest flows in the KSC. Mean annual flow was 218 mm per year in the SSC and 146 mm per year in the KSC.

The ranked annual flow of both sub-catchments of the SRB provides us with the fact that the number of years in which the flow was below the annual average was twenty four years, while fifteen years were those where the flows were greater than the annual average for the SSC. The annual water resources situation of the SSC shows the sixty two percent of the times the flows have been below the annual average, while a thirty eight percent of the times the flows have surpassed the annual average. This gives an indication that in the observed period the flows have been more on the minimal side rather than being on the higher sides most of the time.

Similarly, in the KSC, twenty three years showed flows less than the annual average and sixteen years suggested flows to be higher than annual average. The situation of the river flows in the KSC is not different from the SSC, as the ranked annual flows indicates that fifty nine percent of the years have shown flows to be less than the annual average, while forty one percent have shown that the flows have been more than the annual average.

Table 1.5

Ranked annual flow of Sihala and Kani sub catchments

	Discharge (mm)		
Years	Sihala Sub-catchment	Years	Kani Sub-catchment
1991	451	1991	286
1992	449	1998	283
1994	435	1992	261
1986	378	1995	243

1996	376	1996	238
2003	376	1994	238
1998	320	2003	228
2010	286	1986	221
1995	277	2010	175
1990	269	2008	172
1984	246	1997	170
1997	243	1984	168
2006	233	2015	168
2015	230	2013	166
1985	229	2006	155
1982	217	2005	148
2008	211	2001	143
2000	201	1983	140
1983	197	2016	139
2001	194	2014	136
1993	194	1990	132
1979	194	1979	123
2016	193	1987	117
2014	186	1985	110
1987	181	2000	109
2005	174	1982	109
2011	172	2004	109
2017	169	2009	108
2002	160	2002	104
2009	144	1988	103
1988	134	2011	102
1981	130	2017	102
1999	122	1993	100
1980	119	1999	85
2013	107	2007	78
1989	82	1980	69
2007	81	1981	66
2012	81	2012	57
2004	70	1989	39

1.8. Previous Studies

Hydrological modelling and estimation of future flow projections in different river basins of Pakistan has been carried out, especially in the Upper Indus Basin (UIB). Different hydrological model have been implemented in these studies for example, the University of British Columbia Watershed Model (UBCWM) has been appliedin the Hunza, the Astore, the Siran, the Jhelum and the Kabul river basins by Saeed et al. (2009). Future projections of the study that was conducted in the Mangla basin (that is in northeastern Pakistan) by Babur et al. (2016), suggests an increase in mean annual flow under the RCP 4.5 and the RCP 8.5 emission scenarios, while on seasonal basis the study projects a noticeable increase in winter and spring, while a decrease in flows has been projected for the summer and autumn seasons.

Similarly, the HBV has been employed by (Akhtar, 2008) in the UIB, and according to the study, a reduction of 8 % by 2030 in mean discharge of the UIB is projected. However in another study by (Hasson, 2016) progressing towards the later decades of the twenty first century, a steady increase is projected in the UIB. Another hydrological model that has been used extensively in the estimation and projections of flows in the mountainous catchments, the Snowmelt Runoff Model (SRM) has been implemented by (Tahir, 2011) in Tarbela dam (a reservoir in the UIB), and summer flows have been projected to be twice as they are now by 2075.

The Hydrological Modeling System (HEC-HMS) along with the RCP emission scenarios was employed by Javed, (2018) over the Soan river basin and the flows were projected to increase in the twenty first century. Another study that was conducted by Koike et

al, (2015) over the Soan river basin used the Water and Energy Budget Distributed Hydrological Model (WEB-DHM) along with A1B emission scenario proposed in the Special Report on Emission Scenarios (SRES), and the upsurge in flows of the Soan river basin was also projected.

The (HEC-HMS) has also been implemented in the Jhelum river basin by Mahmood and Jia, (2016), and the mean annual flow has been projected to increase by 10 – 15 % towards the end of century. On seasonal basis, summer flows have shown a decrease, while autumn, spring, and winter flows have projected an increase in the flows. Moreover low and median flows were projected to increase, but a decline in high flow was detected in the future.

1.9. Rationale for study

All these studies mentioned in the above section have been conducted mostly in the UIB, different hydrological modelling approaches have been adopted, along with different future climate scenarios and the projections of different climate models. However, the results have not shown a strict consistency towards one direction (either decreasing or increasing) and also the magnitude of change is not unidirectional throughout the UIB, rather different river basins (catchments) have shown unique hydrological behaviors under changing climate. Somo hydrological modelling of the hydrological characteristics and water resources of different catchments is necessary to further the knowledge base of future freshwater resources under changing climate scenarios in Pakistan.

1.10. Research objectives

The current research aims:

- to perform the hydrological modeling of the Soan River Basin (SRB)by using the HBV-light hydrological model.
- to calibrate and validate the hydrological model for two sub-catchments of the SRB in order to simulate the future flows.
- to assess possible climate changes in the SRB
- to assess possible changes in freshwater resources of the two sub-catchments of the SRB i.e. (Sihala and Kani) on the basis of climate projections under the RCP 4.5 and RCP 8.5 emission scenarios for the time period 2018-2047.

2. MATERIALS AND METHODS

2.1. Study area description

Pakistan lies in the subtropical arid zone and most of the country is subjected to a semi-arid climate. The geography of Pakistan is a profound blend of landscapes varying from plains to deserts, forests, hills and plateaus and ranging from coastal areas of the Arabian Sea in the south to the mountains of the Karakoram Range in the north (FAO, 2012).

The Soan River is located in Potowar region of Pakistan, between 71°45 and 73°35 east longitudes and 32°45 to 33°55 north latitude. It is considered as the major hydrological unit of potowar. Soan riveris the tributary of the mighty Indus river and is a perennial river. Soan River has multiple tributaries namely Ling, Korang, Lai Nulla, and Ghabir River etc. Soan river basin comprised of Rawalpindi division (Rawalpindi, Attock, Chakwal), and Islamabad. Twomajor reservoirs to meet the domestic need of water for millions of citizens of Islamabad and Rawalpindi are the Simly and Rawal dams, constructed on Soan River and its tributary korang river, respectively. Potwar is semi–arid region, except Murree, which is in humid zone. Climatic condition of the SRB is considered as the Subtropical Triple Season Moderate Climate Zone. (FAO, 2012; FAO, 2011; Nazeer et al., 2016; Adnan et al., 2009; Shahid et al., 2017; Ashfaq et al., 2014; WAPDA, 2001).

The headwaters of the Soan River lies in Patriata (Murree) and confluence of the Soan river with the Indus River could be seen near Mianwali, not far from the proposed site of Kalabagh dam. The SRB has been divided into two sub catchments for this study namely the Sihala sub-catchment (SSC) and theKani sub-catchment (KSC) as shown in (Fig 2.1). Both sub-catchments of the SRB are non-glacierized and precipitation is the major inflow to the basin. The total area of SRB is 11253 km^2. The SSC has an area of 882 km^2 and the KSC has an area of 10371 km^2.

2.2. Topographical characteristics of Soan River basin

Land cover map of the SRB is illustrated in (Fig 2.2). Topography of (Sub-watershed 1) i.e. the SSC is relatively different from the topography of (Sub-watershed 2) i.e. the KSC. The SSC starts from 442 m and extends up to 2261 m, while the KSC has an elevation range of 206-2261m. In the KSC not much of the variations in altitudes could be seen, it is primarily a flat terrain area. Sihala sub-catchment on the other hand has diverse topography, as it ranges from the high mountains on the northern side and a relatively flat surface towards the southern side. None of the sub–catchments are glacier dominant. The vegetation ranges from Shrubs in the southern part to the coniferous forests in the Northern part.

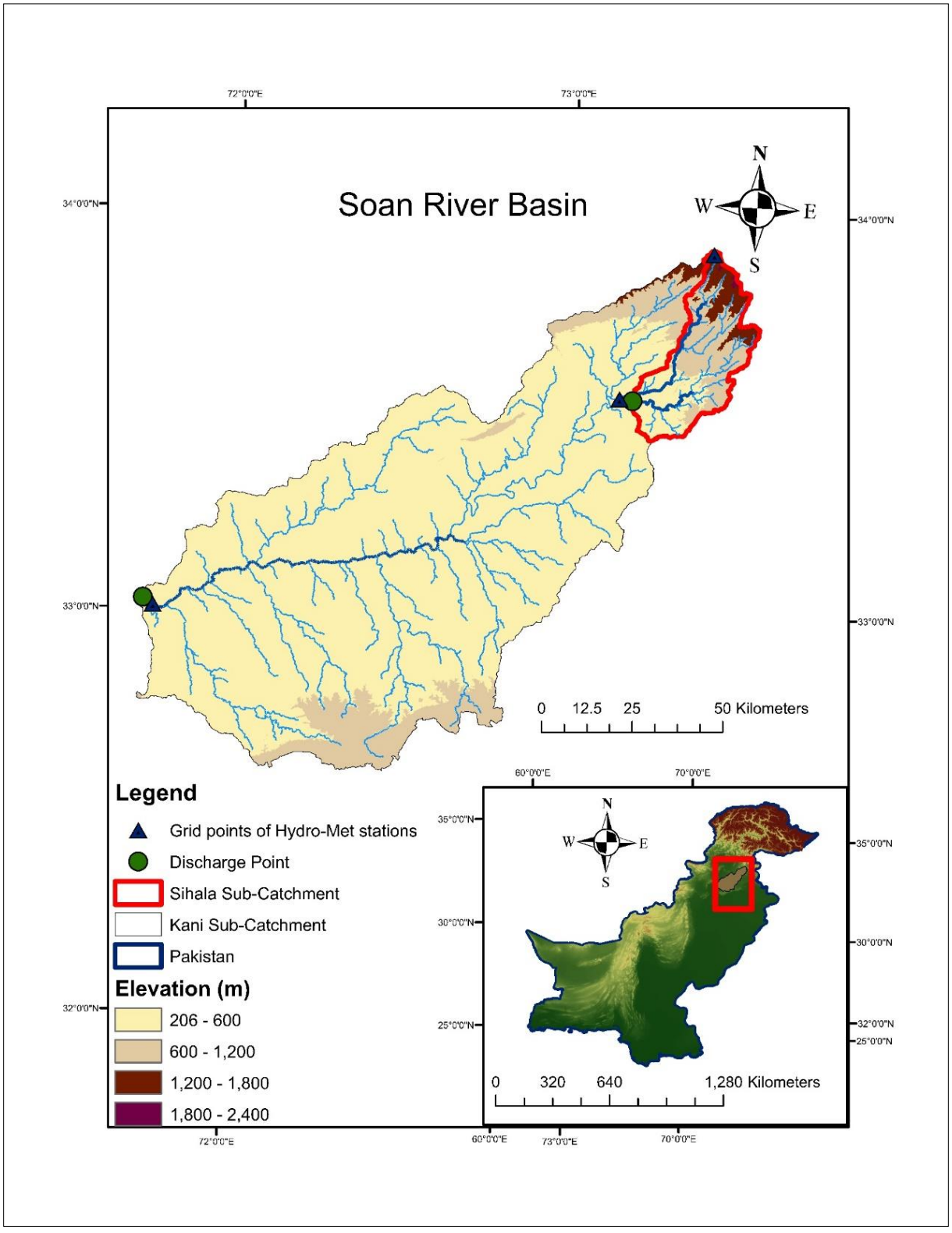

Figure 2.1
Map of the Soan river basin

The land cover ranges from evergreen needle leaf forests, evergreen broadleaf forests to croplands, grasslands, and savannas, as well as, the urban and built up units in the Sihala sub-catchment. Due to the diversity of topographical features, the meteorological characteristics of the SSC are also more diverse than KSC. The KSC is dominated by grasslands, croplands, while open shrub-lands dominates the sub-catchment in the south.

The slope and aspect map of the SSC and the KSC could be seen in appendix i.

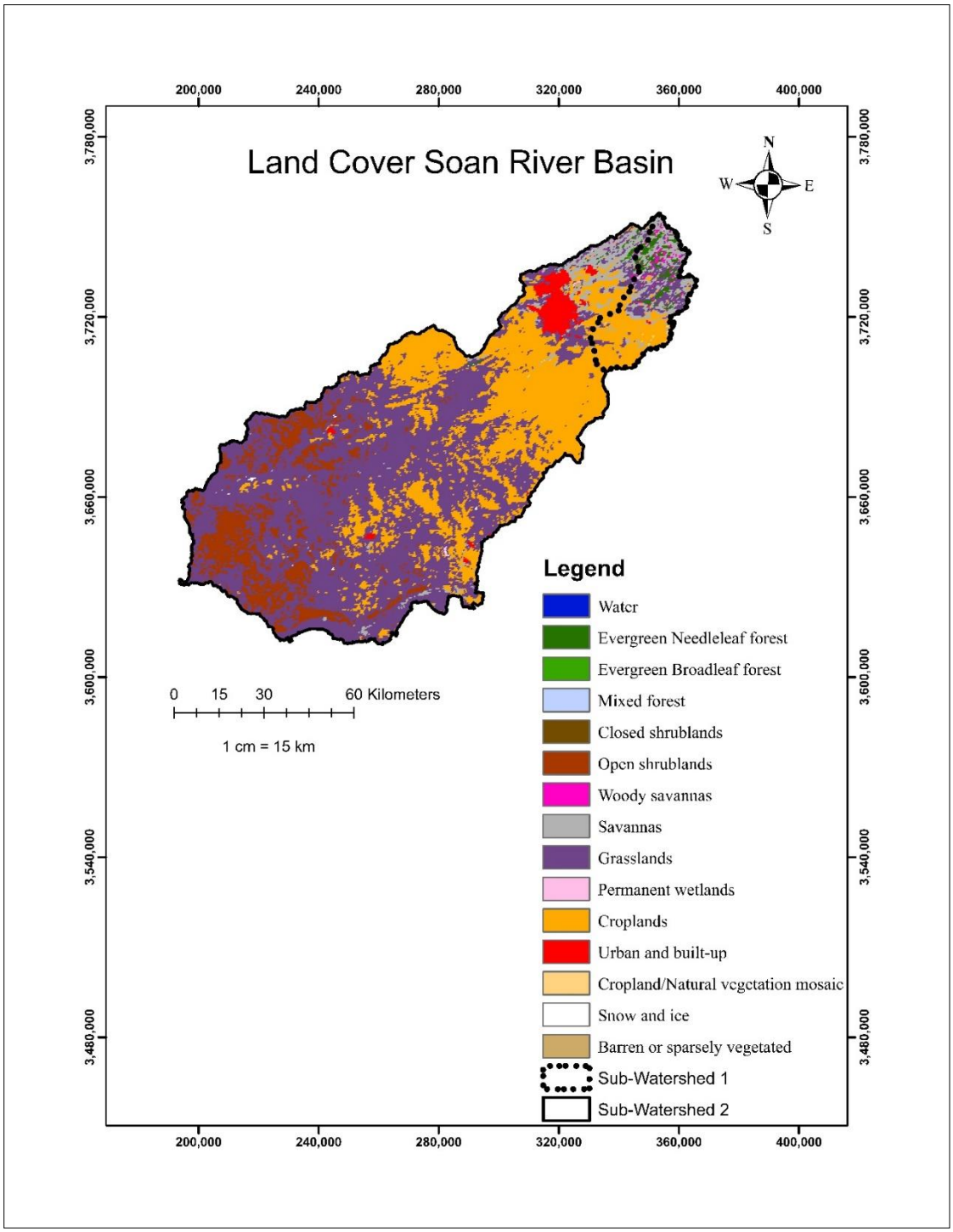

Figure 2.2
Land cover map of Soan river Basin

2.3. Data collection and description

The observed hydrological and climatological data and the projected climatic data for future is explained in the following section.

2.3.1. Climate reanalysis dataset

A climate reanalysis gives a numerical description of the recent climate, produced by combining models with observations. It contains estimates of atmospheric parameters such as air temperature, pressure and wind at different altitudes, and surface parameters such as rainfall, soil moisture content, and sea-surface temperature. The estimates are produced for all locations on

earth, and they span a long time period that can extend back by decades or more (https://www.ecmwf.int/en/research/climate-reanalysis).

2.3.2. Hydro-climatological data

Climatological and hydrological data have been acquired from ERA-Interim archive at ECMWF (European Centre for Medium Range Weather Forecast). "Era-Interim is the latest global atmospheric reanalysis, produced by ECMWF" (Dee et al., 2011). At first ERA-Interim ran from 1989-2017, later in 2011 it was extended for the period of 1979-1989. The spatial resolution of the data set is approximately 79 km on 60 vertical levels from the surface up to 0.1 hectopascal (hPa) at the top. The analysis at 12 Universal Time Coordinated (UTC) involves observations between 03 UTC and 15 UTC. The monthly averages produced for each of the four main synoptic hours (00, 06, 12, and 18 UTC) are referred to as synoptic monthly means (Berrisford and Dee, 2011). Various studies have used Era-Interim datasets (Gevorgyan and Melkonyan, 2015; Kotsias and Lolis, 2018; Wu et al., 2018;).

Daily precipitation (total precipitation), daily surface air temperature (2 meter), and synoptic monthly means of incoming solar radiation (j/m^2) are acquired for the time period 1979-2017. Description of observed hydrological and climatological data can be found in (table 2.1). While high resolution projections of the Swedish Meteorological and Hydrological Institute Rossby Centre Regional Atmospheric Model (SMHI RCA4) under the framework of Coordinated Regional Downscaling Experiment–South Asia (CORDEX–SA), statistically downscaled at 13 km resolution forced with the RCP 4.5 and the RCP 8.5 emission scenarios for the time period 2018-2047 have been used. The description of future projected data can be seen in (table 2.2).

Table 2.1

Description of observed Hydrological and climatological data. (Data source: ECMWF)

Hydro-Climatic parameters	Units	Source	Temporal resolution	Time domain	Grid size	Grid point location	Lat/Lon
Precipitation	m	ECMWF	Daily	1979-2017	0.125° * 0.125°	Murree	33.87/73.45
Temperature	K					Sihala	33.64/73.28
Incoming solar radiation	(j/m^2)		Monthly			Kani	33.02/71.72
Evapotranspiration	mm						
Surface runoff	m		Daily				

Table 2.2

Description of Projected (future) data. (Data source: SMHI RCA4)

Climatological Parameters	Units	Source	Temporal resolution	Time domain	Grid size	Grid point location	Lat/Lon
Precipitation	mm	SMHI RCA4	Daily	2018-2047	0.13°	Murree	33.87/73.45
Temperature (min, max)	°C					Sihala Kani	33.64/73.28 33.02/71.72

2.3.3. Topography and land cover data

The DEM (Digital Elevation Model) of 90m resolution from Shuttle Radar Topography Mission (SRTM) is acquired and the Soan River basin along with its sub-basins is delineated using this DEM in ArcMap (ArcGIS). Hydrology tool that can be found under the Spatial analyst tools has been used to extract the River Basin.

The MODIS Land Cover Type product (MCD12Q1) provides with the land cover suites with a spatial resolution of 500m. Out of five different classification schemes, Land Cover Type 1, that is International Geosphere-Biosphere Programme (IGBP) global

vegetation classification scheme (MODIS User Guide, 2012; Friedl et al., 2010) was adopted in this study. MODIS land-cover products are available in public domain and can be downloaded from https://earthexplorer.usgs.gov/.

The Moderate Resolution Imaging Spectroradiometer (MODIS) Normalized Difference Vegetation Index (NDVI) data product MYD13Q1 is used in this study (Didan, 2015). Normalized Difference Water Index (NDWI) product MODW44 (Carroll et al., 2009)is used in this study to extract water body data (Carroll et al., 2008). These datasets are extracted from the MODIS at 250m spatial resolution and 16 day temporal resolution.

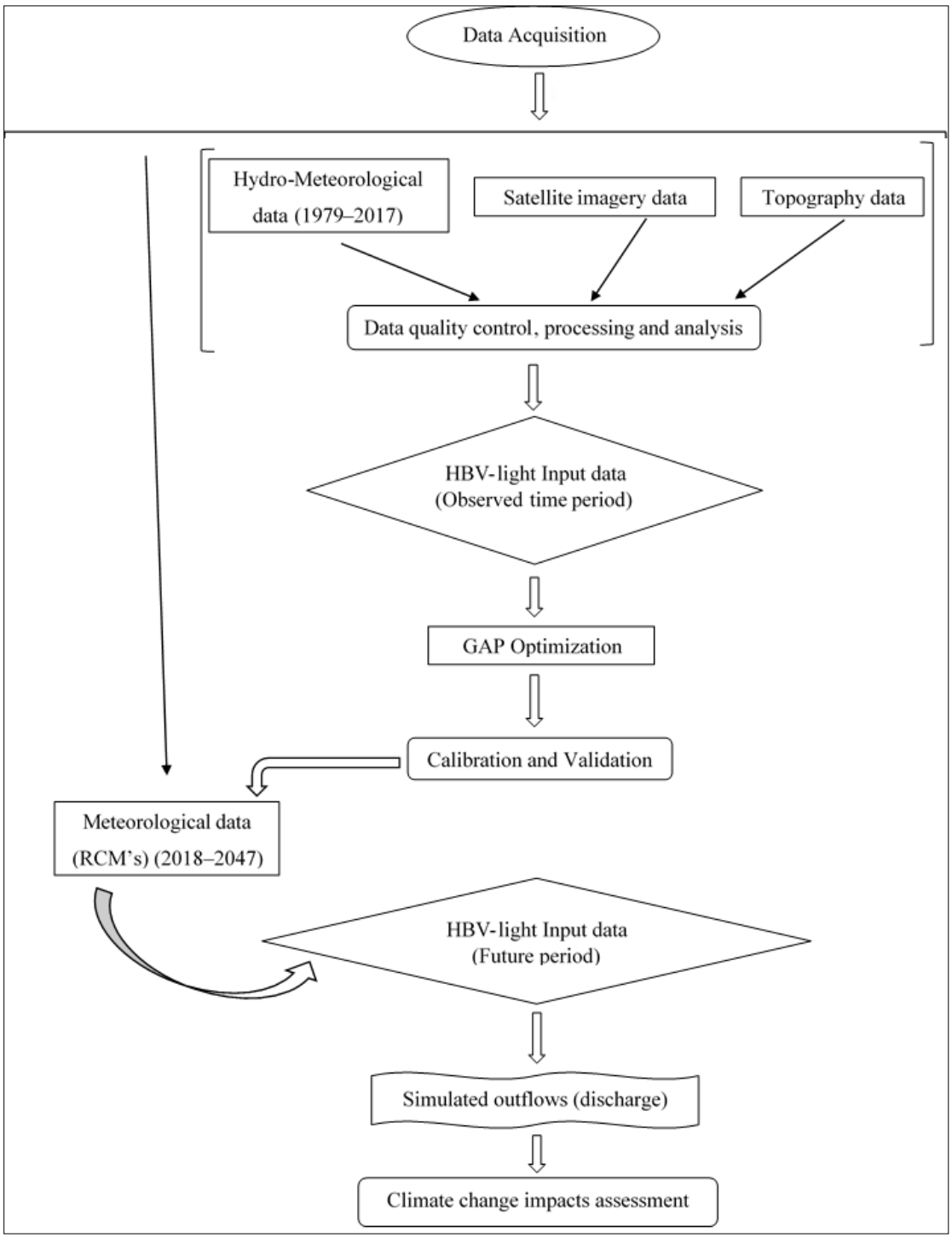

Figure 2.3
An overview of the adopted methodology

2.4. Methodological approach

An overview of the methodology adopted in the present study is presented in (Fig. 2.3). The hydro-meteorological, topographical, and satellite imagery data was acquired, processed and analyzed. After this the input data was s prepared and fed into the HBV-light model. Then the calibration and validation of the model was performed manually in conjunction with Genetic Algorithm to optimize the parameters used for calibration and validation. Afterwards, future climate projection data was induced to the HBV-light and the projected flows were simulated. Finally the climate change impacts assessment on the freshwater resources of the SRB was performed. A more detailed description of the methodology is presented in the paragraphs below.

The DEM (Digital Elevation Model) of 90m resolution from the Shuttle Radar Topography Mission (SRTM) was acquired and the SRB along with its two sub-catchments is delineated using this DEM in ArcMap (ArcGIS).

The hydro-climatological characteristics of the SRB were assessed and analyzed from the data acquired from the European Center for Medium Range Weather Forecast (ECMWF). Hydrology tool that can be found under the Spatial analyst tools has been used to extract the River Basin and its sub-catchments. The MODIS Land Cover Type product (MCD12Q1) with a spatial resolution of 500m was used for land cover classification of the SRB. Both sub-catchments of the SRB are divided into 4 elevation zones with an interval of 600 m each, with an elevation range of 206m up to 2261m for the SSC and 442m up to 2261m for the KSC.

Hydrology tool that can be found under the Spatial analyst tools has been used to extract the River Basin and its sub-catchments. The MODIS Land Cover Type product (MCD12Q1) with a spatial resolution of 500 m is used for land cover classification of the SRB. Both sub-catchments of the SRB are divided into 4 elevation zones with an interval of 600m each, with an elevation range of 206m up to 2261m for the SSC and 442 up to 2261m for the KSC.

Different fractions of vegetation zones are extracted from NDVI and the fraction of area covered with water was assessed using Normalized Difference Water Index (NDWI) from MODIS NDWI data product MODW44). Three vegetation zones were defined, densely vegetated zone, sparsely vegetated zone and Barren land zone. As the aspect variant of the HBV-light is being used in this study so the vegetation zones (three) are assigned with the values of the North, south, and east/west fraction of the total area per elevation zone.

Input files for the HBV-light were prepared, potential evapotranspiration was found out using Turc method. Parameterization and sensitivity analysis were performed and the hydrological model was calibrated and validated. After the calibration and validation the model was induced with the climate projections data of SMHI RCA4 CORDEX-SA and was used to simulate projected flows.

2.5. Input data for HBV-LIGHT

Precipitation, temperature, evapotranspiration, discharge, elevation zones, vegetation zones were used as an input data to drive the hydrological model (HBV-light) is as follows:

Precipitation, Temperature, and Discharge initially have the units meter, Kelvin, and meter respectively. To be used as an input data to the HBV-light model, the units of precipitation, temperature, and discharge have been converted into mm, °C, and mm respectively.

Evapotranspiration that was used as an input to the model was the potential or Reference evapotranspiration. Estimated reference evapotranspiration was found out using Turc method (Shreedhar et al., 2016), this method has different variations (Trajkovic and Stojnic, 2008). "The Turc equation is one of the most accurate empirical equations used to estimate evapotranspiration" (Trajkovic and Kolakovic, 2009). The measurements of mean air temperatures along-with solar radiation (solar radiation was initially in joule per square meter (j/m^2), and was converted to mega joule per square meter (Mj/m^2) are used in the following equation to estimate monthly evapotranspiration, which is as follows eq (2),

$$ET_{\circ} = 0.40\left(\frac{T_{mean}}{T_{mean}+15}\right)(R_s + 50) \quad (2)$$, (Shreedhar et al., 2016)

Where

$ET_{\circ}$= Reference Evapotranspiration (mm/month), R_s = Solar radiation MJ/m^2, and T_{mean} = Average temperature

2.5.1. Elevation and vegetation zones

Both sub basins (Sihala and Kani), are divided into four elevation zones and three vegetation zones. The area and elevations ranges, of elevation zones, and vegetation zones can be seen in appendix ii. Different vegetation zones were found using NDVI (Normalized Difference Vegetation Index) and the fraction of area covered with water was assessed using NDWI (Normalized Difference Water Index). Three vegetation zones were defined, densely vegetated zone, sparsely vegetated zone and Barren land zone. Vegetation zones of the SSC and the KSC are presented in appendix ii.

In this study NDVI values less than 0.2 were considered barren land, water, rocks, 0.2–0.4 moderate vegetation and 0.4–0.8 dense vegetation, these threshold values differ slightly for example Daham et al. (2018) proposed NDVI values of 0 or less for snow, water, clouds, 0.1 or less for barren areas, and 0.3–0.6 for dense vegetation. In another study by Usman et al. (2015) NDVI values for barren areas, rocks, sands, 0.1–0.2 for soils, moderate vegetation 0.2–0.5, and for dense vegetation (forests) values of 0.6–0.9. Values below 0.2 were considered as bare soil and pixels with value above 0.5 were considered fully vegetated by Tang et al. (2015).

Following is a list of input files, and other settings of HBV light model to run the model along with the description.

2.5.2. PTQFILE

PTQ file contains a daily time series of (precipitation (mm), temperature (ºC), and discharge (mm) (Seibert, 2005) for the SSC and the KSC. The values of Sihala sub basin are considered as sub-catchment 1 and the Kani sub basin is the considered as the sub-catchment 2 (outlet sub-catchment).

2.5.3. EVAPFILE

EVAP file contains long term monthly mean values of reference evapotranspiration for both sub basins that have been calculated using Turc method.

2.5.4. TMEAN FILE

TMEAN file contains the long term monthly mean values of the whole basin, this file is optional though.

2.5.5. Catchment properties

PCALT and TCALT are precipitation and temperature gradients. PCALT is change of precipitation with elevation and is given as %/100m, and it generally has values of 10, and TCALT is given in °C/100m with a general values 0.6. Elev of P and elev of T is also given the one value which is the mean value. Mean elevation of lake and area (fraction of the total area of the respective catchment), TT and SFCF which are threshold temperature and snow fall correction factor are assigned with the values for both the sub-catchments separately, and the absolute areas of sub-catchments (two in this study) is also assigned in km^2.

The four elevation zones are assigned with the mean elevation of individual zone. As the aspect variant of model is being used in this study so the vegetation zones (three) have been assigned the values of the North, south, and east/west fraction of the total area per elevation zone, details of which can be seen in appendix ix and x for the SSC and the KSC respectively. The sum area of each sub-catchment should be equal to 1 otherwise further proceeding into running the model will not occur, and number of decimal places while giving the fractional area of each aspect of each vegetation zone should be less so that no error occurs in equating the area to one.

2.6. HBV-light's structure and parameters

The model simulates daily discharge using daily rainfall, temperature and potential evaporation as input. Physical and Process Parameters are two types of parameters, former represents the characteristics of watershed like the area of watershed etc., and later shows the characteristics that are not measurable directly like the depth of surface soil moisture storage, the effective lateral interflow rate, and so on. Parameters of HBV light are shown in (Table. 2.3). Schematics of the HBV light are presented in figure 2.4, which includes the glacier routine of model as well, which is not employed in the present study, but a part of the HBV light.

Precipitation is simulated to be either snow or rain depending on whether the temperature is above or below a threshold temperature, (TT). All precipitation simulated to be snow, i.e. falling when the temperature is below TT, is multiplied by a snowfall correction factor, SFCF. Snowmelt is calculated with the degree-day method. Melt water and rainfall is retained within the snowpack until it exceeds a certain fraction, water holding capacity (CWH), of the water equivalent of the snow. Liquid water within the snowpack refreezes. Rainfall and snowmelt (P) are divided into water filling the soil box and groundwater recharge depending on the relation between water content of the soil box (SM (mm)) and its largest value maximum soil moisture storage (FC (mm)).

Actual evaporation from the soil box equals the potential evaporation if SM/FC is above soil moisture value above which Actual Evapotranspiration (AET) reaches Potential Evapotranspiration (PET) which is (LP) while a linear reduction is used when SM/FC is below LP. Groundwater recharge is added to the upper groundwater box (SUZ (mm)). PERC (mm /day) defines the maximum percolation rate from the upper to the lower groundwater box (SLZ (mm)). Runoff from the groundwater boxes is computed as the sum of two or three linear outflow equations depending on whether SUZ is above a threshold value, UZL (mm), or not .

This runoff is finally transformed by a triangular weighting function defined by the parameter length of triangular weighting function (MAXBAS) to give the simulated runoff (mm/day). If different elevation zones are used, precipitation and temperature changes with elevation are calculated using the two parameters change of precipitation with elevation(PCALT) and change of temperature with elevation(TCALT) (Jan Seibert, 2005).

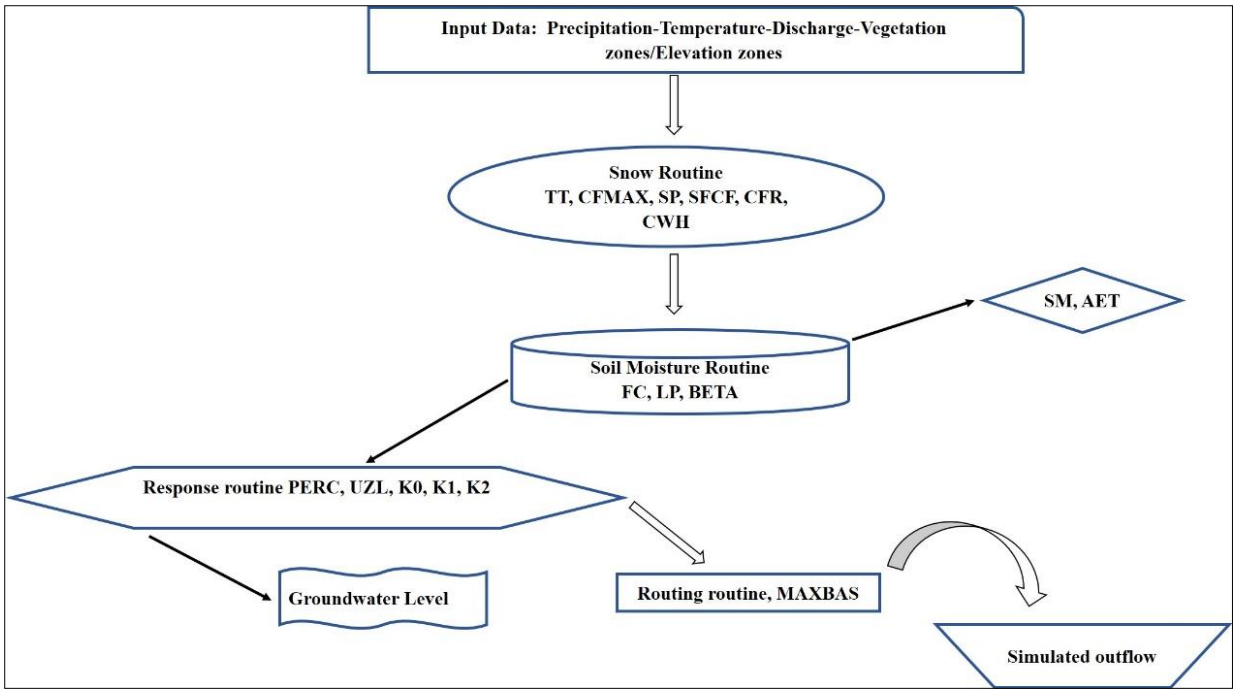

Figure 2.4

Schematics of the HBV-light with different model routines

Table 2.3

HBV light's model setting and parameters of all the four model routines (used in this study) along-with their units and ranges.

Model settings and Routines	Model Parameters with units	Ranges	
		Used Range	Valid Range
Catchment Properties	TT (°C)	-2 – 12	-Infinity – Infinity
	SFCF (-)	0 – 10	0 – Infinity
	PCALT (%/100 m)	5 – 20	-Infinity – Infinity)
	TCALT (%/100 m)	0.4 – 0.8	Infinity – Infinity
	Elevation of P (m)	500	-Infinity – Infinity
	Elevation of T (m)	500	-Infinity – Infinity
Snow Routine	TT (°C)	-2 – 12	- Infinity – Infinity
	CFMAX (mm/day°C)	0 – 2	0 – Infinity
	SP (-)	0 – 5	0 – 1
	SFCF (-)	0 – 2	0 – Infinity
	CFR (-)	0 – 5	0 – Infinity
	CWH (-)	0 – 0.5	0 – Infinity
	CFSlope (-)	0 – 1	0 – Infinity
Soil Moisture	FC (mm)	50 – 600	0 – Infinity
	LP (-)	0 – 1	0 – 1

Routine	BETA (-)	0.1 – 10	0 – Infinity
Response Routine	PERC (mm/d)	0 – 4	0 – Infinity
	UZL (mm)	10 – 75	0 – Infinity
	K0 (1/d)	0 – 0.8	0 – 1
	K1 (1/d)	0 – 0.6	0 – 1
	K2 (1/d)	0.01 – 0.3	0 – 1
Routing Routine	MAXBAS (d)	5 – 20	1– 100
Other	Cet (1/°C)	0 – 0.3	0 – 1

2.7. Parameterization and sensitivity analysis

The determination of contributions of individual inputs to the uncertainty of the model output is referred to as the sensitivity analysis, and execution of sensitivity analysis is precious tool for identification of optimum model parameters (Song et al., 2012; Khatun et al., 2018; Bahremand and Smedt, 2008)

Identification of the parameters that are sensitive to simulated outflow is a vital step before the calibration and validation of a hydrological model (Wijngaard, 2014). HBV light has number of parameters which are adjusted accordingly to reach the maximum objective function which is also the co-efficient of determination; some parameters show more sensitivity than others upon variation. The sensitivity of all the parameters is checked using manual and automated methods (Khatun et al., 2018; Bahremand and Smedt, 2008).

With manual parameterization, over parameterization or unrealistic parameterization could occur. This is the case where the perfect goodness of fit measure could be achieved but some or most of the interpretation of parameter values is beyond justification. So, to cope with this uncertainty manual calibration should be done along with the automatic calibration. Manual method of hit and trial has been used in conjunction with the automatic calibration (explained below in section 2.9.1). Parameters of Snow routine (TT, CFMAX, SFCF,), Soil moisture routine (FC, LP, BETA), response routine (PERC, UZL, K0, K1, K2) and routing routine (MAXBAS, CET), along with gradient parameters (PCALT and TCALT) of Sihala sub-catchment were selected for sensitivity analysis. Remaining parameters (SP, CFR, CWH, and CFSLOPE) were found out to be relatively insensitive to the model output.

2.8. Calibration and validation of HBV-light

Calibration is the estimation of the model parameters that enables the model to closely match the behavior of the real system. Calibration is an inescapable stage of any model before its application. It is the mechanism of approximating model parameter values to enable a hydrologic model to closely match observations like discharge. Conventionally manual trial and error method had been used to calibrate the rainfall-runoff models, such as the HBV, where parameterization is done to attain an adequate fit between observed and simulated time series (Dicam and Szolgay, 2010).

The calibration can be performed by two different alternatives: the manual calibration and automatic calibration.. The technique used for assigning parameter values, which must precede so any practical application, is called parameters (or models) calibration, model parameterization, parameters (or model) optimization. Usually, the calibration is carried out by searching the parameter values that maximize the reliability of the simulation made by the model. Monte-Carlo random sampling is time and resource consuming (Kumarasamy and Belmont, 2018; Lawrence et al., 2009; Dicam and Szolgay, 2010).

The record of daily discharge data that inhibit various hydrological characteristics is essential for calibration and validation of the HBV model with better accuracy. In hydrological models, to simulate larger future datasets longer calibration periods are advantageous (Al-Safi and Sarukkalige, 2017). Model verification is a very important step because it gives information about the real functioning of the model unlike the calibration. After testing the model, it is appropriate to repeat the calibration using the full range of available data, in order to maximize the consistency of the database used to estimate parameter values (Dicam and Szolgay, 2010).

1984-2008 has been selected as the time period for calibration for both the SSC and the KSC, while 2009-2017 has been designated for validation. Five years from 1979-1983 have been used for warming up period. Automatic calibration of the model can be performed by the following ways;

2.8.1. Automatic calibration

Automatic calibration can be done in various ways, but the following are adopted most of the times.

MONTE CARLO RUNS

In the Monte Carlo simulation if there are more than one sub catchment (as in this case there are two sub catchments) the weightage for different objective functions for different sub catchments could be used. Objective function is the goodness of fit measure and if there is only sub catchment then only one objective function (e.g. Reff) could be used with its weight as 1 or multiple objective functions could be used but sum of the weights of the entire objective functions should have to be 1.

If there are multiple sub catchments but one doesn't want to split the weight of the objective function (whether one or multiple are selected) into all the sub catchments then the objective function of the outlet could be used.

If the objective function of the outlet is used the results that Monte Carlo simulation will generate will be stored in the Results folder of as Multi.txt (in case, there is only one sub catchment) or Multi_SubCatchment_i.txt (in case there are more sub catchments, with i the index of the sub catchment). The parameters generated in this file will be effective for calibrating multiple sub catchments, but if the weight of the objective function has been divided into multiple sub catchments like the weight 1 is given to sub catchment 1 and 0 to other sub catchment then the resulted parameters would only be effective for calibration of sub catchment 1, they won't give the same model efficiency for other sub catchments as for the sub catchment 1.

If multiple vegetation zones are selected, parameter value for each zone must be chosen, whether it should compute by random only (R) or whether its value should be equal for all zones (=), increase from zone 1 to 3 (<), or decrease (>) (Seibert, 2005).

GAP OPTIMIZATION

With the genetic calibration algorithm, optimized parameter sets are found by an evolution of parameter sets using selection and recombination. No of population is especially important for this type of automatic calibration. The more the no of populations are selected the more combination sets of different parameters are considered by the model while running, hence increasing the probability of higher goodness of fit measures and the fitness of each set is evaluated against an objective function.

In the population settings along with the no of population there is another option of parameter sets that is equally important in reaching the goal of perfect goodness of fit. So if the parameter set is set to 50 and no of population is 2 and the no of model runs elected is 1000, so for each population the model will run 50 parameter sets and try to determine the perfect goodness of fit measure. So in this case no of model runs will be 2000 (50 for each population until it reaches 1000).

2.9. Model evaluation criteria

Different criteria can be used to assess the fit of simulated runoff to observed runoff:
Visual inspection of plots with Qsim and Qobs
Accumulated difference
Statistical criteria

Lumped metrics such as Nash Sutcliffe Efficiency (NSE), is used to evaluate the model performance (efficiency) and in the HBV-light model, the NSE is also refers to as R_{eff} (Model efficiency), and is described by the following eq (3),

$$1-\frac{\sum(Q_{obs}-Q_{sim})^2}{\sum(Q_{obs}-\overline{Q_{obs}})^2} \quad (3) \quad \text{(Seibert, 2005)}$$

Another objective function that is used to measure the efficiency of the HBV-light is the coefficient of determination (R^2), which is represented by following eq (4),

$$\frac{(\sum(Q_{obs}-\overline{Q_{obs}})(Q_{sim}-\overline{Q_{sim}}))^2}{\sum(Q_{obs}-\overline{Q_{obs}})^2\sum(Q_{sim}-\overline{Q_{sim}})^2} \quad (4) \quad \text{(Seibert, 2005)}$$

Mean difference is another way of determining the model efficiency, it tells the difference in mm/year between the observed flow and the simulated flows. It is described by following eq (5),

$$\frac{\sum(Q_{obs}-Q_{sim})}{n}\times 365 \quad (5) \quad \text{(Seibert, 2005)}$$

Alongside the above mentioned criterion, another criteria that stands out in evaluation the efficiency of mode is the Volume error is described in eq (6) as,

$1-\frac{|\sum(Q_{obs}-Q_{sim})|}{\sum Q_{obs}}$ (6) (Seibert, 2005)

Where Q_{obs} is the observed flow and Q_{sim} is the simulated flow.

These metrics provide an averaged measure of error and are intentionally biased towards large magnitude flows. (NSE) is slightly better than (R^2) for many model applications as it is sensitive to the observed and model simulated means and variances (Kumarasamy and Belmont, 2018). HBV light has other goodness of fit measures as well beside (NSE) and (R^2), like mean difference and volume error and the weightage for other goodness of fit measures is also incorporated.

2.10. Water balance components

Water balance components determine the inflow to the basin, processes occurring within the basin e.g. (evaporation), and finally the outflow of the river basin. The precipitation, evaporation, and discharge are the major water balance components, and the detailed water balance equation is as follows eq (7),

$P - E - Q = \frac{d}{dt}[SP + SM + UZ + LZ + lakes]$ (7) (Hirshfleld, 2010; WMO, 2009)

Where PisPrecipitation,$E$is Evaporation, Q is Discharge, SP is Snowpack, SM is Soil moisture, UZ is upper groundwater zone, LZ is lower groundwater zone, $lakes$ is lake volume.

3. RESULTS AND DISCUSSION

3.1. Parameterization and sensitivity analysis

Results for sensitivity and parameterization analysis are presented in this section. Two types of parameters; Catchment parameters (which include the response routine parameters, routing routine parameters and gradient parameters) and vegetation zone parameters (which includes snow routine parameters and soil moisture routine parameters) are there, and the results are described in the following sequence;

Catchment parameters
Vegetation zone parameters

3.2. Catchment parameters

Results of sensitivity analysis of the routines and parameters of catchment properties of the HBV-light are described in section below.

3.2.1 Runoff response routine parameters

Lower PERC values consequently produce higher flows , the reason because it happened is with lower values of percolation, the high precipitation that occurs in spring and summer season converts into surface runoff, as a result contribution from the upper groundwater box to the lower groundwater storage is not significant, and the high values of discharge could be observed. Similarly, high PERC values tend to contribute more towards groundwater storage and less discharge is observed as seen in (Fig. 3.1).

In figure 3.1, it could be oberved that the lower values of UZL showed high discharge values, while high values of UZL has produced low flows. It means that when UZL which is a threshold parameter, has low values, insignificant contribution to the lower groundwater zone from the upper zone is observed, which produce high flows. Similarly, the high UZL value has produced low flows, because higher UZL flows result in high amounts of groundwater storage.

As seen in figure 3.1, high values of recession co-efficient (K0) produced highy flows and lower values of K0 resulted in low flows, this happened because the with high K0 values the groundwater zone has low potential of water storage, hence upper zone has more amount, resulting in high flows. Low values on K0, on the other hand tend to make lower groundwater zone to have more water and low values of model output flows could be observed. The recession co-efficient K1 also shows the same beaviour in figure 3.1, but the higher values of K1 has yielded higher amounts of flows than in the case of K0, the behaviour of recession co-efficient (K2) also falls in line with the trend of K0, and K1, but in the case of large values of K2, the highly simulated flows are lower than K0 and K1. Another thing in the case of K2 could be seen in figure 3.1, is that, upon smaller values the water in the groundwater box is a bit higher than K0 and K1.

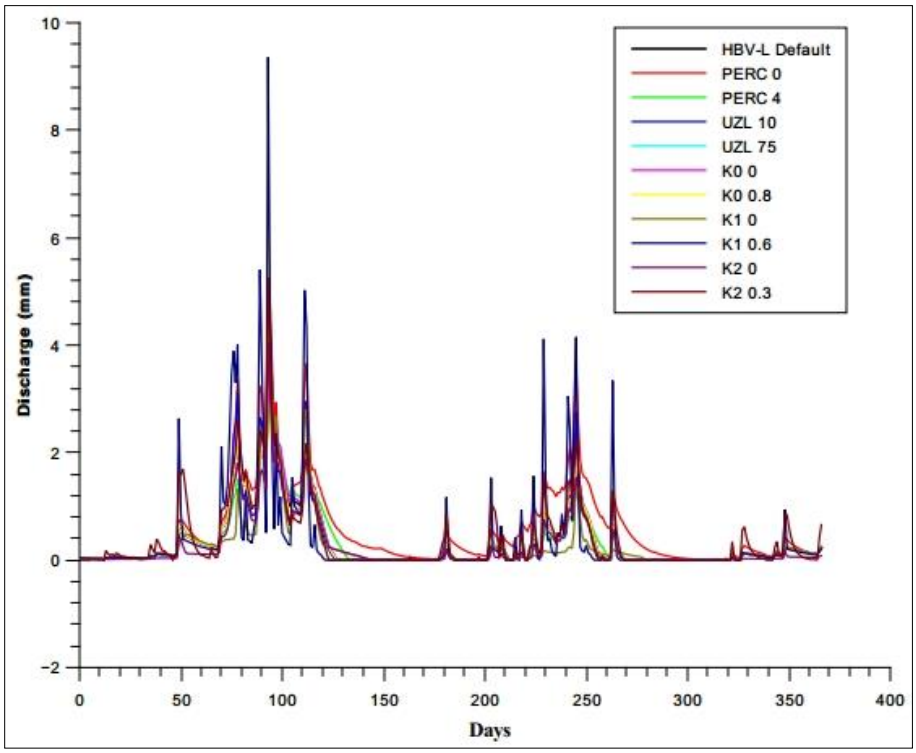

Figure 3.1
Sensitivity analysis of the parameters of response routine of HBV- light model

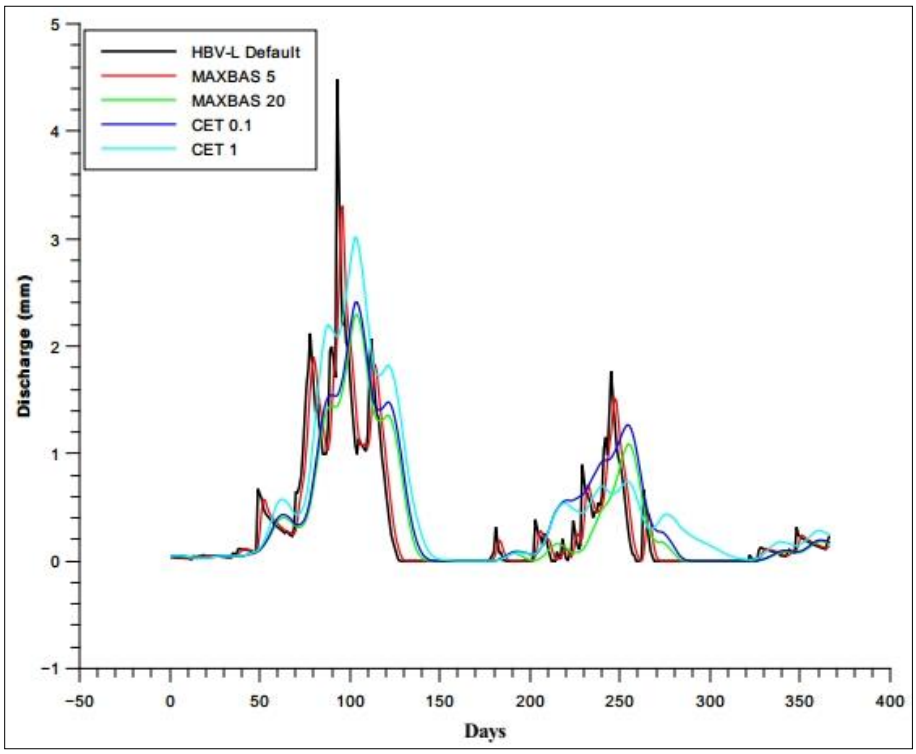

Figure 3.2
Sensitivity analysis of the parameters of routing routine of HBV- light model

3.2.2. Routing routine parameters

With the lower values of MAXBAS, as illustrated in figure 3.2, it could be seen that the peaks have occurred earlier and are considerably high. With high values of MAXBAS, triangulated flow has been given more time and peaks have become gentle and their occurrence has shifted forward. As long as CET is concerned, it could be seen in the figure 3.2, that the large values of CET have produced high flows in the early spring season and small values of CET have produced the high flows, but these high flows are smaller than the one produced with large CET values.

3.2.3. Gradient parameters

Larger values of PCALT as indicated in figure 3.3, have shown a significant increase in the amount of simulated discharge in the spring and summer season, which means with increasing PCALT the precipitaton is increasing and hence producing high flows, while the smaller values of PCALT tends to refer to decrease precipitation and have shown the lower flows consequently.

Sensitivity analysis of TCALT has been shown in (Fig. 3.3). Although througout the year, larger and smaller values of TCALT have resulted in an increase in the discharge in the spring season and a slight increase in late summer season as well. Both small and large values of TCALT have somehow resulted in the similar simulated discharge with an exception, which is the large values of TCALT have shown a slightly increased simulated discharge in the late spring season, while the lower values of TCALT have shown negligible dishcarge in the same time period.

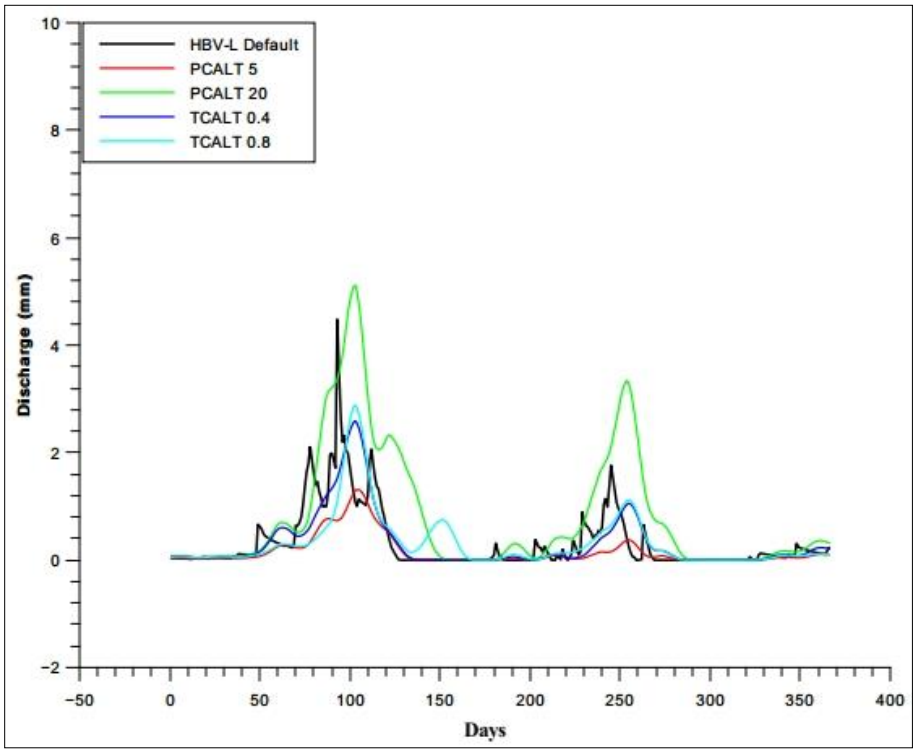

Figure 3.3

Sensitivity analysis of the gradient parameters of HBV- light model

3.3. Vegetation zone parameters

3.3.1. Snow routine parameters

TT is one of the most important parameters, variation in the values of TT could have a drastic effect of model output (simulated discharge). In this case, the higher values of TT have led to an increased amount of simulated discharge, as observed in figure 3.4. It could be seen that, in the later spring season, and the summer seasons the discharge is comprehensively high, as compared with the lower values of TT in the same time of year. In the later summer and early autumn seasons, high flows associated with large values of TT could be observed, an interesting thing that happened is that, even the low values of TT have produced a reasonable flow in this time of the year, although when higher TT values shows higher flows in late spring and mid-summer, the flows simulated with lower TT value were negligible. In the late winter and early spring seasons, higher flows associated with lower values of TT could be observed, while higher TT values have yield negligible flows.

As shown in figure 3.4, lower CFMAX values showed higher discharge in early spring, and mid to late summer, while the high values of CFMAX showed an increase in the simulated discharge in the said period, but these increased flows are not even near to those which were produced as a result of low CFMAX values, generally high CFMAX values have produced low flows and lower CFMAX values have shown high flows.

Generaly, lower SFCF values have produced negligible amount of simulated discharge, as depicted in figure 3.4, large values of SFCF have led to an increase simulated dishcarge in the early to mid spring season, and throughout the rest of the time flows have been negligible as well with the large values of SFCF.

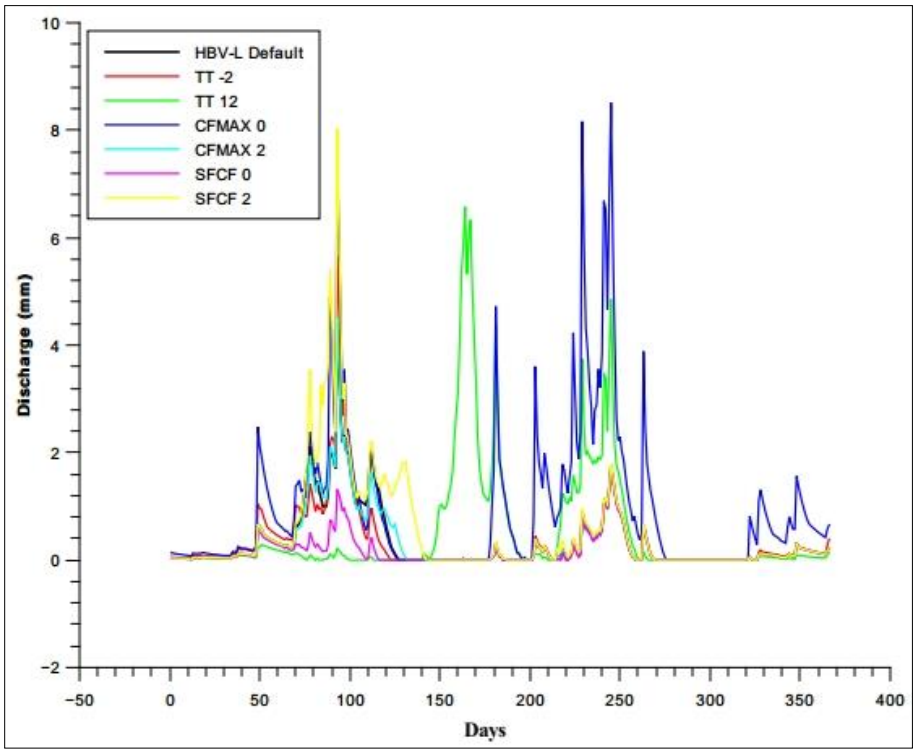

Figure 3.4
Sensitivity analysis of the parameters of snow routine of HBV- light model

3.3.2. Soil moisture routine parameters

Smaller FC values are associated with the high flows, as it could be seen in the figure 3.5, the reason being the less FC means the water stored in the soil water zone is not much, hence not a significant amount of evapotranspiration could take place, consequently producing high flows. Peaks of simulated discharge could be observed in the early spring time with lower FC values, while for the same period of time the large values of FC have also shown an increased discharge, but this discharge is not as much as the one produced with smaller FC values. Generally, higher FC values have shown a very reduced amount of simulated discharge throughout the year.

Large values of LP have resulted in the enhanced simulated discharge in the early spring season, which is not very evident for the rest of the year.As illustratted in figure 3.5, small values of LP on the other hand have shown the same behaviour, except the high flows produced with smaller LP values were not as high as produced with the larger values of LP.

It could be observed in figure 3.5, the smaller BETA values have shown an increased amount of simulated discharge in the early spring, and mid to late summer, meanwhile the higher values of BETA have produced negligible amount of simulated discharge in the said period and generally throughout the year as well.

3.4. Parameterization, calibration and validation

Results obtained during parameterization process, and use for calibration and validation of the HBV-light are presented in the following section.

3.4.1. Optimum parameters for calibration

The optimum parameters of three different vegetation zones, lake properties and four model routines that were found out during parameterization, and used for the calibration and validation of HBV-light model for the Sihala and Kani sub-catchments are shown in (Table 3.1).

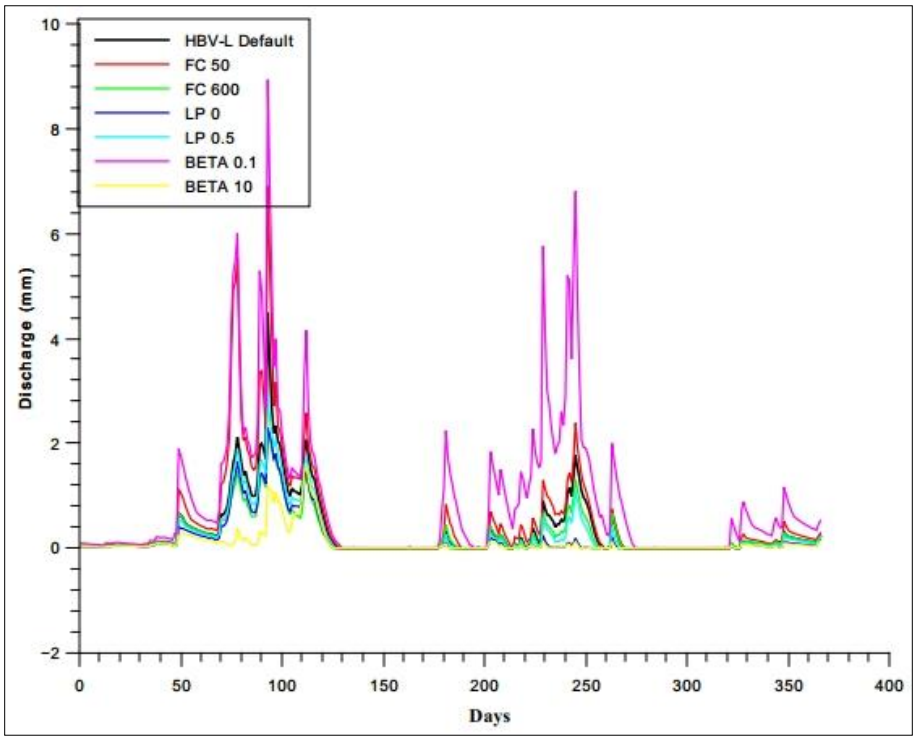

Figure 3.5

Sensitivity analysis of the parameters of soil moisture routine of HBV- light model

Table 3.1

Optimum parameters selected to calibrate the model. 1* = Dense vegetation zone, 2* = Moderate vegetation zone, and 3* = barren land, water, rocks zone Elevation of P* and Elevation of T* is taken as the elevation value of grid point of data, for the respective sub-catchment.

Lake Properties						
TT	7			1		
SFCF	2.8			4		
PCALT	9			15		
TCALT	0.58			0.61		
Elevation of P*	530			500		
Elevation of T*	530			500		
	Sihala Sub-catchment Vegetation zone			Kani Sub-catchment Vegetation zone		
	1*	2*	3*	1*	2*	3*
Snow Routine						
TT	5	8	1	11.3	0	1
CFMAX	0.01	0.01	0.01	0.01	0.01	0.01
SP	0.01	0.01	0.01	1	1	1
SFCF	1E-05	1E-05	1E-05	1E-07	2E-06	6E-05
CFR	0.05	0.05	0.05	0.05	0.05	0.05

CWH	0.01	0.01	0.01	0.01	0.01	0.01
CFSlope	1	1	1	1	1	1
Soil Moisture Routine						
FC	180	140	100	300	260	200
LP	1	1	1	1	1	1
BETA	0.73	0.25	0.01	0.46	0.25	0.05
Response Routine						
PERC	0.02			0.03		
UZL	57			45		
K0	0.58			0.52		
K1	0.065			0.038		
K2	0.05			0.037		
Routing Routine						
MAXBAS	3.4			2.8		
Other						
Cet	0.13			0.15		

3.4.2. Water balance components resulting from calibration and validation of Sihala and Kani sub-catchment

Different water balance components like, sum of simulated discharge, observed discharge, precipitation, Actual evapotranspiration, Potential evapotranspiration, and contribution of Q0 (Surface flow), Q1 (inter flow), and Q2 (base flow), that have emerged as a result of Calibration and validation for Sihala and Kani sub-catchments are presented in Table 3.2.

Table 3.2

Water balance of the Sihala and Kani sub-catchments as a result of Calibration and validation

Sihala sub-catchment	Calibration	Validation
Water Balance	mm/year	mm/year
Sum Qsim	230	192
Sum Qobs	244	178
Sum Precipitation	508	462
Sum AET	310	301
Sum PET	2345	2372
Contribution of Q0	0.053	0.009
Contribution of Q1	0.78	0.825
Contribution of Q2	0.17	0.166
Kani sub-catchment	Calibration	Validation
Water Balance	mm/year	mm/year
Sum Qsim	170	162
Sum Qobs	160	131
Sum Precipitation	408	406
Sum AET	182	185
Sum PET	3767	3828
Contribution of Q0	0.054	0.013
Contribution of Q1	0.889	0.930
Contribution of Q2	0.058	0.057

Where, Qsim = model simulated flow, Qobs = observed flow, AET = actual evapotranspiration, PET = potential evapotranspiration, Q0 = Surface flow, Q1 = Inter flow, and Q2 = Base flow.

3.4.3. Calibration and validation results of the Sihala and the Kani sub-catchment

Observed and simulated discharge resulted from calibration and validation of the SSC and the KSC is presented in (Fig. 3.6). The HBV-light has found out to be efficient both during calibration and validation of the two sub-catchments of the SRB.

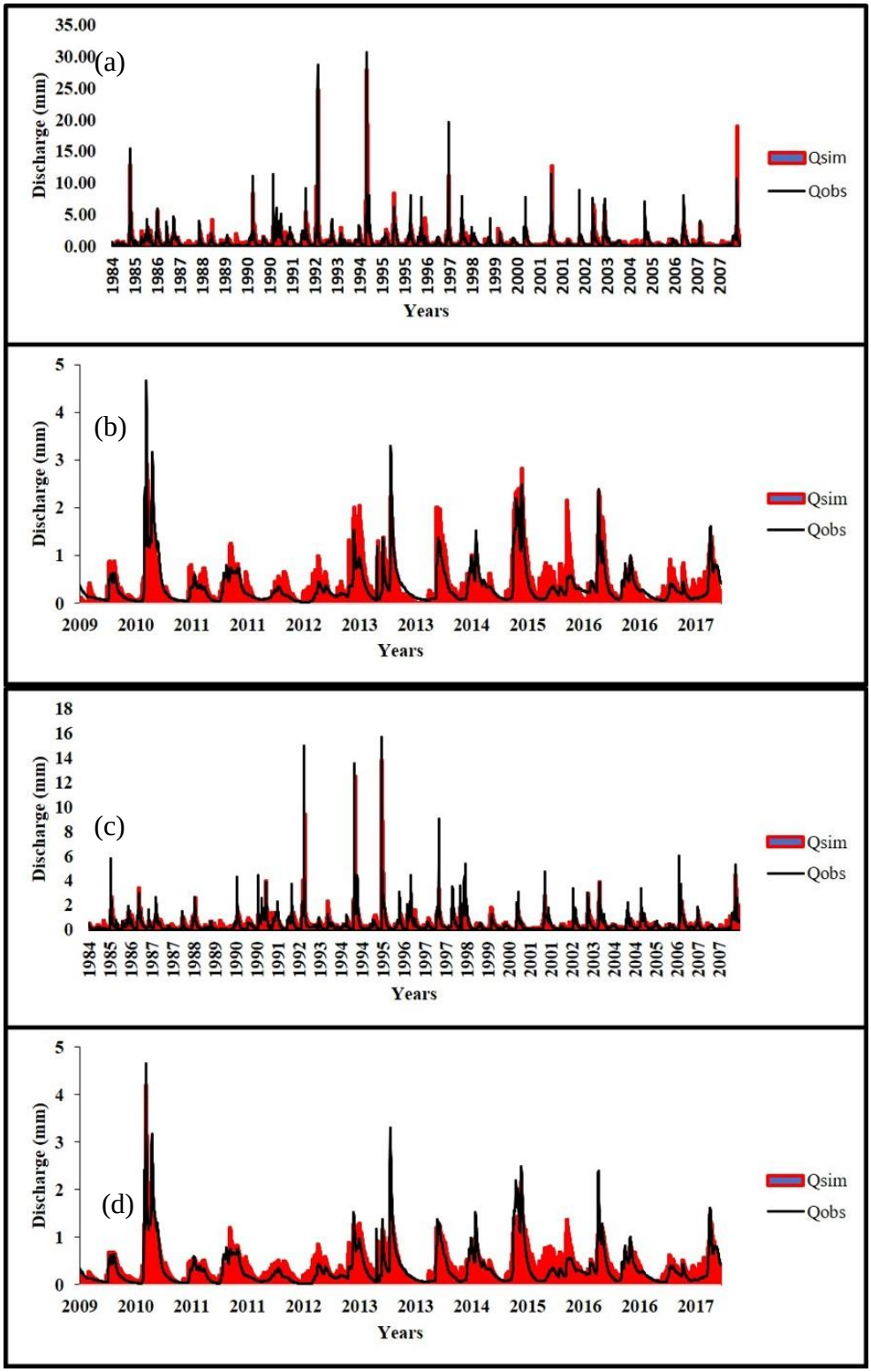

Figure 3.6

Calibration and Validation results for Sihala and Kani Sub-catchment (a) Calibration of Sihala sub-catchment (b) Validation of Sihala sub-catchment (c) Calibration of Kani sub-catchment (d) Validation of Kani sub-catchment.

3.4.4. Calibration periods with different goodness of fit measure values

NSE is a measure of goodness-of-fit and is independent of the flow magnitude. It ranges from -infinity to 1 and one being the perfect fit (Zhang et al., 2013; Mostafaie et al., 2018), the NSE tends to accentuate the high discharges (Huo and Liu, 2018). The NSE also measures the capability of the model to predict variables that differs from the mean and provides the proportion of the initial variance accounted for by the model (Javan et al., 2015).

Nash sutcliffe efficiency for calibration of sihala sub-catchment scored a value of NSE = 0.75, while kani sub-catchment scored values of NSE = 0.72, which are considered as good and very good. Asl-Rousta and Mousavi. (2019), Pluntke et al. (2014), and Asl-Rousta et al. (2018) suggests NS > 0.65 as good and NS> 0.75 as very good. NS> 0.7 have been considered good by (Lawrence et al., 2009.). The values of volume error have a perfect fit that equals 1.

Different objective functions with their relative values for calibration and validation for Sihala sub-catchment and kani sub-catchment are illustrated in (table 3.3).

Table 3.3

Goodness of fit measures for Calibration and validation ofthe Sihala and the Kani sub-catchments.

		NSE	R^2	Mean Difference (mm)	Volume Error (%)
Sihala sub-catchment	Calibration	0.75	0.75	13.36	0.95
	Validation	0.72	0.72	-14.39	0.92
Kani sub-catchment	Calibration	0.72	0.73	-10.27	0.94
	Validation	0.72	0.76	-31.46	0.76

3.5. Projected changes in yearly discharge of the Sihala and the Kani sub catchments

Projected changes in the discharge of the SSC and the KSC under the RCP 4.5 and the RCP 8.5 on the yearly basis are shown in the (Fig 3.7). The discharge of the SSC and the KSC is projected to show the positive change of direction (increase) and the magnitude of positive change is more significant under the RCP 8.5 emission scenario than the RCP 4.5 emission scenario. On yearly basis the increase in discharge may be attributed to the increased projected precipitation, evapotranspiration and the temperatures. The increase in precipitation tends to outweigh the increase in evapotranspiration, hence attributing towards the high flow projections. Another noticeable difference is that the magnitude of increase is stronger in the SSC than the KSC that may be attributed to different physical, geographical and topographical characteristics of the two respective sub-catchments. An average yearly increase of 467 % and 593 % is projected for the SSC under the RCP 4.5 and the RCP 8.5 emission scenarios. While a mean yearly increase of 270 % and 316 % is projected under the RCP 4.5 and the RCP 8.5 emission scenarios for the KSC.

For the SSC, discharge under the RCP 4.5 emission scenario is seen to be between 1000 and 2000 mm for 12 years, 200-1000 mm for 18 years. While 19 years showed the discharge to be between 1000 and 3300 mm a year, and less than 1000 mm for the rest of the 11 years, under RCP 8.5 emission scenario. Discharge in the baseline period of the SSC was like this, 16 years showed the discharge to be between 200-450 mm, while 23 years showed that the flows remained between 60-250 mm a year.

For the KSC the discharge is projected to be between 100 and 400 mm for 13 years, and 400-820 mm for 17 years under the RCP 4.5 emission scenario, however 19 years showed the discharge to be between 400 to 1500 mm a year, and less than 400 mm for rest of the 11 years, under the RCP 8.5 emission scenario. To have a better view of how the projected changes differ from the observed period, it is important to give here the values of discharge for the observed period as well. So, out of 39 years in the baseline period, 31 years showed the discharge to be between 30-180 mm, while 8 years showed that the flows remained between 220-280 mm a year.

3.6. Projected changes in yearly precipitation of the Sihala and the Kani sub catchments

Precipitation tends to show an increase under both emission scenarios the RCP 4.5 and RCP 8.5 for the SSC and the KSC, as illustrated in figure 3.8. An average yearly increase of 206 % and 241 % is projected under the RCP 4.5 and the RCP 8.5 emission scenario for the SSC, respectively. However the projected increase in the KSC is not as strong in magnitude as the SSC has exhibited, with an average yearly increase of 108 % and 126 % under the RCP 4.5 and the RCP 8.5 emission scenarios, respectively.

Under the RCP 4.5 emission scenario 23 years out of 30 years projects that the precipitation is projected to vary between (1100-2300 mm), 7 years showed less 1000 mm a year. While under the RCP 8.5 emission scenario 27 years showed that the precipitation seems to vary between (1000-3000 mm), and 3 years showed the precipitation to be less than 1000 mm, so the highest increase is projected under the RCP 8.5 emission scenario.

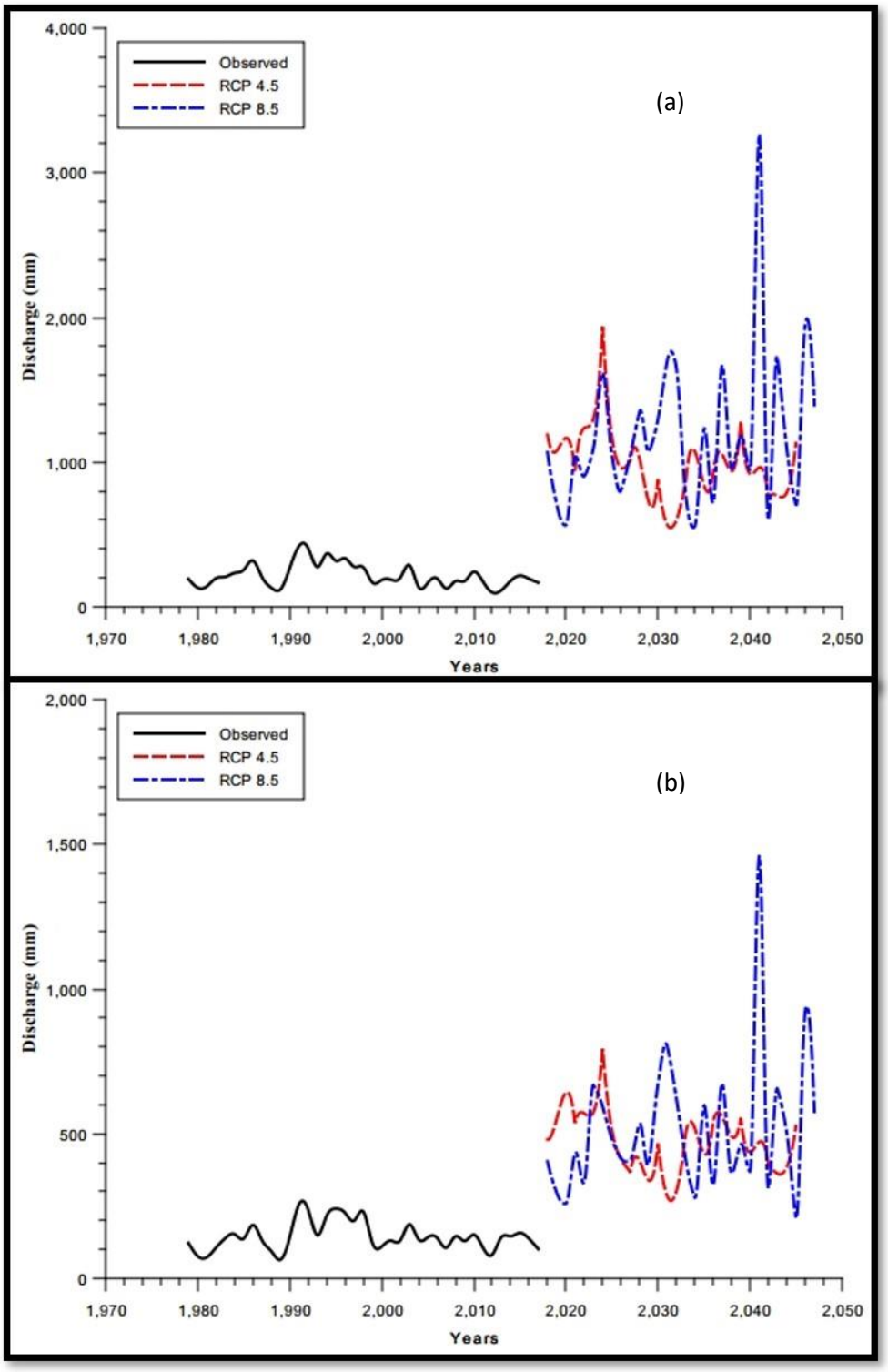

Figure 3.7

Projected changes in yearly discharge of (a) the Sihala sub-catchment and (b) the Kani sub-catchment under the RCP 4.5 and RCP 8.5 for the time period (2018-2047), as compared to baseline period (1979-2017). Data source (ECMWF and SMHI RCA4).

The yearly precipitation of the KSC is projected to increase under the RCP 4.5 and RCP 8.5 emission scenarios except with a decrease in precipitation under the RCP 4.5 emission scenario in the year 2033. Six years out of projected 30 years, under the RCP 4.5 emission scenario showed that the precipitation seem to vary between (1000-1300 mm), and 24 years showed that the precipitation seem to be less than 1000 mm. Under the RCP 8.5 emission scenario precipitation in 22 years is projected to be less than 1000 mm and for 8 years it seems to be between (1000-2000 mm).

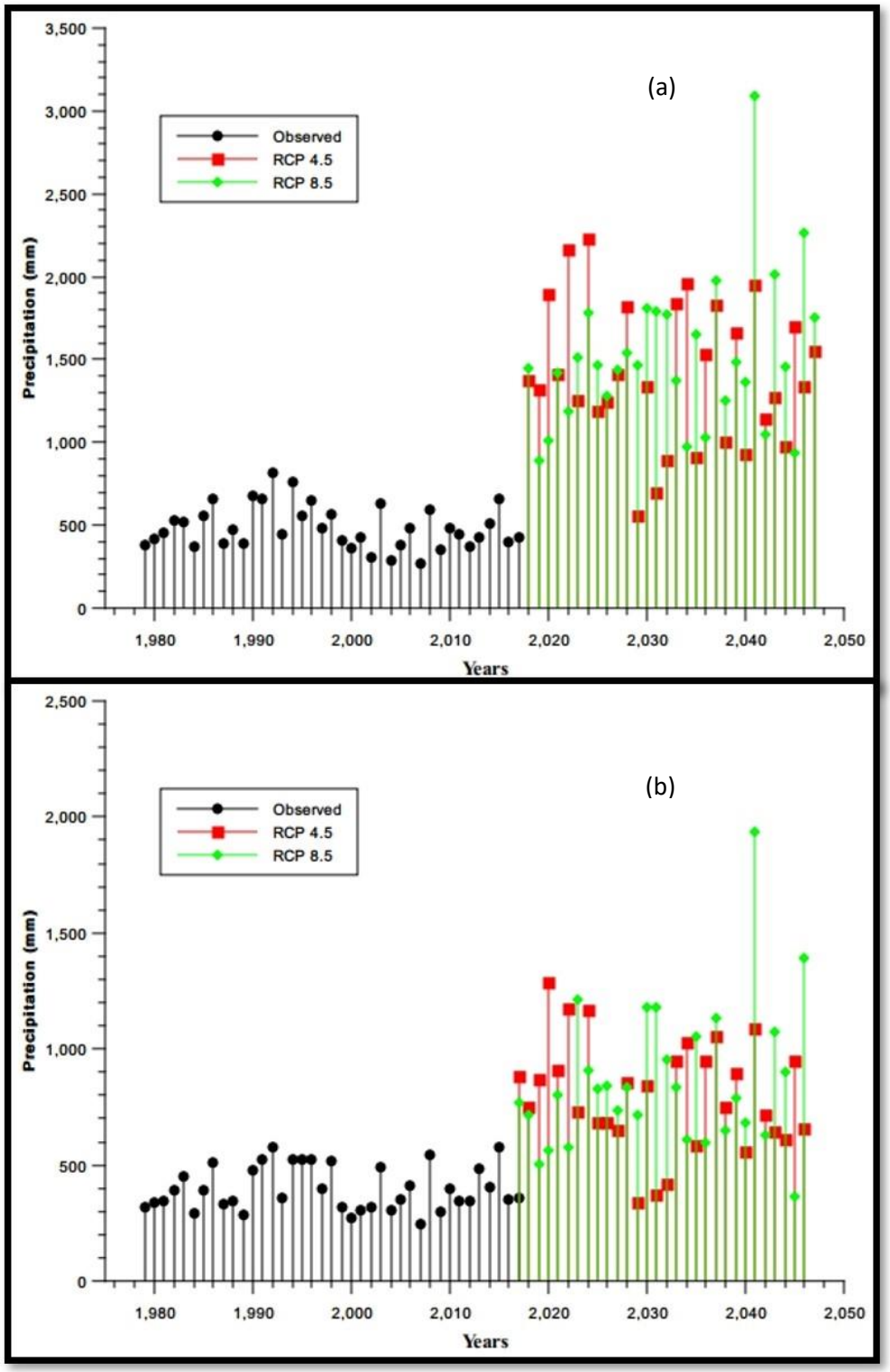

Figure 3.8

Projected changes in yearly precipitation of (a) the Sihala sub-catchment and (b) the kani sub-catchment under the RCP 4.5 and RCP 8.5 for the time period (2018-2047), as compared to baseline period (1979-2017). Data source (ECMWF and SMHI RCA4).

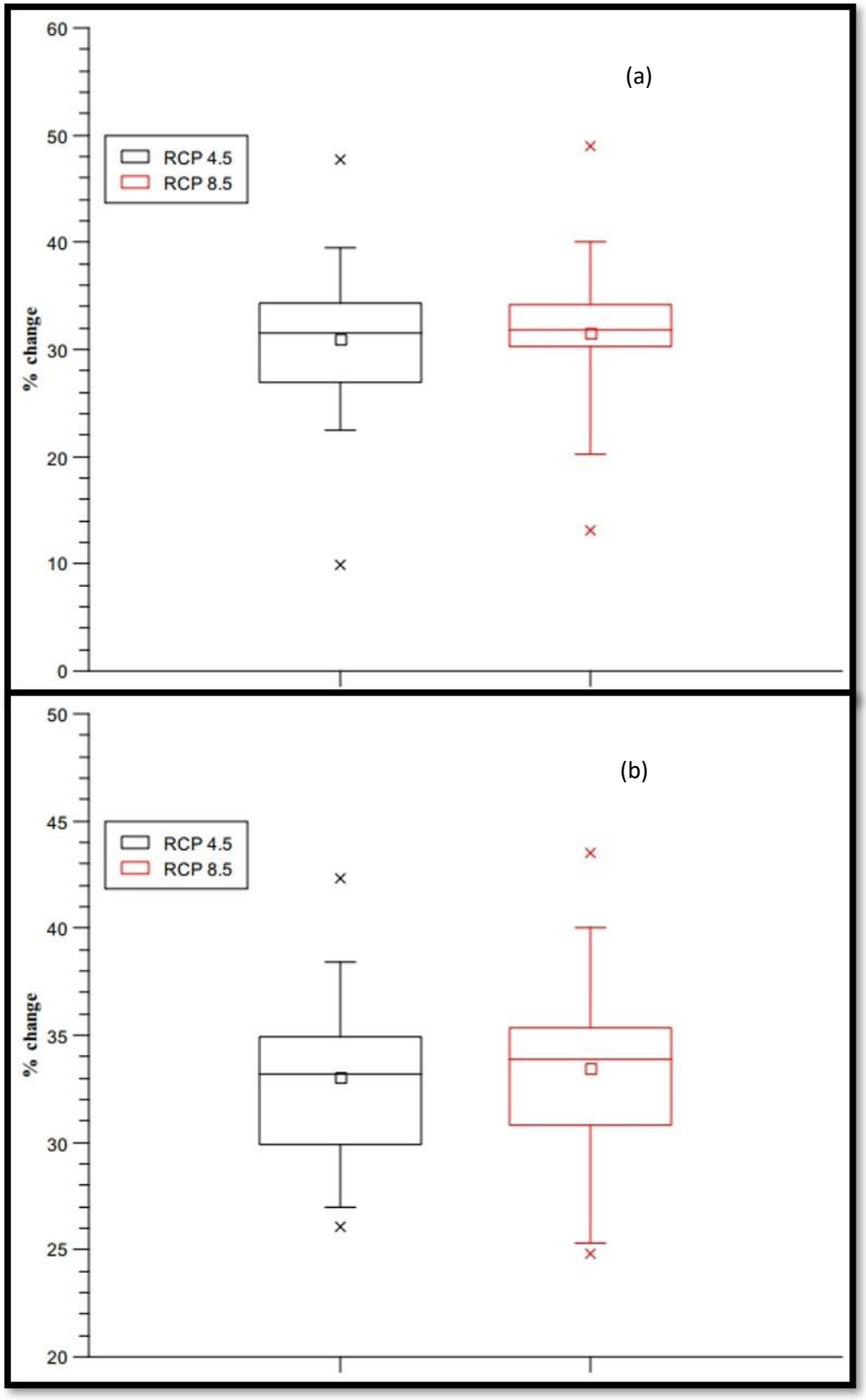

Figure 3.9

Percent changes in yearly evapotranspiration of (a) the Sihala sub-catchment and (b) the kani sub-catchment under the RCP 4.5 and RCP 8.5 for the time period (2018-2047), as compared to baseline period (1979-2017). Data source (ECMWF and SMHI RCA4).

3.7. Projected changes in yearly evapotranspiration of the Sihala and the Kani sub catchments

Evapotranspiration is seen to increasing as well under both the emission scenarios for both the sub-catchments of the SRB. The magnitude of change in evapotranspiration of the KSC is stronger than the SSC under the RCP 4.5 and the RCP 8.5 emission scenarios.

In the SSC, evapotranspiration is projected to be 121 mm/year and 129 mm/year, which is an increase of around 31 %and 31.5 % on average under the RCP 4.5, and the RCP 8.5 emission scenarios, respectively (Fig. 3.9).

Projected changes in yearly evapotranspiration of the KSC suggests that evapotranspiration seems to be 139 mm per year under the RCP 4.5and the RCP 8.5 emission scenarios, respectively, as compared to baseline period values of 107 mm per year.

3.8. Projected changes in yearly temperatures of the Sihala and the Kani sub catchments

Temperatures also tend to increase under both the emission scenarios for both the sub-catchments of the SRB. In the SSC, temperatures are projected to be 20 °C and 22 °C, under the RCP 4.5, and the RCP 8.5 emission scenarios, respectively, as compared to 17 °C in observed period, as illustrated in (Fig. 3.10). Higher temperatures could also be observed in the future time period of the KSC. Mean annual temperatures seem to have same value under both the RCPs. In the observed time period, mean annual temperature was 13 °C and is projected to be 22 °C under the RCP 4.5, RCP 8.5 emission scenario respectively.

3.9. Projected changes in monthly discharge of Sihala and the Kani sub catchments

The discharge, whether it is going to increase or decrease depends on the variations in the other water balance components e.g. precipitation, evapotranspiration, temperature. At higher temperatures water holding capacity in the atmosphere increase, hence increase in rainfall may occur, and with the high rainfall amounts an increase in the discharges is expected (as precipitation is the sole inflow source to the study catchments, the major driver of changes in discharge is precipitation). Projected increase in the future precipitation overweighs the increase in evapotranspiration, so despite of increasing evapotranspiration the projected discharge is still increasing. Precipitation tends to increase on the monthly basis under both scenarios RCP 4.5 and RCP 8.5, with a few exceptions, and the increase is not uniform in terms of magnitude over all the months.

Mean monthly discharge in the SSC seems to increase under both changing climate scenarios, as shown in (Fig. 3.11). Discharge in March is projected to decrease under the RCP 4.5 emission scenario and seems to remain stable under the RCP 8.5. Increase is seen in January flows under the RCP 4.5 emission scenario and decrease is projected under the RCP 8.5 emission scenario, while in February both future emission scenarios showed a decrease in the volume of discharge. Projected increase in the discharge of all the remaining months could be seen.

In the KSC, discharge seems to decrease in the month of February under RCP 4.5 and increase under RCP 8.5, while in March it is projected to decrease under the RCP 4.5 and increase under the RCP 8.5. All the other months showed a projected increase in discharge till mid of the 21st century, as shown in (Fig. 3.11).

3.10. Projected changes in monthly precipitation of Sihala and the Kani sub catchments

The change in projected increase of precipitation in the months that received higher amounts of rainfall in the baseline period is less than the change that occurred in the months of low precipitation in the baseline period in the future time slice near the mid of the 21st century. As shown in table 3.4, in the SSC, February was the only month that showed a decrease in the projected amount of precipitation, under RCP 4.5 and the RCP 8.5, and March was the only month to receive projected lower amounts in the future under the RCP 4.5 and higher amounts of precipitation under the RCP 8.5. All other months tend to show an increase in the precipitation under both scenarios.

Projected changes in monthly precipitation of the KSC under RCP 4.5 and RCP 8.5 are shown in table 3.4. Months of January and February showed a decrease in the projected amount of precipitation, under the RCP 4.5 and RCP 8.5, while in March, precipitation is projected to decrease under the RCP 4.5 and seems to increase under the RCP 8.5. Increase in projected changes of precipitation in the rest months could be seen, and the change is pretty much consistent under both climate change scenarios, the RCP 4.5 and RCP 8.5.

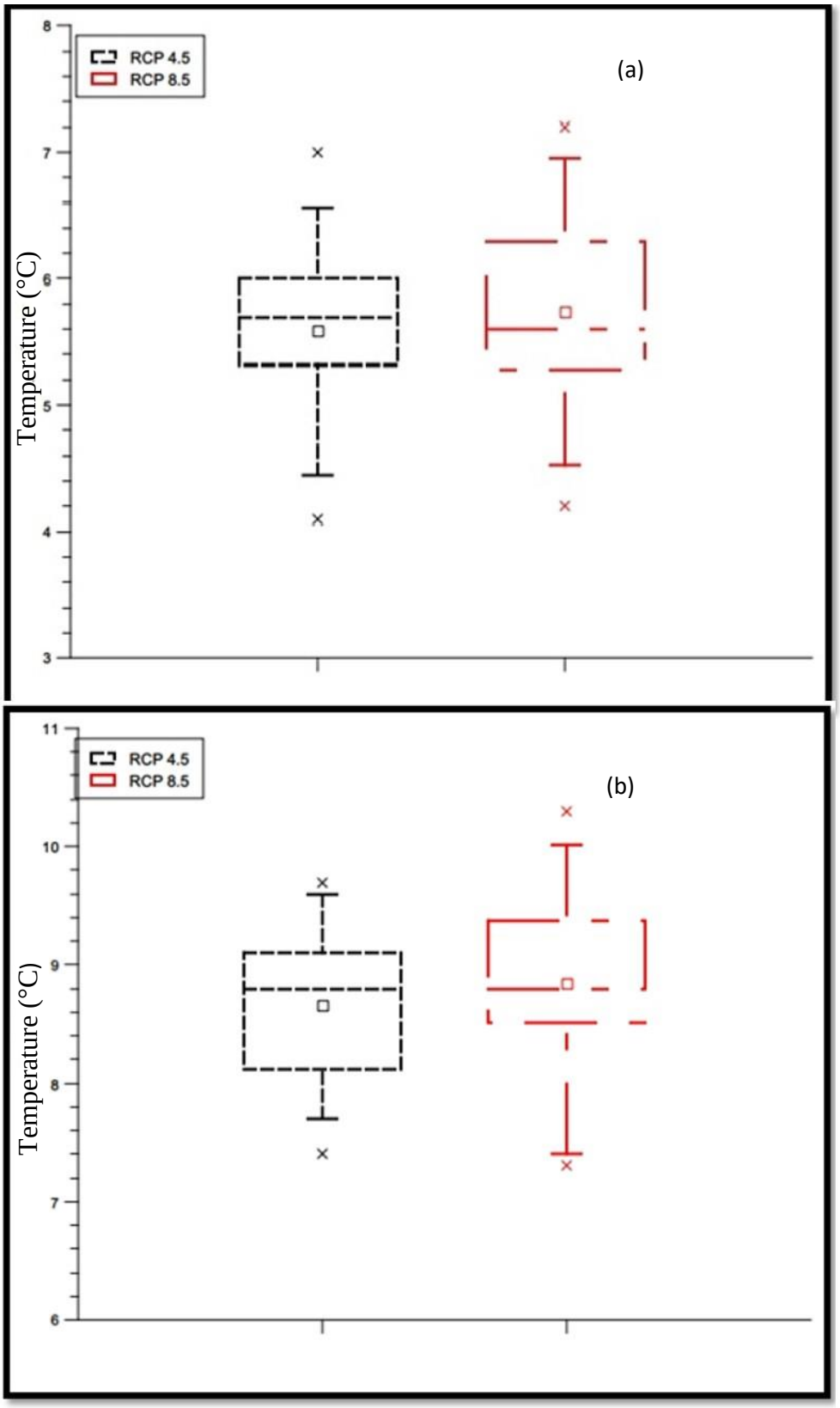

Figure 3.10

Projected changes in yearly temperature of (a) the Sihala sub-catchment and (b) the kani sub-catchment under the RCP 4.5 and RCP 8.5 for the time period (2018-2047), as compared to baseline period (1979-2017). Data source (ECMWF and SMHI RCA4).

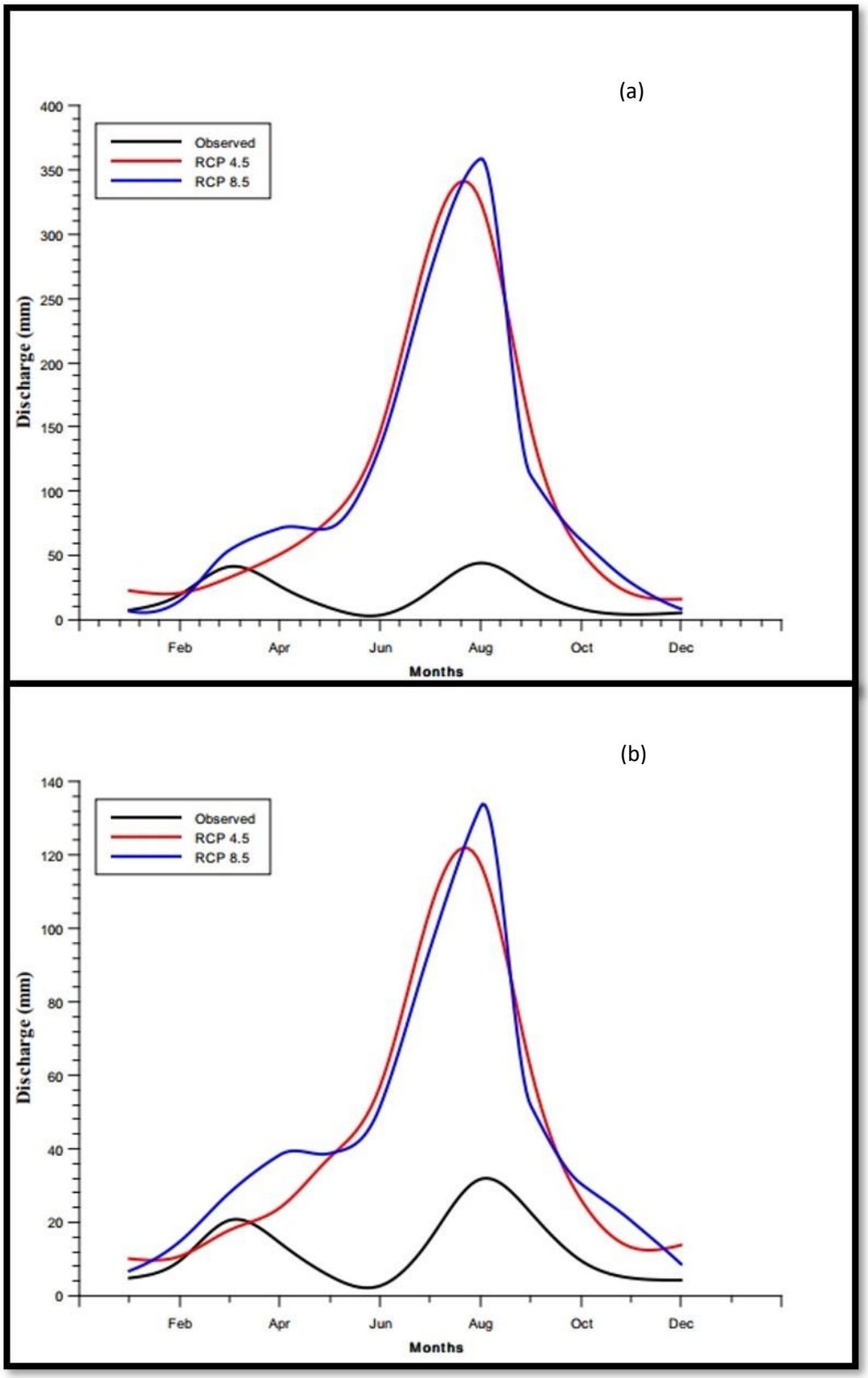

Figure 3.11

Projected monthly change in discharge of (a) the Sihala sub-catchment and (b) the kani sub-catchment under the RCP 4.5 and RCP 8.5 for the time period (2018-2047), as compared to baseline period (1979-2017). Data source (ECMWF and SMHI RCA4).

Table 3.4

Projected changed in Precipitation of the Sihala and Kani Sub-catchments for the time period (2018-2047). Data source (SMHI RCA4).

	Precipitation (%)			
	Sihala Sub-catchment		Kani Sub-catchment	
Months	RCP 4.5	RCP 8.5	RCP 4.5	RCP 8.5
Jan	1.45	7.27	-20.8	-19.9
Feb	-34.87	-11.04	-45.1	-14.2
Mar	-22.87	33.55	-23.7	23.1
Apr	117.86	211.20	76.4	169.2
May	799.30	849.59	442.2	425.1
Jun	678.09	885.25	244.4	301.9
Jul	311.47	274.95	157.9	123.8
Aug	373.37	339.93	198.3	182.1
Sep	397.30	334.64	203.0	158.2
Oct	209.90	543.06	88.0	278.1
Nov	37.08	128.66	14.2	122.6
Dec	135.12	1.00	90.4	-11.8

3.11. Projected changes in monthly evapotranspiration of Sihala and Kani sub catchments

From table 3.5, it could be observed that the mean monthly evapotranspiration, under RCP 4.5 and RCP 8.5 is projected to be 11 mm as compared to 8 mm in the observed time period, in the SSC while projected changes in monthly evapotranspiration of the KSC under the RCP 4.5 and RCP 8.5 have been illustrated in table 3.5. Mean monthly evapotranspiration, under the RCP 4.5 and RCP 8.5 seems to be 11 mm as compared to the baseline of 8 mm.

Table 3.5

Projected changed in Evapotranspiration of the Sihala and Kani Sub-catchments for the time period (2018-2047). Data source (SMHI RCA4).

	Evapotranspiration (%)			
	Sihala Sub-catchment		Kani Sub-catchment	
Months	RCP 4.5	RCP 8.5	RCP 4.5	RCP 8.5
Jan	340.8	368.9	190.9	199.4
Feb	127.9	131.9	99.0	100.3
Mar	155.6	156.1	88.6	89.3
Apr	24.7	22.3	29.1	27.9
May	18.2	19.4	18.4	19.2
Jun	10.9	11.1	13.1	13.3
Jul	9.5	9.9	12.9	13.3
Aug	7.0	7.9	11.5	12.2
Sep	12.9	13.6	15.7	16.1
Oct	29.2	29.5	28.7	29.2
Nov	53.7	50.7	48.8	47.1
Dec	159.9	159.1	122.3	121.4

3.12. Projected changes in monthly temperatures of Sihala and Kani sub catchments

Projected changes in the temperature of the Sihala and the Kani sub-catchments are given in table 3.6. An increase of up to 7.5 °C is projected for the SSC under the RCP 4.5, while a rise of up to 7.7 °C is projected under the RCP 8.5. Overall a mean monthly increase is projected for the Sihala sub-catchment, as suggested by the SMHI RCA4.More warming is projected for the KSC under both the

average and the extreme emission scenarios. An outstanding increase of up to 10.3°C and 10.5 °C is projected under the RCP 4.5 and the RCP 8.5 as per the SMHI RCA4 for the Kani sub-catchment.

Table 3.6
Projected changed in Evapotranspiration of the Sihala and Kani Sub-catchments for the time period (2018-2047). Data source (SMHI RCA4).

	Temperature (°C)			
	Sihala Sub-catchment		Kani Sub-catchment	
Months	RCP 4.5	RCP 8.5	RCP 4.5	RCP 8.5
Jan	4.9	5.4	7.5	8.0
Feb	5.7	5.9	8.4	8.6
Mar	7.2	7.2	9.9	10.1
Apr	7.5	6.7	10.3	9.7
May	7.1	7.7	10.0	10.5
Jun	5.9	6.1	9.4	9.7
Jul	5.3	5.5	9.6	9.9
Aug	3.9	4.5	8.3	8.9
Sep	5.5	5.9	9.0	9.3
Oct	6.2	6.3	8.8	9.0
Nov	5.3	5.0	7.6	7.3
Dec	4.9	4.9	7.5	7.4

3.13. Projected changes in seasonal discharge of the Sihala and the Kani sub catchments

Seasonal discharges in both sub-catchments of the Soan river basin are of particular peculiarity and diversity. The discharge of the Spring, Summer, Autumn, and the Winter for the Sihala and Kani sub-catchments are presented in the following section.

3.13.1. Projected changes in spring discharge

(Fig. 3.12) illustrates the spring discharge in the SSC. Discharge is projected to increase from an average of 73 mm in observed period to 157 mm and 197 mm under both changing climate scenarios, i.e. the RCP 4.5 and RCP 8.5, respectively. While the discharge in the KSC in spring seems to increase from an average of 12 mm in observed period to 79 mm and 105 mm under RCP 4.5 and RCP 8.5, respectively, as illustrated in (Fig. 3.12).

3.13.2. Projected changes in summer discharge

In the SSC, average summer discharge is projected to increase from average of 73 mm in observed period to 816 mm and 764 mm under RCP 4.5 and RCP 8.5, respectively, as illustrated in (Fig. 3.13). This is the highest change (increase) as compared to all the seasons. Projected changes in summer discharge of the Kani sub-catchment under the RCP 4.5 and RCP 8.5 are shown in (Fig. 3.13). Discharge in summer might increase under the RCP 4.5 and the RCP 8.5. However, the magnitude of change is more concentrated under the RCP 4.5 than the RCO 8.5. In the observed period mean flow in the winter was 17 mm, while it seems to be 294 mm for average greenhouse gas emission scenario and 279 mm with extreme emission scenario.

3.13.3. Projected changes in autumn discharge

In the SSC, it could be observed in the figure 3.14, that, discharge in autumn is projected to increase from an average of 41 mm in observed period to 180 mm and 203 mm under both changing climate scenarios, i.e. RCP 4.5 and RCP 8.5, respectively. In the KSC Discharge is seen to increase from an average of 13 mm in observed period to 87 mm and 102 mm under both changing climate scenarios, i.e. RCP 4.5 and RCP 8.5, respectively, as given in (Fig. 3.14).

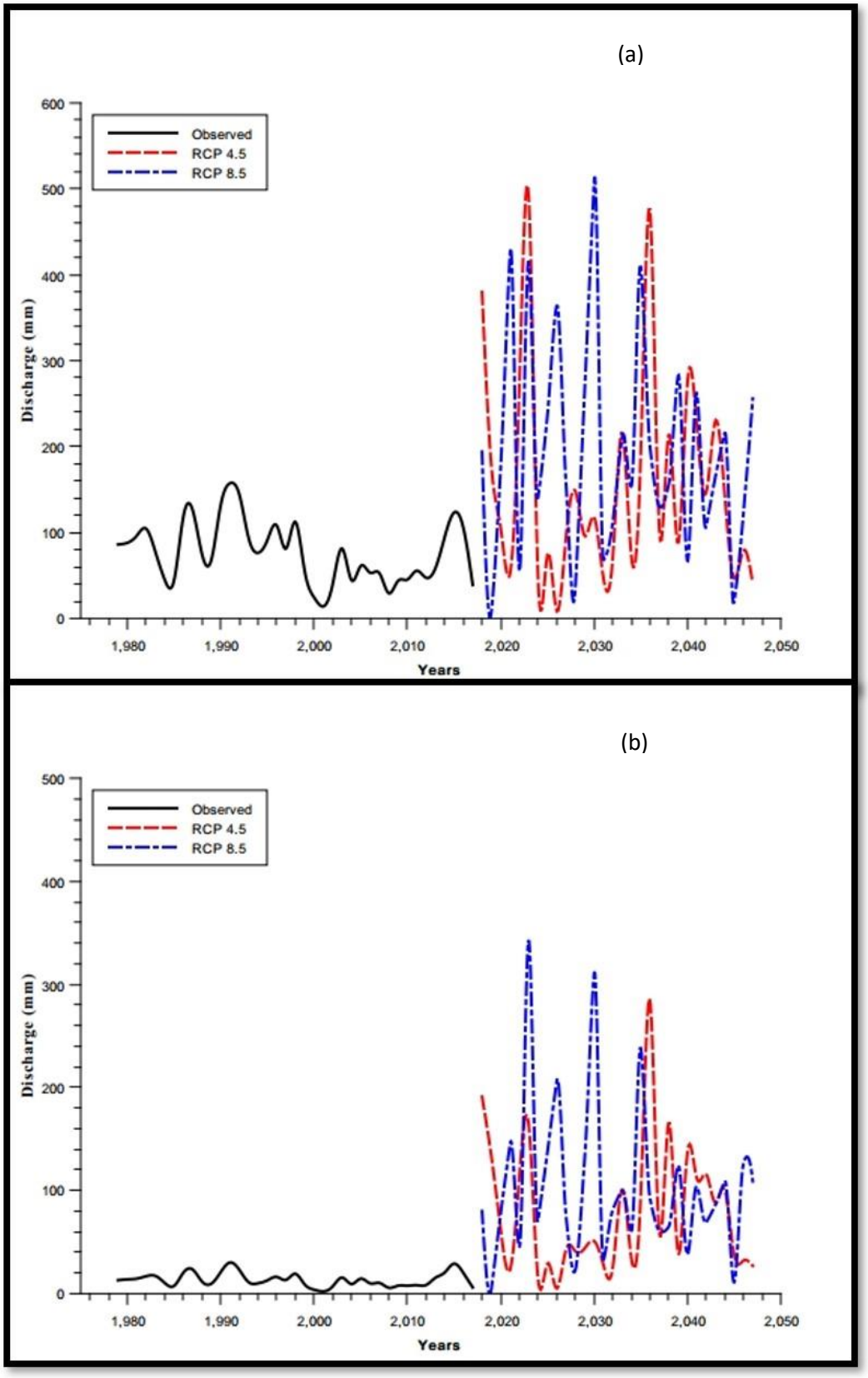

Figure 3.12

Projected changes in spring discharge of (a) the Sihala sub-catchment and (b) the kani sub-catchment under the RCP 4.5 and RCP 8.5 for the time period (2018-2047), as compared to baseline period (1979-2017). Data source (ECMWF and SMHI RCA4).

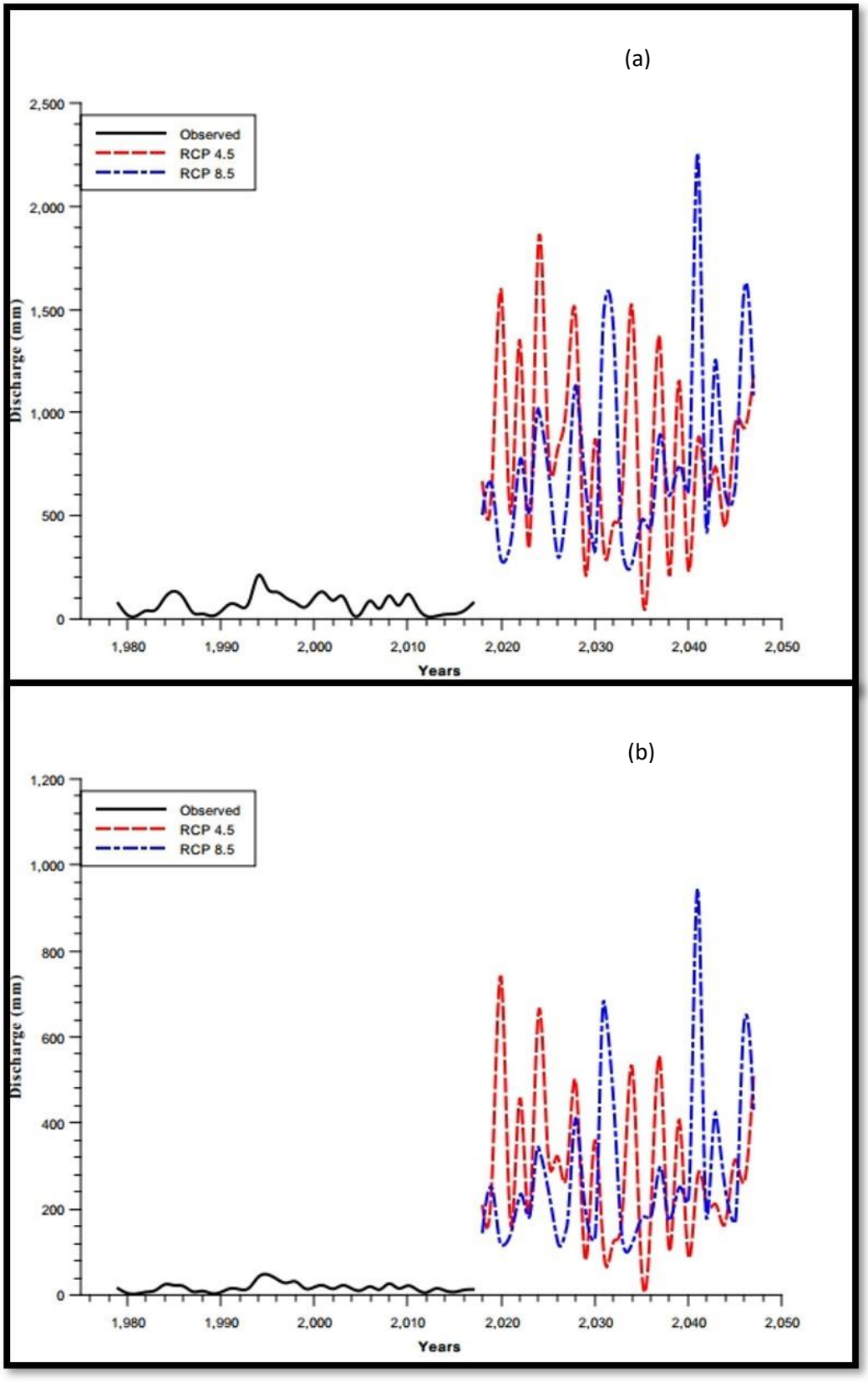

Figure 3.13

Projected changes in summer discharge of (a) the Sihala sub-catchment and (b) the kani sub-catchment under the RCP 4.5 and RCP 8.5 for the time period (2018-2047), as compared to baseline period (1979-2017). Data source (ECMWF and SMHI RCA4).

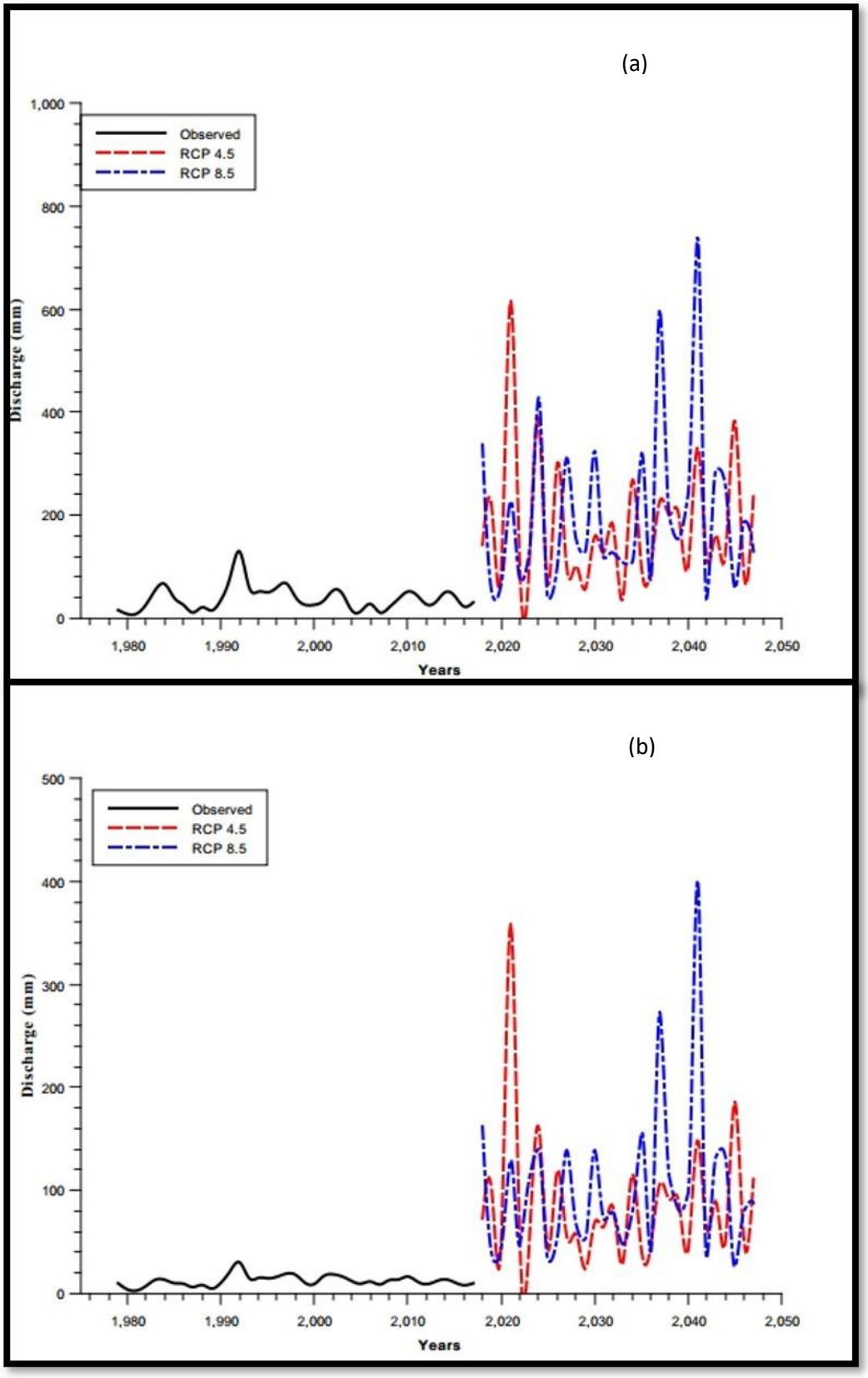

Figure 3.14

Projected changes in autumn discharge of (a) the Sihala sub-catchment and (b) the kani sub-catchment under the RCP 4.5 and RCP 8.5 for the time period (2018-2047), as compared to baseline period (1979-2017). Data source (ECMWF and SMHI RCA4).

3.13.4. Projected changes in winter discharge

Discharge in winter showed an interesting result, it is projected to increase under the RCP 4.5 and decrease under the RCP 8.5. As it is depicted in figure 3.15, that, in the observed period mean flow in the winter was 32 mm, while it seems to be 54 mm in average greenhouse gas emission scenario and 30 mm with extreme emission scenario. Positive change is more comprehensive under the RCP 4.5 than the negative change under the RCP 8.5. Projected changes in winter discharge of Kani sub-catchment under the RCP 4.5 and RCP 8.5 are shown in (Fig. 3.15). Discharge seems to increase from average of 6 mm in observed period to 34 mm and 30 mm under RCP 4.5 and RCP 8.5, respectively.

3.14. Projected changes in seasonal precipitation of the Sihala and the Kani sub-catchments

Projected changes in seasonal precipitation of Sihala sub-catchment, for spring, summer, autumn, and winter have been shown in (Fig. 3.16). The changesin spring precipitation are like this;238 mm to 313 mm of mean seasonal precipitation in spring is projected under RCP 4.5 and RCP 8.5, as compared to 121 mm in the observed period, so under both the climate change scenarios the precipitation tends to show both positive and negative change (increase) in the future, however the positive change outweighs the negative change under both the emission scenarios. Precipitation increase is substantially more under RCP 8.5 than RCP 4.5. In the spring season of observed time period, mean seasonal precipitation was 32 mm, while under the RCP 4.5 it is projected to be 179 mm and 236 mm under the RCP 8.5. An overall increase in spring precipitation is projected for the KSC under both the emission scenarios (Fig. 3.16).

Similarly, in summers, mean precipitation in the observed period was 187 mm, and will be 851 and 840 mm under RCP 4.5 and RCP 8.5, respectively, as it could be seen in the (Fig. 3.16).Mean Precipitation in the summer season showed that under both emission scenarios it will increase, while under the RCP 8.5 the increase is less in magnitude than RCP 4.5, mean precipitation is projected to be 435 mm and 416 mm under RCP 4.5 and RCP 8.5, respectively, and was 54 mm in the observed time in the KSC (Fig. 3.16).

In the autumn season of observed time period, mean seasonal precipitation was 54 mm, while under RCP 4.5 it will be 185 mm and 231 mm under RCP 8.5, in the SSC as seen in (Fig. 3.16). The precipitation is increased more under RCP 8.5 than RCP 4.5 in the SSC.A hundred and ten mm to 144 mm of mean seasonal precipitation in autumn is projected under the RCP 4.5 and RCP 8.5, as compared to 17 mm in the observed period for the SSC (Fig. 3.16).

As far as winters are concerned, both negative and positive changes are projected in rainfall, but the negative change outweighs the positive change under both the emission scenarios. Mean Precipitation in the winter season showed that under RCP 4.5 it will slightly increase, while under RCP 8.5 it seem to slightly decrease, mean precipitation is projected to be 138 and 121 mm under RCP 4.5 and RCP 8.5, respectively, and was 125 mm in the observed time, as illustrated in (Fig. 3,16). In the KSC, both negative and positive changes are projected in rainfall, but the positive change outweighs the negative change under both the emission scenarios. In winters, mean precipitation in the observed period was 30 mm, and is projected to be 77 mm under RCP 4.5 and RCP 8.5 (Fig. 3.16).

3.15. Projected changes in seasonal evapotranspiration of the Sihala and the Kani sub-catchments

Projected changes in seasonal evapotranspiration of Sihala sub-catchment, for spring, summer, autumn, and winter are illustrated in (Fig. 3.17). Mean seasonal evapotranspiration seems to increase, under both climate change scenarios, for all the seasons, with respect to the observed seasonal evapotranspiration. It is projected to be 32 mm under RCP 4.5 and RCP 8.5, while it was 25 mm in the observed period, in spring. While in the KSC, spring evapotranspiration seems to be increasing, it is projected to be 36 mm under the RCP 4.5 and RCP 8.5, and it was 28 mm in the historical time period (Fig. 3.17).

As shown in figure 3.17, mean seasonal evapotranspiration, under the RCP 4.5 and RCP 8.5 is projected to be 38 mm as compared to 35 mm in the observed time period, in the summer of the SSC. Mean summer evapotranspiration showed an increase and seems to be 41 mm under both climate change scenarios, while it was 36 mm in the observed period in the KSC.

While in autumn, evapotranspiration is projected to be 7mm under both average and extreme climate change scenarios, and it was 2 mm in the historical time period in the SSC, and mean seasonal evapotranspiration in autumn, under the RCP 4.5 and RCP 8.5 is projected to be 35 mm, while it was 28 mm in the observed period in the KSC.

Mean winter evapotranspiration also showed an increase, and could be 19 mm under both climate change scenarios, while it was 7 mm in the observed period, in the SSC, as illustrated in (Fig. 3.17). Mean seasonal evapotranspiration in winter, under RCP 4.5 is seen to be 25 mm and 26 mm under RCP 8.5, as compared to 11 mm in the observed time period for the KSC (Fig. 3.17).

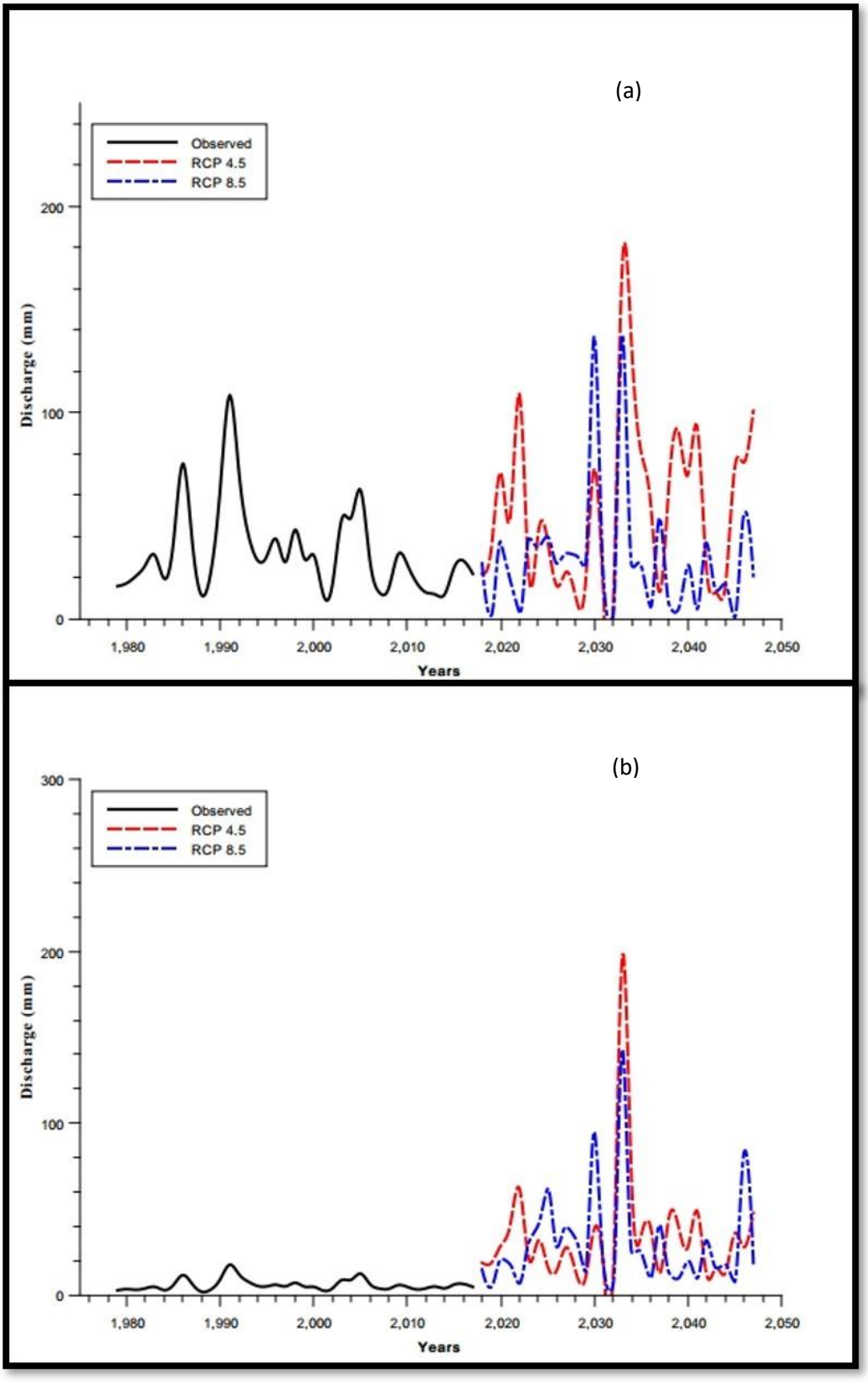

Figure 3.15

Projected changes in winter discharge of (a) the Sihala sub-catchment and (b) the kani sub-catchment under the RCP 4.5 and RCP 8.5 for the time period (2018-2047), as compared to baseline period (1979-2017). Data source (ECMWF and SMHI RCA4).

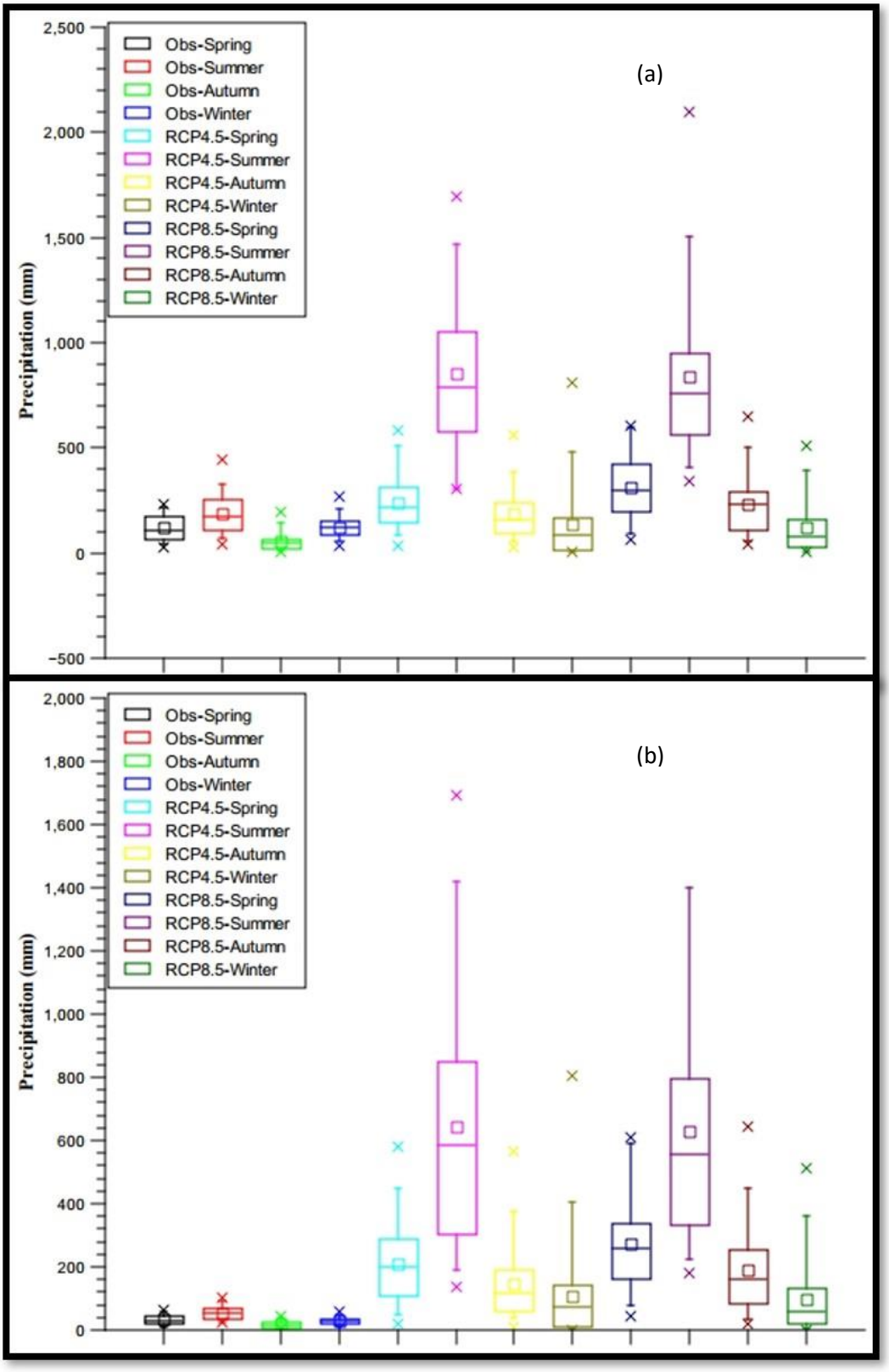

Figure 3.16

Projected changes in seasonal precipitation of (a) the Sihala sub-catchment and (b) the kani sub-catchment under the RCP 4.5 and RCP 8.5 for the time period (2018-2047), as compared to baseline period (1979-2017). Data source (ECMWF and SMHI RCA4).

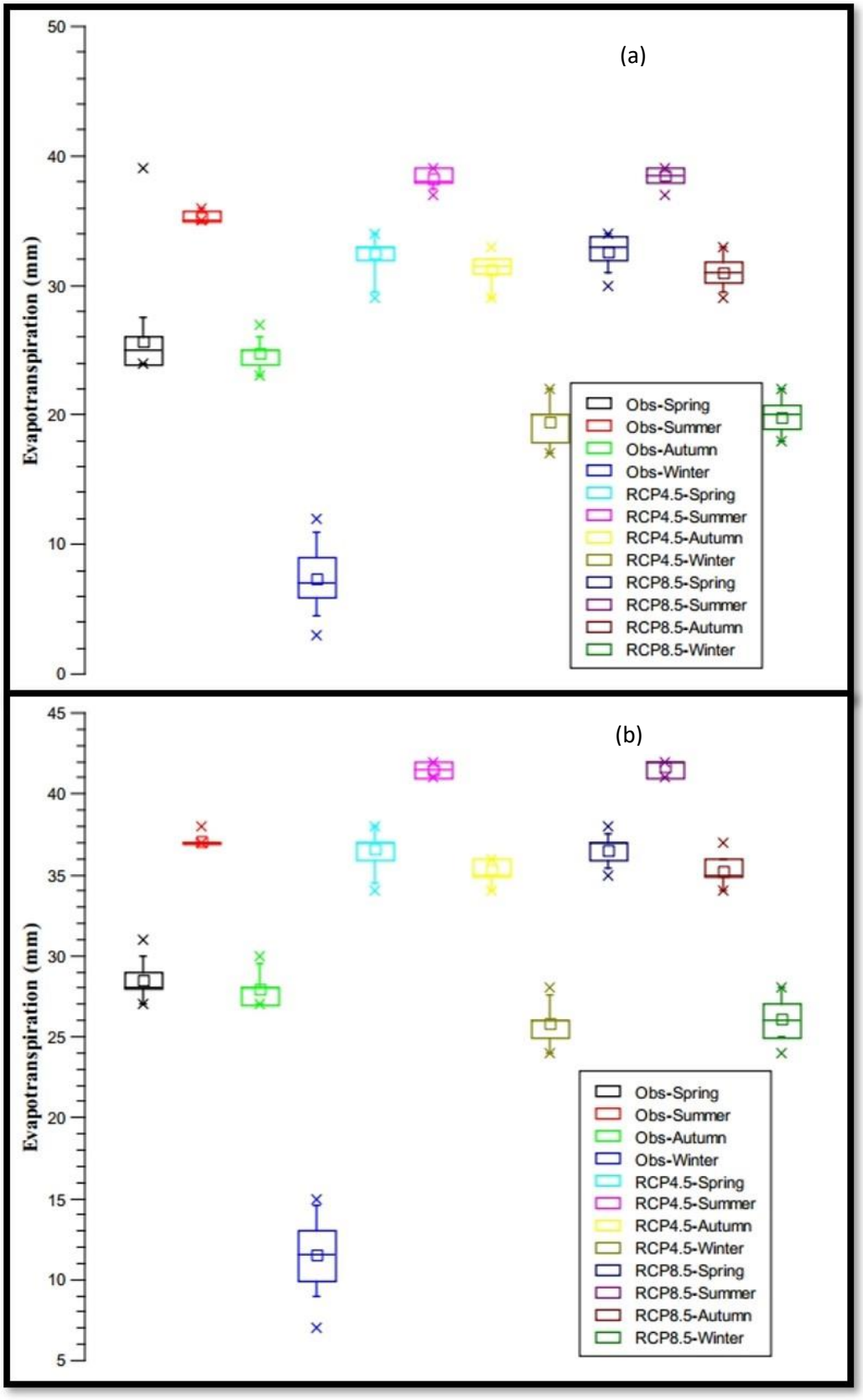

Figure 3.17

Projected changes in seasonal evapotranspiration of (a) the Sihala sub-catchment and (b) the kani sub-catchment under the RCP 4.5 and RCP 8.5 for the time period (2018-2047), as compared to baseline period (1979-2017). Data source (ECMWF and SMHI RCA4).

(a)

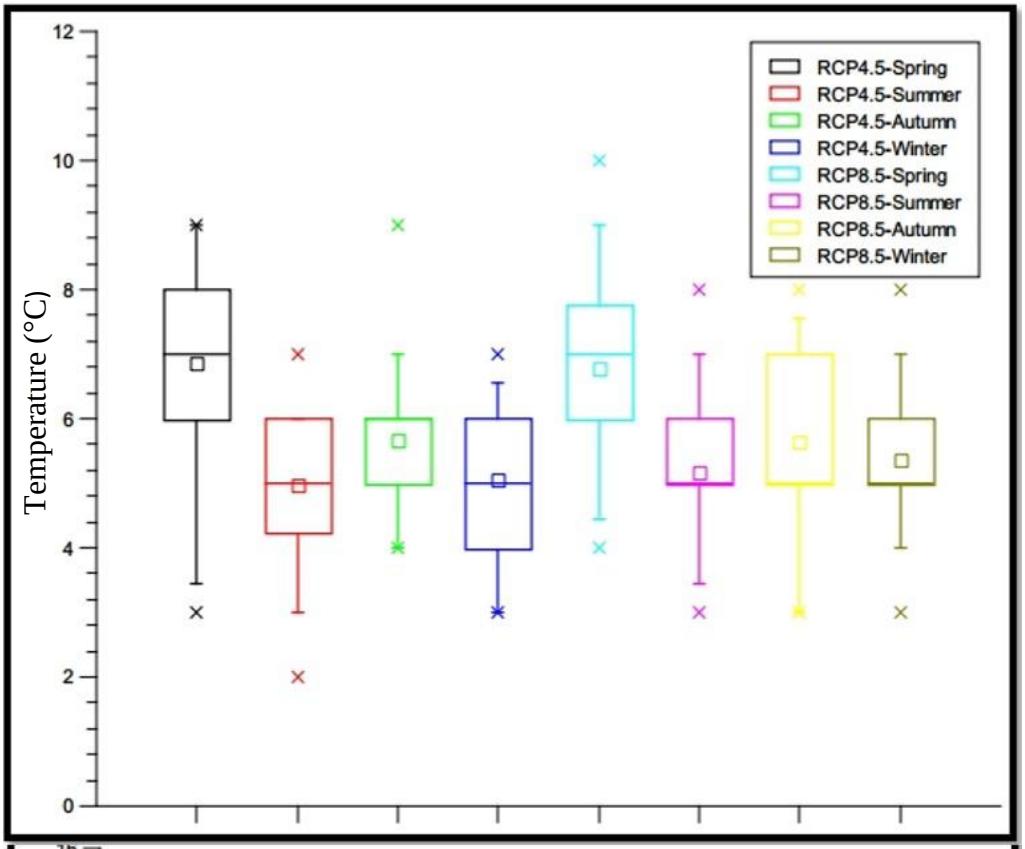

(b)

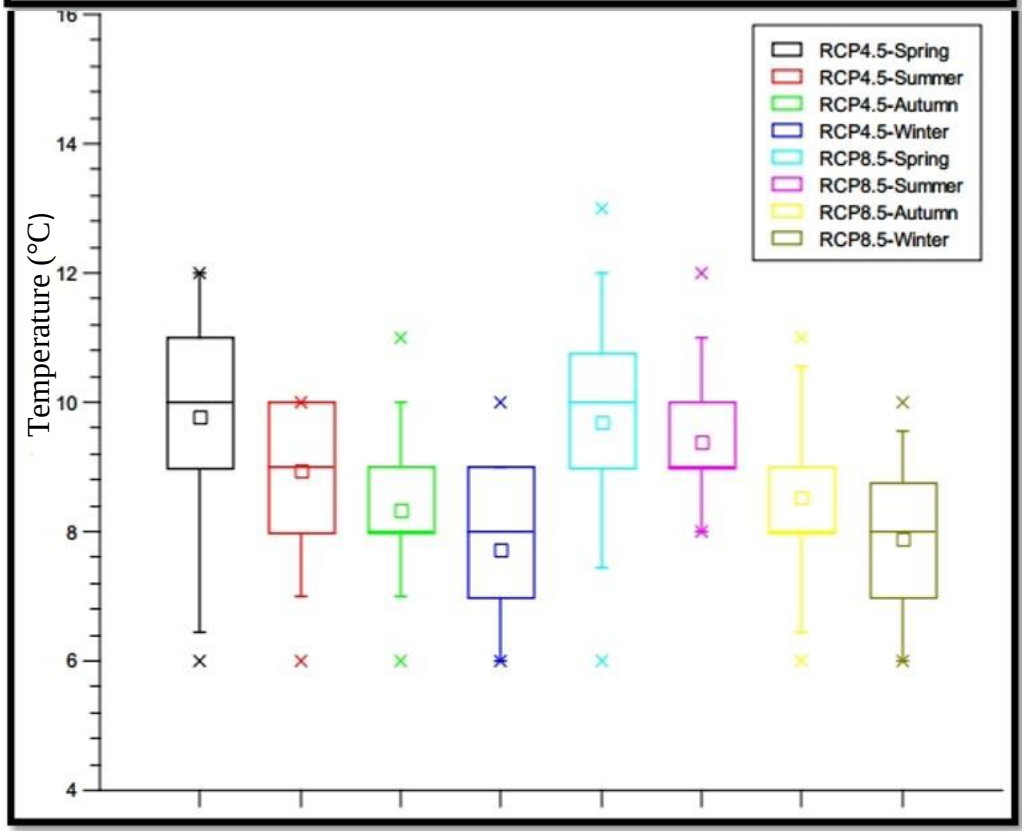

Figure 3.18

Projected changes in seasonal temperatures of (a) the Sihala sub-catchment and (b) the Kani sub-catchment under the RCP 4.5 and RCP 8.5 for the time period (2018-2047), as compared to baseline period (1979-2017). Data source (ECMWF and SMHI RCA4).

3.16. Projected changes in seasonal temperatures of the Sihala and the Kani sub-catchments

Projected changes in temperatures for all the four seasons, namely, spring, summer. Autumn, and winter for the SSC and the KSC are given in (Fig. 3.18). Mean temperature under the RCP 4.5 and RCP 8.5 seems to be 18 °C as compare to 11 °C in the observed time period, in spring season, in the SSC. However, more warming is projected in the KSC with a projected mean temperature of 23 °C under both climate change scenarios, as compared to 14 °C in the observed time span in the spring season.

In summers, mean temperature is seen to be 25 °C and 26 °C under RCP 4.5 and RCP 8.5 respectively, relative to 20 °C that was in the observed period in the SSC. Mean temperature under the RCP 4.5 and RCP 8.5 is projected to be 32 °C as compare to the baseline temperature of 23 °C, in summers, in the KSC.

In the SSC, temperature is projected to be 17 °C under both emission scenarios, as compared to 11 °C in the observed time period, in the autumn season, as seen in (Fig. 3.18). However, average temperature under the RCP 4.5 and RCP 8.5 is seen to be 22 °C as compare to 14 °C in the observed time period, in autumn, in the KSC.

While in the SSC, in winters, average temperature under the RCP 4.5 and RCP 8.5 might be 7 °C as compare to the baseline temperature of 2 °C, as shown in (Fig. 3.18). Average temperature in winter under the RCP 4.5 and RCP 8.5 is projected to be 11 °C, rather than 3 °C that was in the observed period, in the KSC.

3.17. Model limitations and uncertainties in hydrological impact assessments

In this study reanalysis dataset form ECMWF was employed to define and analyze the hydrological and climatological characteristics of two sub-catchments of the SRB. A conceptual hydrological model was used to simulate the potential changes in the future flows of basin. Before the calibration and validation of hydrological model HBV-light parameterization was carried out to identify the parameters that are highly sensitive to the model's goodness of fit measure. HBV-light has around 21 parameters for a standard model routine. Not all the parameters are equally sensitive to model's efficiency, some are more and some are less or even none. So to find out which parameters affected the efficiency of model, Parameterization was done.

It was found out that the TT, which is Threshold temperature, CFMAX which is degree-Δt factor, SFCF which is snowfall correction factor, FC maximum soil moisture storage, LP soil moisture value above which AET reaches PET, BETA parameter that determines the relative contribution to runoff from rain or snowmelt, PERC threshold parameter, UZL threshold parameter, K0 storage (or recession) coefficient 0, K1 storage (or recession) coefficient 1 , K2 storage (or recession) coefficient 2, MAXBAS length of triangular weighting function, Cet potential evaporation correction factor, PCALT change of precipitation with elevation, TCALT change of temperature with elevation, elevation of precipitation data, elevation of temperature are the most sensitive parameters, that plays a crucial role in the model calibration..

Literature on uncertainty in impacts analyses has focused mainly on the uncertainties in impacts that result from the uncertainties in future climate. Uncertainties in climate change impacts on water resources are mainly due to the uncertainty in precipitation inputs and less due to the uncertainties in greenhouse gas emissions. GCM structure is the largest source of uncertainty, next are the emissions scenarios, and finally hydrological modeling. Uncertainty exists at all stages of regional climate change impact assessments of water resources (Bott, 2014; IPCC, 2007, Breach et al., 2016; Xu and Luo, 2015).

4. CONCLUSION

Present study was conducted over the Soan River Basin (SRB), which is a semi-arid basin and highly vulnerable to climate changes. This study unveiled the differences between the yearly, monthly and the seasonal climatic changes and their subsequent impacts on the freshwater resources of the basin. Prominent differences in the climate changes, magnitude of climate changes, and the implications of these climate changes on hydrological characteristics of the Sihala and the Kani sub-catchments exists. Compared to the Kani sub-catchment (KSC), the catchment that lies in the northern part of the basin, the Sihala sub-catchment (SSC) had more apparent wetting, with a larger upsurge in river discharge

The SRB was divided into two sub-catchments. Hydro-climatological characteristics and the land cover classification of both the sub-catchments were assessed and analyzed. Both sub-catchments were divided into four elevation and three vegetation zones and their north, south, east-west aspect was found out with their fractional areas. The HBV light was calibrated and validated for both the sub-catchments. After that HBV light was induced with future climate projections of the SMHI RCA4. The HBV light then simulated the projected flows. The conclusions drawn from results of the present study are presented below:

1. Increase in yearly precipitation, evapotranspiration, and temperature was projected for both the sub-catchments and consequently, projected flows showed an increase on yearly basis for both the sub-catchments i.e. Sihala and Kani.

2. Mean monthly precipitation is projected to decrease for the winter to spring transitioning months, and increase for the rest of the months, along with projected increase in evapotranspiration, and the temperature. Projected flows showed both decreasing and increasing trends on monthly basis for both the sub-catchments.
3. Mean seasonal precipitation, is projected to increase in all seasons, except winter in the SSC, where the decrease is dominant over the increase, evapotranspiration and temperature are projected to increase. Highest increase in flows amongst all the seasons is projected for the summer season in the SSC under both the emission scenarios. However the winter seems to see the decrease in flows under the RCP 8.5. Overall an increasing pattern of flows could be observed for the rest of the seasons.

Attributable to extremely high variability in projected precipitation more an intense storm with more flooding is expected. Greater interannual variability may result in less precipitation in some years and more in others. More rain and less snow owing to extraordinary high seasonal temperature variability in Spring is projected. Snow is projected to melt sooner in spring. More evapotranspiration and drier vegetation and soils in the sub-catchments are predicted. More frequent and severe droughts in some years followed by extreme stream flows in others are projected. Earlier spring runoff is seen in the projections which may enhance chances of lake formation in upper sub-catchment. More summer stream flow is also projected which may result in downstream inundation of the lower sub-catchment.

RECOMMENDATIONS

The findings of this study have significant implications for management of water resources and a better understanding of hydrological implications of climate change in this semi-arid catchment. It is also helpful to the water managers in designing, identifying or bridging the gaps of suitable allocation schemes. The results might be helpful in identification of areas where the action is needed for example increasing the reservoir storage capacity, and development of flood risk management plans in case of high projected flows, and in case of low flow projections, cooperation should exist in terms of information sharing, among different stakeholders to develop and implement water plans. It will also be beneficial for other sectors and stakeholders including the civil engineers (in terms of infrastructure building), the core funding agencies on national and international level that deals with the mega projects.

This researchpresents adequate results which are robust enough to extract major trends, however uncertainties lies as well. So, further research could be carried out in the SRB, in order to make improvements. HBV light should be provided with more vegetation zones for more effective assessment of land cover changes. As the basin is scarcely researched, and the fact that uncertainties exists among different hydrological models and climatic projections obtained from different general and reegional climate models, different hydrological models alongwith different outputs from different GCMs and RCMs (individually and in the form of ensembles) along with different emission scenarios should be employed. Hydrological models could be calibrated for the study basin by using both the station based data and the gridded data.

The mid century projections of stream-flows pertaining to model results predicts the heavy streamflow and ample availability of water for Ghabir dam (a proposed project of Water and Power Development Authority (WAPDA) under the WAPDA vision 2025) which would be a small dam with a potential of irrigated agriculture development of 15000 acres, and hydropower generattion of 150 kw (WAPDA, 2001), and would also help conserve fresh water to enhance the number of beneficiaries.

APPENDIX-i

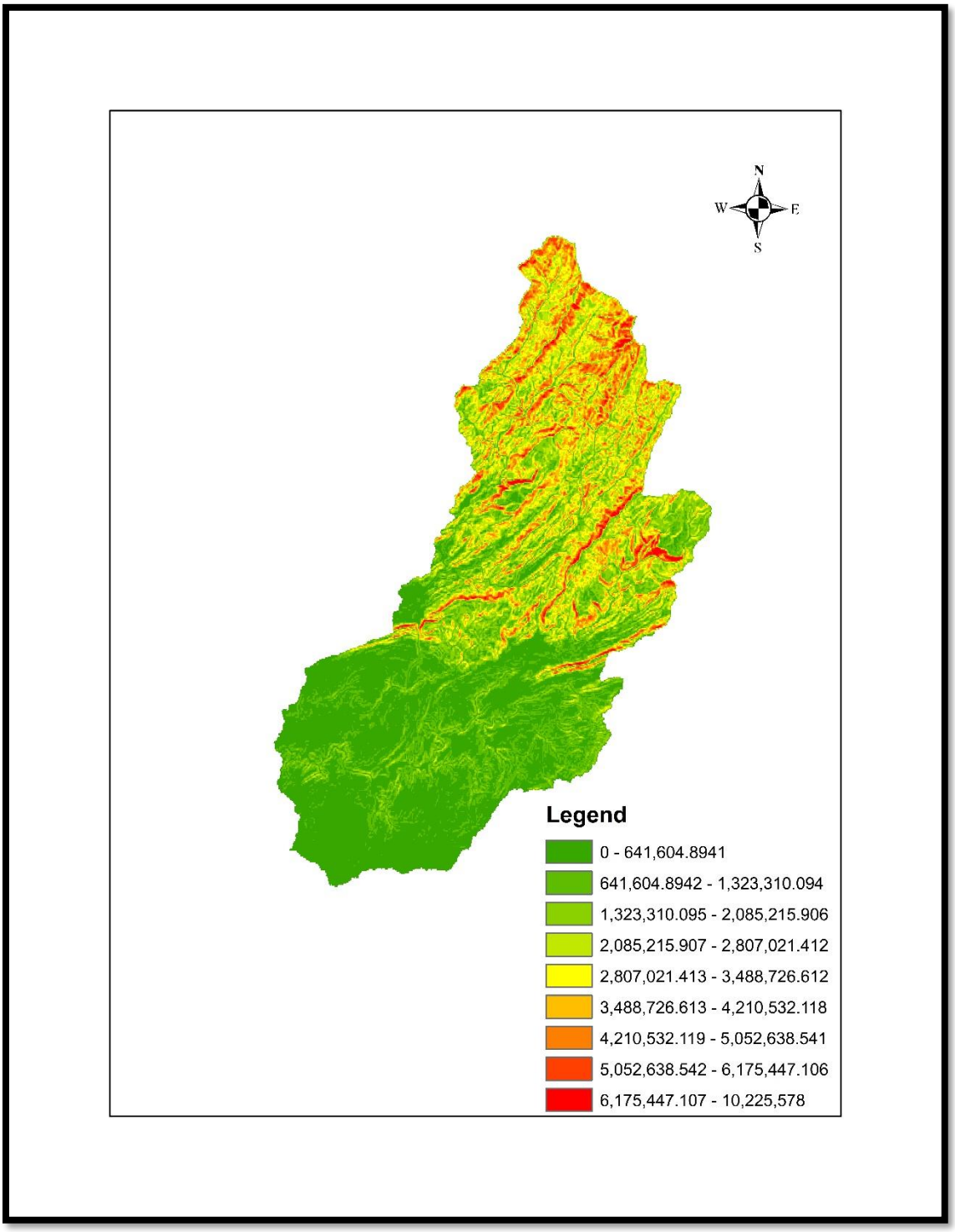

Figure I Slope map of Sihala sub-catchment.

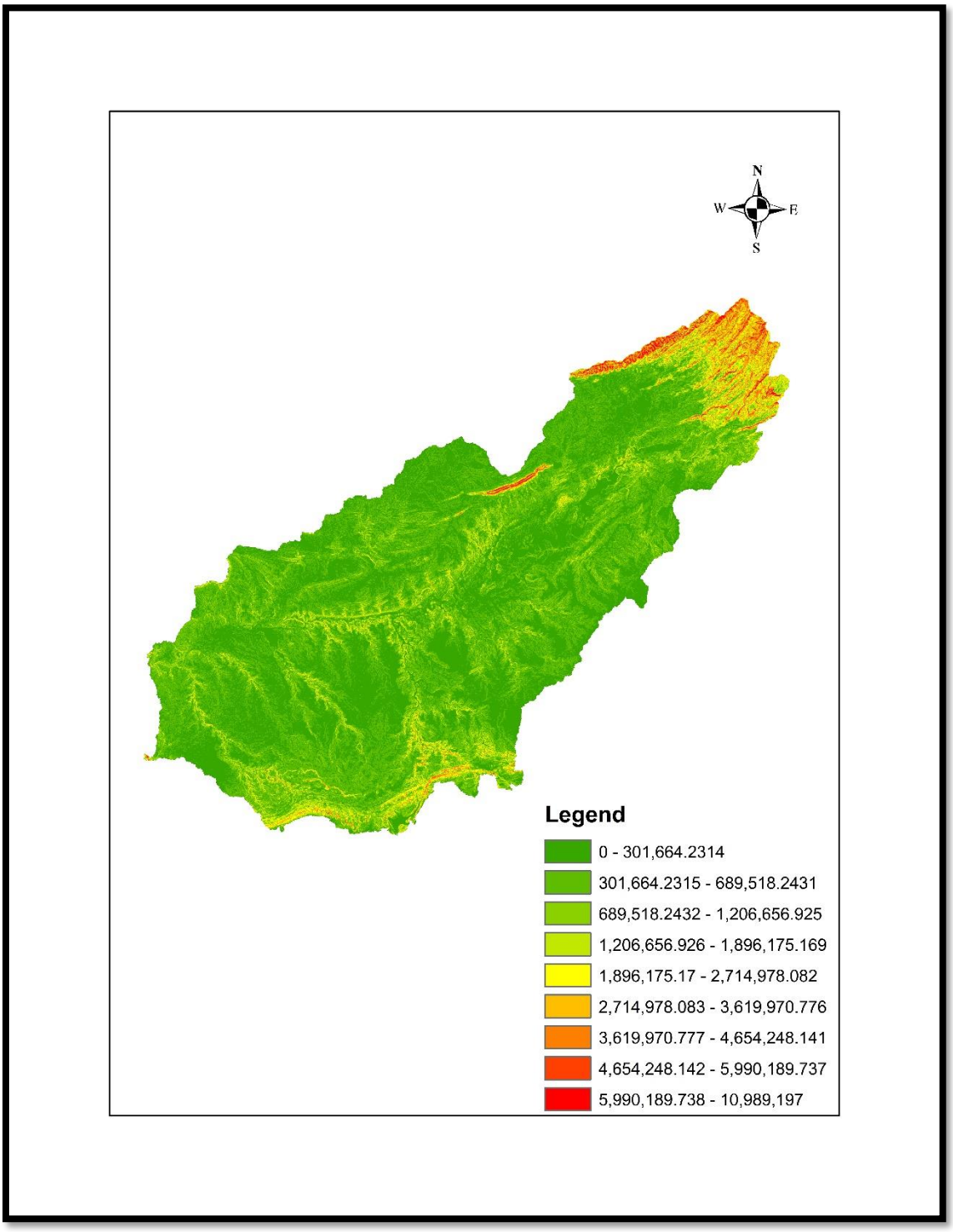

Figure II Slope map of Kani sub-catchment.

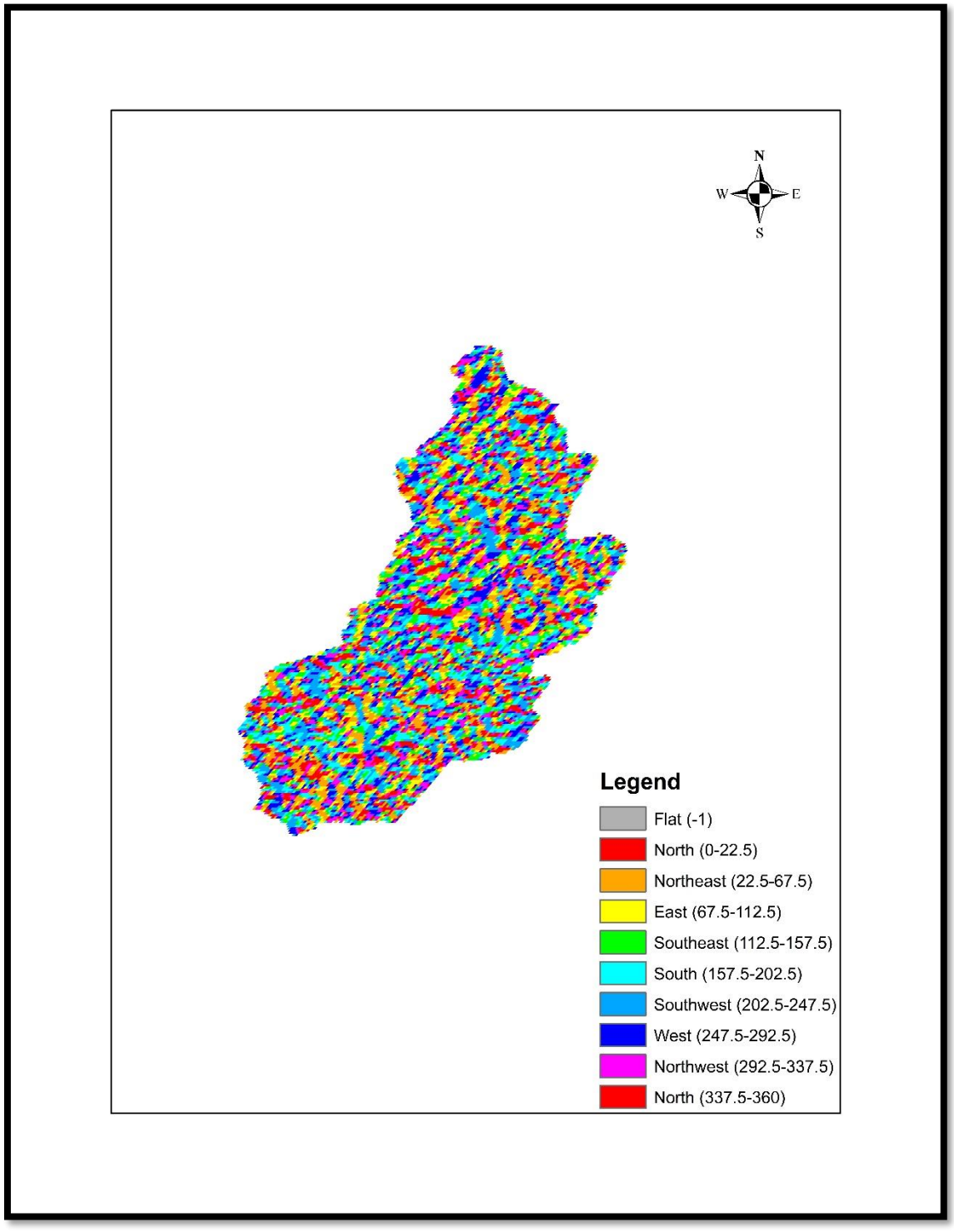

Figure III Aspect of Sihala sub-catchment.

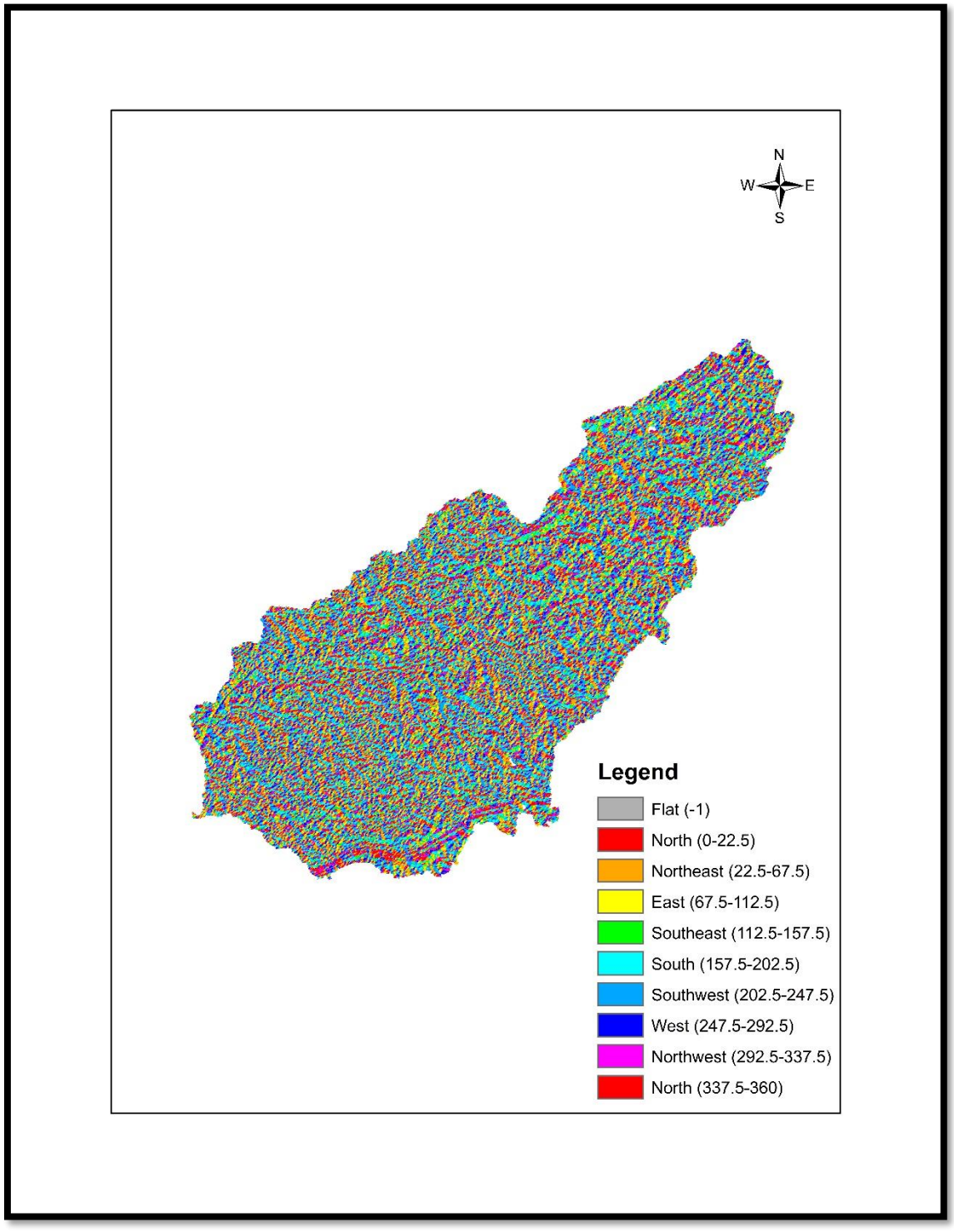

Figure IV Aspect of Kani sub-catchment.

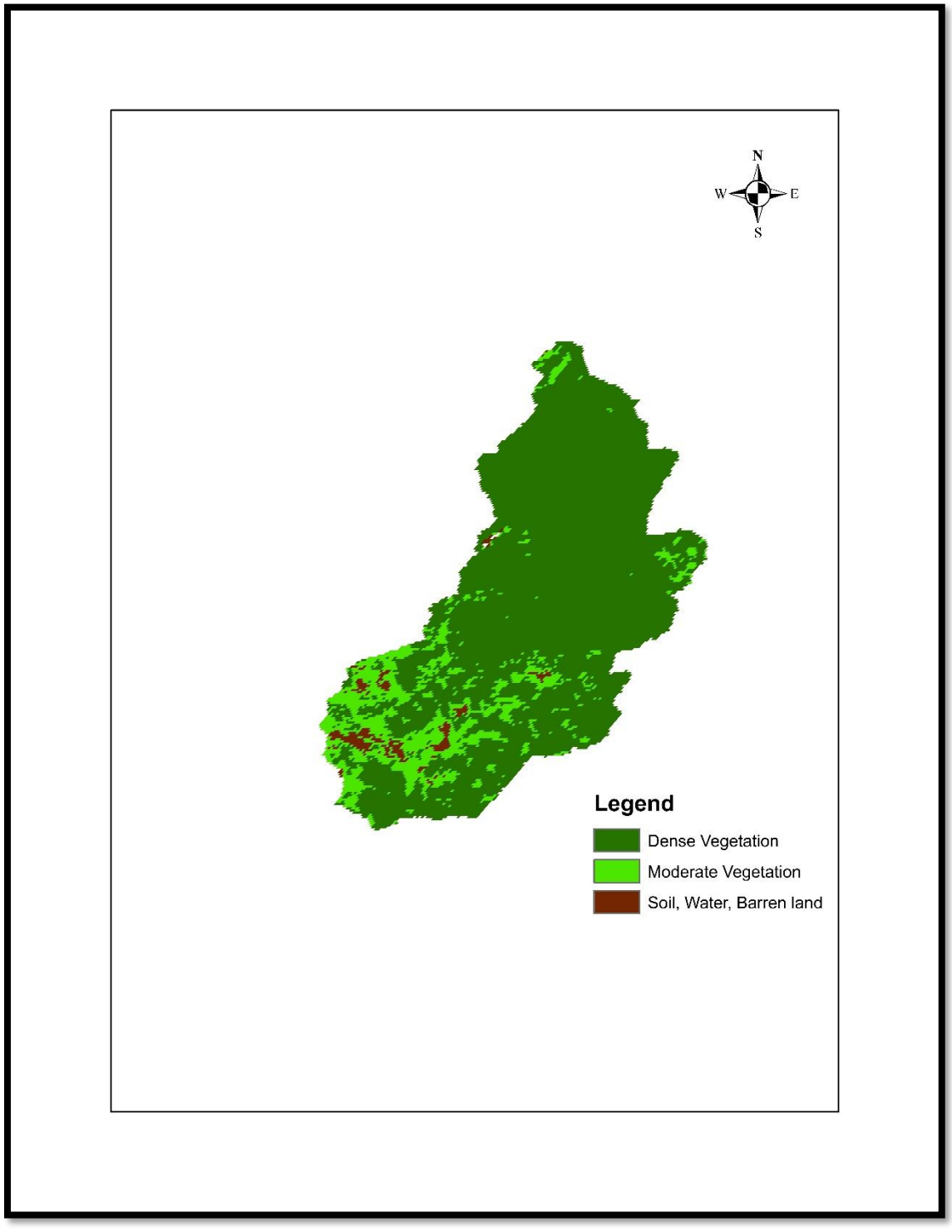

Figure V Vegetation zones of Sihala sub-catchment.

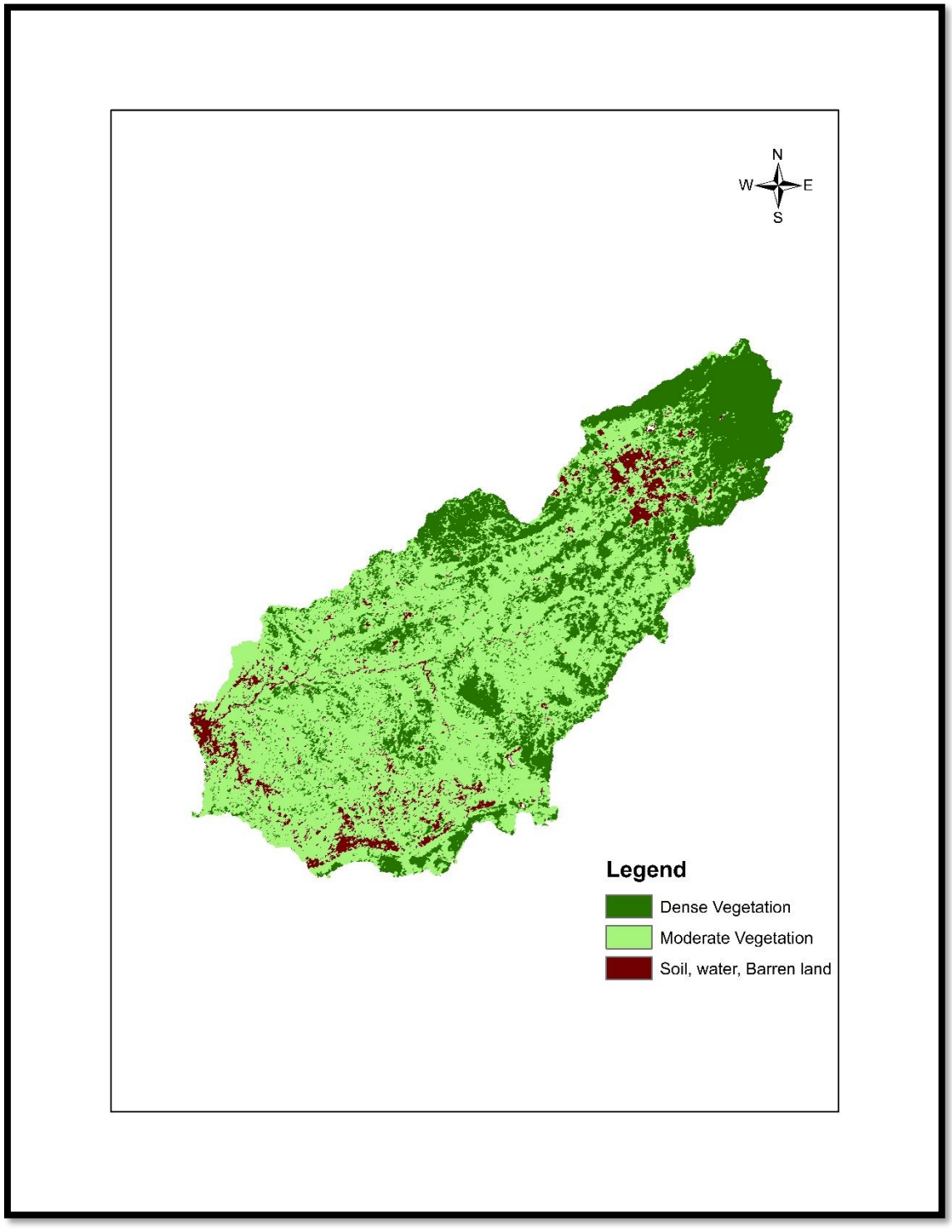

Figure VI Vegetation zones of Kani sub-catchment.

APPENDIX-ii

Table I Sihala sub-catchment with three vegetation zones, and four elevation zones along with area used as input to HBV-light.

	Area (km^2)	Mean Elevation (m)	Elevation Range (m)	Vegetation zone I (Dense Vegetation km^2)	Vegetation zone II (Moderate Vegetation km^2)	Vegetation zone III (Soil, Water, Barren land km^2)
Sihala Sub-catchment	882	1351.5	442-2261	738	127.15	17.25
Level 1	299	521	442-600	174	109	15.73
Level 2	414	900.5	601-1200	400	12.7	1.32
Level 3	153	1500.5	1201-1800	145.5	7.37	0.073
Level 4	15	2031	1801-2261	14	1.3	0.073

Table II. Kani sub-catchment with three vegetation zones, and four elevation zones along with area used as input to HBV-light.

	Area (km^2)	Mean Elevation (m)	Elevation Range (m)	Vegetation zone I (Dense Vegetation km^2)	Vegetation zone II (Moderate Vegetation km^2)	Vegetation zone III (Soil, Water, Barren land km^2)
Kani Sub-catchment	10371	1233.5	206-2261	2906	6862	603
Level 1	8806	403	206-600	2046	6312	551.5
Level 2	1336	900.5	601-1200	662	534	52.14
Level 3	198	1500.5	1201-1800	183	15	0
Level 4	17	2031	1801-2261	15.49	1.43	0.0733

Table III. Sihala sub-catchment with aspects (N-NE-NW,S-SE-SW,E-W) of three vegetation zones, and four elevation zones along with area used as input to HBV-light.

Dense Vegetation	Area (km^2)	Mean Elevation (m)	N-NE-NW	S-SE-SW	E-W
Level 1	174	521	66	64	30
Level 2	400	900.5	139	148	78
Level 3	145.5	1500.5	53	59	32
Level 4	14	2031	3.39	5	3.5

Moderate Vegetation	Area (km^2)	Mean Elevation (m)	N-NE-NW	S-SE-SW	E-W
Level 1	109	521	37	38.7	17.17
Level 2	12.7	900.5	3.47	4.33	1.7
Level 3	7.37	1500.5	2.47	1.89	2.07
Level 4	1.3	2031	0.53	0.18	0.39

Soil, Water, Barren land	Area (km^2)	Mean Elevation (m)	N-NE-NW	S-SE-SW	E-W
Level 1	15.73	521	4.88	5.88	2.35
Level 2	1.32	900.5	0.34	0.43	0.28
Level 3	0.073	1500.5	0	0	0
Level 4	0.073	2031	0.073	0	0

Table IV. Kani sub-catchment with aspects (N-NE-NW,S-SE-SW,E-W)of three vegetation zones, and four elevation zones along with area used as input to HBV-light.

Dense Vegetation	Area (km^2)	Mean Elevation (m)	N-NE-NW	S-SE-SW	E-W
Lakes	13.29				
Level 1	2046	403	900	925	220
Level 2	662	900.5	233	282	147
Level 3	183	1500.5	64	62	36
Level 4	15.49	2031	4	5	3
Moderate Vegetation	Area (km2)	Mean Elevation (m)	N-NE-NW	S-SE-SW	E-W
Level 1	6312	403	2956	2670	676
Level 2	534	900.5	197	182	81
Level 3	15	1500.5	6	3.26	3.42
Level 4	1.43	2031	0.54	0.3	0.34
Soil, Water, Barren land	Area (km^2)	Mean Elevation (m)	N-NE-NW	S-SE-SW	E-W
Level 1	551.5	403	160	170	42
Level 2	52.14	900.5	16.39	20.23	8.14
Level 3	0	1500.5	0	0	0
Level 4	0.073	2031	0	0	0

REFERENCE

1. Abebe, E., and Kebede, A., 2017. Assessment of Climate Change Impacts on the Water Resources of Megech River Catchment, Abbay Basin, Ethiopia. Open Journal of Modern Hydrology, 7, no.2, 141-152.
2. Adnan, S., Mahmood, R., and Khan, A. H., 2009. Water Balance Conditions in Rainfed Areas of Potohar and Balochistan Plateau During 1931-08. World Applied Sciences Journal ,7, no.2, 162-169.
3. Aguilera, H and Murillo-Díaz, J, M., 2009. The effect of possible climate change on natural groundwater recharge based on a simple model: A study of four karstic aquifers in SE Spain.Environmental Geology, 5, no.7.
4. Ali, S.S., Baloch, K.A., and Masood, S., 2017. Water sustainability in Pakistan: Key issues and challenges. State Bank of Pakistan's Annual Report 2016-17, 93-103. Retrieved from http://www.sbp.org.pk/reports/annual/arFY17/Chapter-07.pdf
5. Al-Safi, H. I. J., and Sarukkalige, P. R., 2017. Assessment of future climate change impacts on hydrological behavior of Richmond River Catchment. Water Science and Engineering, 10, no.3, 197–208.
6. Akhtar, M., 2008. the Climate Change Impact on Water Resources of Upper Indus Basin-Pakistan University of the Punjab , Lahore-Pakistan. Phd Thesis.
7. Arnell, N. W., and Lloyd-Hughes, B., 2014. The global-scale impacts of climate change on water resources and flooding under new climate and socio-economic scenarios. Climatic Change, 122, no.1-2, 127-140.
8. Ashfaq, A., Ashraf, M., and Bahzad, A., 2014. Spatial and Temporal Assessment of Groundwater Behaviour in the Soan Basin of Pakistan.Technical Journal, University of Engineering and Technology Taxila,19, no.1. 12-22
9. Asl-Rousta, B., Mousavi, S. J., Ehtiat, M., and Ahmadi, M., 2018. SWAT-Based Hydrological Modelling Using Model Selection Criteria. Water Resources Management, 32, no.6, 2181-2197.
10. Asl-Rousta, B., and Mousavi, S. J., 2019. A TOPSIS-Based Multicriteria Approach to the Calibration of a Basin-Scale

SWAT Hydrological Model. Water Resources Management, 33, no.1, 439-452.
11. Babur, M., Babel, M. S., Shrestha, S., Kawasaki, A., and Tripathi, N. K., 2016. Assessment of climate change impact on reservoir inflows using multi climate-models under RCPs-the case of Mangla Dam in Pakistan. Water (Switzerland), 8, no.9.
12. Bahremand, A., and Smedt, F., 2008. Distributed hydrological modeling and sensitivity analysis in Torysa Watershed, Slovakia. Water Resources Management, 22, no.3, 393-408.
13. Bates, B. C., Kundxewicz, Z. W., Wu, S., and Palutikof, J. P., 2008. Observed and projected changes in climate as they relate to water. IPPC - Techincal Paper 4. Climate Change and Water. Retrieved from http://www.ipcc.ch/pdf/technical-papers/ccw/chapter2.pdf
14. Bergstörm, S., 1992. THE HBVMODEL -its structure and applications , no.4
15. Berrisford, P., Dee, D., Poli, P., and Simmons, A., 2011. ERA Report Series, no.1, Version 2.0, 1-2-17. https://www.ecmwf.int/en/elibrary/8174-era-interim-archive-version-20
16. Bjørnæs, C., 2013. A guide to Representative Concentration Pathways. Retrieved fromhttp://www.iiasa.ac.at/web/home/research/researchPrograms/TransitionstoNewTechnologies/RCP.en
17. Bott, R., 2014. Climate Change 2014 Impacts, Adaptation, and Vulnerability Part B: Regional Aspects. Igarss 2014. https://doi.org/10.1007/s13398-014-0173-7.2
18. Breach, P. A., Simonovic, S. P., and Yang, Z., 2016. Global Climate Model Selection for Analysis of Uncertainty in Climate Change Impact Assessments of Hydro-Climatic Extremes. American Journal of Climate Change, 5, no.04, 502-525.
19. Carroll, M., Dimiceli, C., Townshend, J., Noojipady, P., and Sohlberg, R., 2008. UMD Global 250 meter Land Water Mask User Guide. Rivers. Retrieved from http://landcover.org/library/guide/techguide_watermask.pdf
20. Carroll, M. L., Townshend, J. R., Dimiceli, C. M., Noojipady, P., and Sohlberg, R. A., 2009. A new global raster water mask at 250 m resolution. International Journal of Digital Earth, 2, no.4, 291-308.
21. Daham, A., Han, D., Rico, M., and Anke, R., 2018. Analysis of NVDI variability in response to precipitation and air temperature in different regions of Iraq , using MODIS vegetation indices. Environmental Earth Sciences, 77, no.10, 1-24.
22. Dee, D. P., Uppala, S. M., Simmons, A. J., Berrisford, P., Poli, P., Kobayashi, S., Vitart, F., 2011. The ERA-Interim reanalysis: Configuration and performance of the data assimilation system. Quarterly Journal of the Royal Meteorological Society, 137, no.656, 553–597.
23. Dicam, D., and Szolgay, I. J., 2010. Alma Mater Studiorum-Università Di Bologna Facolta' Di Ingegneria Corso Di Laurea In Ingegneria Per L'ambiente E Il Territorio Ls.Calibration of rainfall-runoff models Summary of contents. Retrieved from https://core.ac.uk/download/pdf/11806898.pdf
24. Didan, K., 2015. MYD13Q1 MODIS/Aqua Vegetation Indices 16-Day L3 Global 250m SIN Grid V006 [Data set]. NASA EOSDIS Land Processes DAAC. doi: 10.5067/MODIS/MYD13Q1.006
25. Didovets, I., Lobanova, A., Bronstert, A., Snizhko, S., Maule, C. F., and Krysanova, V., 2017. Assessment of climate change impacts on water resources in three representative ukrainian catchments using eco-hydrological modelling. Water (Switzerland), 9, no.3.
26. Dingding, Y., Caiping, Z., Hua, O., and Chuanyou, C., 2012. Characteristics of Variation in Runoff Across the Nyangqu River Basin in the Qinghai-Tibet Plateau. Journal of Resources and Ecology, 3,no.1, 80-86.
27. Eregno, F., 2009. Comparison of Hydrological Impacts of Climate Change Simulated by WASMOD and HBV Models in Different Climatic Zones China, Ethiopia, and Norway. Master's Thesis, Universty of Oslo.
28. European Commission., 2015. Guidance document on the application of water balances for supporting the implementation of the WFD. https://doi.org/10.2779/352735
29. FAO, A., 2011. Indus river basin. Aquastat, 1-14. Retrieved from http://www.fao.org/nr/water/aquastat/basins/indus/index.stm
30. FAO., 2012. Irrigation in Southern and Eastern Asia in figures. AQUASTAT Survey - 2011. FAO Water report 37. Retrieved from http://www.fao.org/docrep/016/i2809e/i2809e.pdf
31. Friedl, M. A., Sulla-Menashe, D., Tan, B., Schneider, A., Ramankutty, N., Sibley, A., and Huang, X., 2010. MODIS Collection 5 global land cover: Algorithm refinements and characterization of new datasets. Remote Sensing of Environment, 114, no.1, 168-182.
32. Gebre, S. L., 2015. Potential Impacts of Climate Change on the Hydrology and Water resources Availability of Didessa Catchment, Blue Nile River Basin, Ethiopia. Journal of Geology and Geosciences, 4, no.1, 1-7.
33. Gevorgyan, A., and Melkonyan, H., 2015. Regional impact of the Armenian highland as an elevated heat source: ERA-Interim reanalysis and observations. Climate Dynamics, 44, no.5-6, 1541-1565.
34. Gunasekara, N., Kazama, S., Yamazaki, D.,Oki, T., 2014. Analysing regional aspects of climate change and water resources. Water Resources Management, 28, no.1, 169-184.
35. Harasawa, H., Lal, M., Wu, S., Anokhin, Y., Punsalmaa, B., Honda, Y., … Hanson, C. E., 2007. IPCC 4th Assessment Report, Working Group II, Asia Chapter, 469-506. Retrieved

from https://www.ipcc.ch/site/assets/uploads/2018/02/ar4-wg2-chapter10-2.pdf
36. Hasson, S., 2016. Future Water Availability from Hindukush-Karakoram-Himalaya upper Indus Basin under Conflicting Climate Change Scenarios. Climate, 4, no.3, 1-28.
37. Hoegh-Guldberg, O., Jacob, D., and Taylor, M., 2018. Special Report on Global Warming of 1.5 °C - Chapter 3: Impacts of 1.5o C global warming on natural and human systems, 243.
38. Hoff, H., 2009. Global water resources and their management. Current Opinion in Environmental Sustainability, 1, no.2, 141-147.
39. Hirshfleld, F., 2010. The Impact Of Climate Change and harvest of Mountain Pine Beetle stands on Streamflow in Northern British Columbia.Phd Thesis.The University of Northern British Columbia.
40. Huo, J., and Liu, L., 2018. Application research of multi-objective Artificial Bee Colony optimization algorithm for parameters calibration of hydrological model. Neural Computing and Applications, 4.
41. IPCC., 2007. Chapter 3 - Freshwater Resources. Agriculture, 17, no.3, 469-506. https://doi.org/10.2134/jeq2008.0015br
42. IPCC., 2001. Climate change: impacts, adaptation, and vulner- ability. Contribution of Working Group II to the third assess- ment report of the Intergovernmental Panel on Climate Change. Cambridge University Press, 1032. Retrieved from https://www.ipcc.ch/ipccreports/tar/wg2/pdf/wg2TARchap1.pdf
43. IPCC., 2010. Gaps in knowledge and suggestions for further work. IPCC, no.8, 1-6.
44. IPCC.,2014. Intergovernmental Panel on Climate Change, Fifth Assessment report (AR5), Part A, Working Group II Final.
45. Islam, Z. M., 2013. Modeling the Hydrology and Water Resources Management of South Saskatchewan River Basin under the Potential Combined Impacts of Climate Change and Climate Anomalies. Phd thesis. University of Alberta, Canada
46. Jajarmizadeh, M., Harun, S., and Salarpour, M., 2012 A review on theoretical consideration an types of models in hydrology. Journal of Environmental Science and Technology, 5, no.5, 249-261
47. Javed, M., 2018. Hydrological response to climate change on Soan river catchment. Master's thesis. National University of Science and Technology (NUST).
48. Javan, K., Lialestani, M. R. F. H., and Nejadhossein, M., 2015. A comparison of ANN and HSPF models for runoff simulation in Gharehsoo River watershed, Iran. Modeling Earth Systems and Environment, 1, no.4, 41.
49. Jia, G., Liu, Z., Lixin Chen, L., and Yu, X., 2017. Distinguish water utilization strategies of trees growing on earth-rocky mountainous area with transpiration and water isotopes.Ecology and Evolution, 7.
50. Jones, J. A., 2011. Hydrologic responses to climate change: considering geographic context and alternative hypotheses. Hydrological Processes, 25, no.12, 1996-2000.
51. Khatun, S., Sahana, M., Jain, S. K., and Jain, N., 2018. Simulation of surface runoff using semi distributed hydrological model for a part of Satluj Basin: parameterization and global sensitivity analysis using SWAT CUP. Modeling Earth Systems and Environment, 4, no.3, 1111–1124.
52. Koike, T., Koudelova, P., Jaranilla-sanchez, P. A., Bhatti, A. M., Nyunt, C. T., and Tamagawa, K., 2015. River management system development in Asia based on Data Integration and Analysis System (DIAS) under GEOSS. Science China Earth Sciences, 58, 76-95.
53. Kotsias, G., and Lolis, C. J., 2018. A study on the total cloud cover variability over the Mediterranean region during the period 1979-2014 with the use of the ERA-Interim database. Theoretical and Applied Climatology, 134, no.1-2, 325-336.
54. Kumarasamy, K., and Belmont, P., 2018. Calibration parameter selection and watershed hydrology model evaluation in time and frequency domains. Water (Switzerland), 10, no.6.
55. Ky, R., 2014. Impact of Climate Change on Water Resources. Journal of Earth Science and Climatic Change, 5, no.3.
56. Lawrence, D., Haddeland, I., and Langsholt, E., 2009. Calibration of HBV hydrological models using PEST parameter estimation. Retrieved from http://publikasjoner.nve.no/report/2009/report2009_01.pdf
57. Mahmood, R., and Jia, S., 2016. Assessment of Impacts of Climate Change on the Water resources of the transboundary Jhelum river basin of Pakistan and India. Water, 8, no.6, 246.
58. McCabe. G. J. and Wolock. D. M., 2014. Spatial and temporal patterns in conterminous United States streamflow characteristics. Geophysical Research Letters. 41. DOI: 10.1002/2014GL061980
59. Mostafaie, A., Forootan, E., Safari, A., and Schumacher, M., 2018. Comparing multi-objective optimization techniques to calibrate a conceptual hydrological model using in situ runoff and daily GRACE data. Computational Geosciences, 22, no.3, 789-814.
60. National Water Policy., 2018. Ministry of water resources ,Government of Pakistan. Retrieved from https://ffc.gov.pk/wp-content/uploads/2018/12/National-Water-Policy-April-2018-FINAL_3-1.pdf
61. Nazeer, S., Ali, Z., and Malik, R. N., 2016. Water Quality Assessment of River Soan (Pakistan) and Source Apportionment of Pollution Sources Through Receptor

Modeling. Archives of Environmental Contamination and Toxicology, 71, no.1, 97-112.
62. Nepal, S., 2016. Impacts of climate change on the hydrological regime of the Koshi river basin in the Himalayan region. Journal of Hydro-Environment Research, 10. 76-89.
63. Pluntke, T., Pavlik, D., and Bernhofer, C., 2014. Reducing uncertainty in hydrological modelling in a data sparse region. Environmental Earth Sciences, 72, no.12, 4801-4816.
64. Report, T., 1999. Groundwater recharge - climatic and vegetation induced variations. Simulations in the Eman and Aspo areas in southern Sweden.
65. Rosanna, A., and David, H., 2014. Southeast Asia Climate Analysis and Modelling Framework. Met Office.
66. Saeed, F., S. Jehangir, M. Noaman-ul-Haq, W. Shafeeq, M. Z. Hashmi, G. Ali and A.M. Khan., 2009. Application of UBC and DHSVM Models for Selected Catchments of Indus Basin Pakistan, GCISC-RR-11, Global Change Impact Studies Centre (GCISC), Islamabad, Pakistan.
67. Seibert, J., 2005. User ' s Manual.
68. Seibert, J., and Vis, M. J. P., 2012. Teaching hydrological modeling with a user-friendly catchment-runoff-model software package, 3315–3325.
69. Sitterson, J., Knightes, C., Parmar, R., Wolfe, K., Muche, M., and Avant, B., 2017. An Overview of Rainfall-Runoff Model Types. U.S. Environmental Protection Agency, (issue September), 0-29.
70. Shahid, M., Cong, Z., and Zhang, D., 2017. Understanding the impacts of climate change and human activities on streamflow: a case study of the Soan River basin, Pakistan. Theoretical and Applied Climatology, 1-15.
71. Shreedhar, S., Venkatesh, B., and Purandara, B. K., 2016. a Comparison of Five Potential Evapotranspiration Methods for Biligihole Watershed in Western Ghats of India. International Journal of Scientific and Engineering Research, 7, no.4, 1398–1412.
72. Song, X., Zhan, C., Xia, J., and Kong, F., 2012. An efficient global sensitivity analysis approach for distributed hydrological model. Journal of Geographical Sciences, 22, no.2, 209-222.
73. Tahir, A. A., 2011. Impact of climate change on the snow covers and glaciers in the Upper Indus River Basin and its consequences on the water reservoirs (Tarbela Dam) – Pakistan. Phd Thesis
74. Tang, B., Shao, K., Li, Z., Wu, H., and Tang, R., 2015. An improved NDVI-based threshold method for estimating land surface emissivity using MODIS satellite data.International Journal of Remote Sensing ,36, no.19-20, 4864-4878.
75. Trajkovic, S., and Kolakovic, S., 2009. Evaluation of reference evapotranspiration equations under humid conditions. Water Resources Management, 23, no.14, 3057–3067.
76. Trajkovic, S., and Stojnic, V., 2008. Effect of wind speed on accuracy of Turc method in a humid climate. Facta Universitatis - Series: Architecture and Civil Engineering, 5, no.2, 107–113.
77. UNDP., 2017. The Vulnerability of Pakistan's Water Sector to the Impacts of Climate Change: Identification of Gaps and Recommendations for Action. Retrieved from http://www.pk.undp.org/content/dam/pakistan/docs/Environmentand Climate Change/Report.pdf
78. United Nations., 2019. The Nnited Nations world water development report, Titled; Leaving no one behind. https://doi.org/9789231003097
79. User Guide for the MODIS Land Cover Type Product (MCD12Q1)., 2012. 1-50. Retrieved from https://www.bu.edu/lcsc/files/2012/08/MCD12Q1_user_guide.pdf
80. Usman, M., Liedl, R., Shahid, M. A., and Abbas, A., 2015. Land use / land cover classification and its change detection using multi-temporal MODIS N DVI data, 25, no.12, 1479–1506.
81. Vormoor, K., Rössler, O., Bürger, G., Bronstert, A., and Weingartner, R., 2017. When timing matters-considering changing temporal structures in runoff response surfaces. Climatic Change, 142, no.1-2, 213–226.
82. WAPDA., 2001. Development portfolio. WAPDA vision 2025. Retrieved from https://www.waterinfo.net.pk/sites/default/files/knowledge/Wapda%20Development%20Portfolio.pdf. Date of access, 6 august 2019.
83. Wayne, G. P., 2013. The Beginner's guide to Representative Concentration Pathways (RCPs). SkepticalScience, Version 1.0, 1–24.
84. Wijngaard, R.R., 2014. Hydroological response of the Ötztal glacierized catchments to future clim mate change. Master's thesis.Utrecht University, Netherlands.
85. WMO., 2009. Guide to Hydrological Practices.Volume II Management of Water Resources and Application of Hydrological Practices. No. 68
86. Wu, L., Qin, J., Wu, T., and Li, X., 2018. Trends in global ocean surface wave characteristics as represented in the ERA-Interim wave reanalysis for 1979-2010. Journal of Marine Science and Technology (Japan), 23, no.1, 2-9.
87. Xu, H., and Luo, Y., 2015. Climate change and its impacts on river discharge in two climate regions in China. Hydrology and Earth System Sciences, 19, no.11, 4609-4618
88. Zhang, R., Santos, C. A. G., Moreira, M., Freire, P. K. M. M., and Corte-Real, J., 2013. Automatic Calibration of the SHETRAN Hydrological Modelling System Using MSCE. Water Resources Management, 27, no.11, 4053-4068.
89. Zhao, Y., 2015.Investigation of uncertainties in assessing climate change impacts on the hydrology of a Canadian river watershed. PhD Thesis.